



Dominik Hilber, BSc

**Development of a fast-sampling device for the automatic rapid transfer of exact volumes of fluids from a bioreactor**

**MASTER'S THESIS**

to achieve the university degree of

Diplom-Ingenieur

Master's degree programme: Biomedical Engineering

submitted to

**Graz University of Technology**

Supervisor

Ao.Univ.-Prof. Dipl.-Ing. Dr.techn. Hermann Scharfetter

Institute of Medical Engineering

## **AFFIDAVIT**

I declare that I have authored this thesis independently, that I have not used other than the declared sources/resources, and that I have explicitly indicated all material which has been quoted either literally or by content from the sources used. The text document uploaded to TUGRAZonline is identical to the present master's thesis dissertation.

---

Date

---

Signature

## Abstract

Intracellular metabolite analysis is a key technology to identify biomarkers and metabolic bottlenecks in cellular systems for pharmaceutical and biotechnological applications. The determination of unbiased metabolite levels requires the transfer of a known amount of cells from the bioreactor without altering the cellular state. Afterwards the cellular metabolism must be stopped as fast as possible. Unfortunately, currently no instrument is commercially available which fulfills these requirements. In this context two approaches (volumetric cell and mass measurement) were pursued to sample a known volume. Independent of the approaches the device consists of a sampling tube, a 5-valve module and a vacuum pump. Using a volumetric cell of a defined volume resulted in sample volume of  $1.2\text{ml} \pm 2\%$  and 57% sample-to-sample carryover. This could be improved by using a mass measurement and a sampling tube made of fluorinated ethylene propylene instead of steel. This reduced carry over to under 5%. The obtained prototype is capable of aseptically transferring 0.5-100 ml of cell broth at a flow rate of approximately 2ml/s.

**Keywords:** rapid sampler, intracellular metabolite analysis, metabolomics, mass measurement, carry over

## Kurzfassung

Intrazelluläre Metaboliten Analyse ist eine Schlüsseltechnologie um Biomarker und Engstellen in zellulären Systemen zu identifizieren. Dies ist vor allem für pharmazeutische und biotechnologische Anwendungen wichtig. Um zuverlässige Metabolitenkonzentrationen zu messen, muss eine bekannte Menge an Zellflüssigkeit entnommen und deaktiviert werden ohne diese zu verändern. Es sind zur Zeit keine Geräte kommerziell verfügbar, welche diese Anforderungen erfüllen. Im Rahmen dieser Masterarbeit wurden 2 Ansätze verfolgt (volumetrische Messzelle und Massenbestimmung). Für beide Ansätze bestand der Aufbau aus einem Entnahmerohr, einer 5-Ventile Einheit und einer Vakuumpumpe. Mit Hilfe der volumetrischen Messzelle konnte ein definiertes Volumen (1.2ml), mit einer Genauigkeit von  $\pm 2\%$  und einen Übertrag von 57% entnommen werden. Diese konnte durch den Einsatz einer Massenmessung und eines Entnahmerohres aus Fluorethylen-Propylen verbessert werden. Dadurch wurde der Übertrag auf unter 5% reduziert. Mit Hilfe des Prototyps ist es möglich Zellproben im Bereich von 0.5 bis 100ml, bei einer Flußgeschwindigkeit von 2ml/s, zu entnehmen.

**Schlüsselwörter:** Rapid Sampler , Intrazelluläre Metaboliten Analyse, Metabolomics, Massenbestimmung, Übertrag

# Contents

<b>1</b>	<b>Introduction</b>	<b>1</b>
1.1	Why fast sampling . . . . .	1
1.2	Fast sampling approaches . . . . .	2
1.3	Quantification of the Volume . . . . .	6
1.4	Requirements . . . . .	8
1.5	Design decision . . . . .	9
1.6	Development Tools . . . . .	9
1.6.1	Electronic Circuit Simulation . . . . .	9
1.6.2	PCB Design . . . . .	10
1.6.3	Firmware-Development . . . . .	10
1.6.4	Software Development . . . . .	10
1.6.5	Matlab . . . . .	11
<b>2</b>	<b>Methodes and materials</b>	<b>12</b>
2.1	Materials . . . . .	12
2.2	Basic device . . . . .	16
2.3	Sampling procedure . . . . .	19
2.4	Electronical Hardware and Firmware . . . . .	22
2.4.1	Overview . . . . .	22
2.4.2	Power Supply . . . . .	23
2.4.3	Valve and Valve Driver . . . . .	24
2.4.4	Display . . . . .	25
2.4.5	Keyboard . . . . .	26
2.4.6	Pressure sensor . . . . .	27
2.4.7	Weight sensor . . . . .	31
2.4.8	Timer . . . . .	41
2.4.9	Memory Management . . . . .	41
2.4.10	Interpreter . . . . .	43
2.4.11	Connectors . . . . .	44
2.5	Software . . . . .	45
2.6	Matlab model . . . . .	45
2.7	Verification of the sampling device . . . . .	47
2.7.1	Setup for experiments . . . . .	47
2.7.2	Accuracy of the mass . . . . .	47
2.7.3	Carry over . . . . .	48

2.7.4	Sampling water from a bioreactor (only Version 1) . . . . .	50
2.7.5	Sampling cultivation broth from a bioreactor (only Version 2) . . .	51
2.7.6	Step response of the mass measurement (only Version 2) . . . . .	53
2.7.7	Temperature drift of the mass measurement (only Version 2) . . . .	53
2.7.8	Calibration of the mass measurement . . . . .	54
<b>3</b>	<b>Results</b>	<b>55</b>
3.1	Results of the simulation using the Matlab model of the tubing systems . .	55
3.2	Verification Version 1 . . . . .	57
3.2.1	Verification of the volumetric cell . . . . .	57
3.2.2	Verification of the carry over . . . . .	60
3.2.3	Verification with a bioreactor . . . . .	65
3.3	Verification Version 2 . . . . .	67
3.3.1	Analyzes of the dynamic behavior of the weight sensor . . . . .	67
3.3.2	Temperature drift . . . . .	69
3.3.3	Verification of the mass measurement . . . . .	71
3.3.4	Verification of the carry over . . . . .	74
3.3.5	Verification with biological samples . . . . .	77
<b>4</b>	<b>Discussion</b>	<b>81</b>
4.1	Technical requirements . . . . .	81
4.1.1	General . . . . .	81
4.1.2	Pressure sensor . . . . .	81
4.1.3	Weight sensor (Only Version 2) . . . . .	82
4.1.4	Thermal verification of the mass measurement . . . . .	84
4.1.5	Analysis of the dynamic behavior of the system for Version 2 . . . .	85
4.2	Knowledge of the mass . . . . .	87
4.2.1	Version 1 . . . . .	87
4.2.2	Version 2 . . . . .	89
4.2.3	Comparison of the two versions with other published devices . . . .	91
4.3	Carry over . . . . .	91
4.3.1	Version 1 . . . . .	92
4.3.2	Version 2 . . . . .	93
4.3.3	Comparison of the two Versions with published devices . . . . .	94
4.4	Sample transfer time . . . . .	95
4.4.1	Version 1 . . . . .	95
4.4.2	Version 2 . . . . .	95
4.4.3	Comparison of the two Versions and the literature . . . . .	96

4.5	Amount of cleaning liquid . . . . .	96
4.5.1	Version 1 . . . . .	97
4.5.2	Version 2 . . . . .	97
4.6	Modification of the sample volume . . . . .	97
4.6.1	Version 1 . . . . .	97
4.6.2	Version 2 . . . . .	98
4.6.3	Comparison of the two versions . . . . .	98
4.7	Installation . . . . .	98
4.8	Other features . . . . .	98
4.9	Conclusion . . . . .	100
<b>5</b>	<b>Literature</b>	<b>102</b>
<b>6</b>	<b>Appendix</b>	<b>108</b>
<b>7</b>	<b>Manual</b>	<b>108</b>
7.1	Parts of the Device . . . . .	108
7.2	Sampling Device . . . . .	109
7.2.1	Set-Up . . . . .	109
7.2.2	User Interface . . . . .	111
7.2.3	Sampling . . . . .	111
7.2.4	Cleaning . . . . .	112
7.3	Software . . . . .	112
7.3.1	Installation . . . . .	112
7.3.2	Overview . . . . .	114
7.3.3	Establishing a connection . . . . .	114
7.3.4	Measure values . . . . .	116
7.3.5	Adapting the Sequence . . . . .	117
7.3.6	Calibration . . . . .	120
7.4	Trouble shooting . . . . .	121

## Symbols, Abbreviation

**A** ... Amplification

**ADC** ... Analog-Digital Converter

**AV** ... Air Valve

**B** ... Integer Value

**BSD** ... Berkeley Software Distribution

**C** ... Capacitor

**CO** ... Carry Over

**D** ... Diode

**GPL** ... General Public License

**IAmp** ... Instrumentation Amplifier

**IC** ... Integrated Circuit

**IDm** ... Inner Diameter (by tubes)

**IDE** ... Integrated Development Environment

**ISR** ... Interrupt Service Routine

$\mu\mathbf{C}$  ... Microcontroller

$m_{scale}$  ... Mass measured with a analytic balance

$m_{device}$  ... Mass measured by the sampling device

**OD** ... Optical Density

**ODm** ... Outer Diameter (by tubes)

**OP** ... Operational Amplifier

**OS** ... Operating System

**PCB** ... Printed Circuit Board

**R** ... Resistor

**RV** ... Reactor Valve

**SV** ... Sample Valve

**SPI** ... Serial Peripheral Interface

$t_{cleaning}$  ... Cleaning Time

$t_{fill}$  ... Filling Time

$t_{release}$  ... Release Time

$t_{sampling}$  ... Sampling Time

**U** ... Voltage

**USB** ... Universal Serial Bus

**VV** ... Vacuum Valve

**VC** ... Volumetric Cell

**WV** ... Waste Valve

# 1 Introduction

## 1.1 Why fast sampling

The phenotype of a cell is characterized by the levels of enzymes and metabolites representing the active reaction network. This network is very complex and for *Escherichia coli* for example, there are more than 1000 enzymatic reactions with over 900 metabolites involved. For energy production and cellular growth alone 193 reaction paths are known. [56] Consequently determination of intracellular metabolites is important to identify phenotype and metabolite relationships. Over the last years intracellular metabolite analysis has been developed to an important tool to identify metabolic bottlenecks in microbial-based processes or health-associated biomarkers for medical application. This process can lead to future diagnostics and new pharmaceuticals.

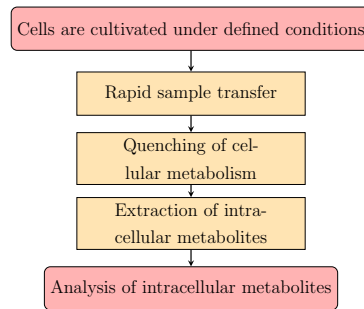


Figure 1: Working steps essential in the determination of intracellular metabolites

To gain information about the composition and levels of intracellular metabolites a sophisticated sample preparation procedure is carried out. As shown in Figure 1 this procedure involves 5 steps.

First a cell culture is grown in a defined environment. For batch analyses a defined amount of substrate is added which is then consumed by the cells. For continuous cultivation the environment is kept in a steady state. And for dynamic analyses the steady state is altered by changing one parameter of the environment. This could be for example a glucose injection or a change in the oxygen flow rate. After this alteration, samples are drawn in defined intervals. With this procedure the metabolic response of the cells can be monitored on the level of intracellular metabolites in the cells. [33]

Due to the high intracellular conversion rates ( $1mMs^{-1}$  for Adenosintriphosphat (ATP) [9]) and low concentrations of the metabolites ( $1mM$  for ATP [9]) the sample transfer from

the reactor has to be fast and an instantaneous deactivation of the cellular metabolism is necessary. This deactivation is called quenching and is done by mixing the drawn sample with a so called quenching solution. Broadly accepted solutions are cold methanol [22, 56, 61] or liquid nitrogen [14, 21].

In a next step the metabolites are extracted from the cell. This could be done by using high temperature, extreme pH, organic solvents, mechanical stress or a combination of these options [62]. Alternatively the sample could also be deactivated and extracted simultaneously by using perchloric acid [18, 57].

Finally the obtained metabolite extracts are analyzed by high performance liquid chromatography (HPLC) techniques coupled to mass spectrometry.

This master thesis focuses on the first part of the sample-work up - the sampling.

To obtain a reliable sample 4 factors are critical.

- First of all the transfer of the sample from the reactor has to be fast. Therefore if the sampling takes too long, metabolite levels will not be representative.
- Furthermore, contamination of a drawn sample, with liquid from a previous one, has to be avoided. This contamination is called carry over (CO).
- Knowledge of the exact sample volume transferred from the cultivation vessel is vital to determine levels of intracellular metabolites without bias, therefore the sampling volume must be known or reproducible.
- The metabolism of the cells must be inactivated instantly, therefore the sample and the quenching solution must be mixed during or at the end of the sampling procedure.

## 1.2 Fast sampling approaches

A commonly used method is to draw the sample manually by means of a volumetric pipette. For this purpose the cultivation vessel is opened and a defined volume of fermentation/cultivation broth is transferred to a flask containing the quenching solution. This flask is then closed and shaken to mix the sample with the quenching solution. This method does not need any special installation but has some disadvantages:

- The reactor has to be opened to draw the sample. This can lead to contamination of the content. For example for anaerobic cultivation a contamination of the culture with air has to be avoided.
- The sample transfer time depends highly on the skills of the person who effects the transfer. This limits reproducibility. [3]
- Also the amount of the sample drawn could vary among different users.
- Due to handling mistakes, it is possible that the sample touches the wall of the Falcon-tube before entering the quenching solution. This poses the issue that the the sample could create ice crystals, which can lyse the cell and thus the metabolites will leak into the quenching solution, which will results in too low metabolite levels. [3]

In order to address these issues and to fulfill the previously discussed requirements fast sampling methods were developed.

Four different main types of rapid sampling approaches can be distinguished. [15]

- **Valve with minimum dead space**

In this first approach the sample is drawn through only one valve and therefore the dead space of the whole system is minimal. [3,29,41,57] The valve can be mounted on top, bottom or on the side of the reactor. The sampling vessel contains a quenching liquid and is evacuated with vacuum. Once the tube is docked onto the valve, the valve opens automatically [3, 29] or manually [41, 57] and the liquid is transferred into the tube.

The amount of transferred liquid depends on the duration the valve is opened and the pressure difference between reactor and tube. Therefore the sampled volume can vary.

If the valve is mounted on top of the reactor, no modification of the reactor is required, but the sampling vessel has to be specially designed to allow the sampling liquid to enter the tube from the bottom. [41,57]

Mounting the valve on the side or bottom of the reactor has the advantage that no special tube is required, but the reactor has to be modified. [41,57]

- **Direct mixing with a quenching liquid in a sample coil**

For this approach the sample is mixed directly, after entering the sampling tube, with a quenching liquid (e.g. perchloric acid), which is kept at a temperature of  $-40^{\circ}C$ . This quenching liquid also extracts the metabolites from the cells. This

mix is then drawn into a sampling coil, which is frozen at  $-80^{\circ}\text{C}$ , once the sampling process has been completed. [10, 34]

The position of the liquid in the coil correlates with its sampling time stamp. Therefore it is possible to analyze fast dynamic behavior, by drawing only one sample and cutting the coil into parts of equal length. The exact time stamp for one specific part depends on the flow rate of the liquid. To generate the flow the reactor and the quenching liquid container are put under pressure. If this pressure varies the time stamp changes.

- **Sampling using a tubing system with valves**

In this approach the tubing system is first cleaned by drawing a defined amount of liquid from the reactor into a waste container. This is necessary to reduce carry over from the previous samples. After completion of the cleaning phase the liquid is transferred to the sample container, which contains a quenching liquid. [18, 22, 47]

Sample transfer is driven by pressure difference between the reactor and the sample container. To generate this difference two setups are possible. One option is the use of a vacuum pump, which is connected to the sampling vessel and the waste container. The other option is to put the reactor under pressure.

The sample container can be connected to the top, bottom or side [18, 22] of the reactor and the sample can be drawn through vacuum [18] or overpressure [22].

This method requires, due to the larger tubing system, a cleaning procedure. This increases the sampling time and the amount of liquid consumed.

- **Sampling using constant flow**

Using this method a line of sampling vessels is filled successively. Therefore a constant flow is generated by using hydrostatic pressure [56] or by using a peristaltic pump [9]. The sample container are changed by a valve system [9] or a step motor [56]. To reduce carry over a special geometry of the tubing system, which creates a turbulent flow, is used. [9]

If a peristaltic pump is used, the sample could be redrawn from the top, bottom or side of the reactor. By using hydrostatic pressure only sampling from the bottom is possible.

During the literature search it turned out, that there is no rapid sampler commercially available today. Another disadvantage of most published and patented instruments is that they are applicable only to a certain type of cultivation vessel and many of them even

require special installations to be built in cultivation vessels which typically ends up with irreversibly altered vessels. Consequently these sampling devices are not compatible with other cultivation vessels or vessel types which greatly reduce their general applicability in the lab.

However, the greatest disadvantage of all hitherto known sampling devices is that the exact sample volume is not known and can only be estimated. Gravimetric determination of the sample volume subsequent to the sampling event is not an option because metabolite samples must be processed as quickly as possible to preserve the metabolite state.

With the exception of [9] where cell broth is continuously sampled at a constant flow by using a peristaltic pump, sampling is driven by the overpressure and hydrostatic pressure present in the cultivation vessel. To increase the pressure difference between cultivation vessel and sample container, the sample container can be evacuated [3, 29, 57]. The flow rate of the cell broth through the tubing of the sampling device is largely determined by this pressure difference.

In addition fluid properties such as viscosity affect the flow rate and therefore the sample volume. Consequently changes in cultivation volume (due to fed batch operation and sampling; alters hydrostatic pressure;) and overpressure in the reaction vessel (by cell growth, increased aeration and CO<sub>2</sub> production) as well as differences in the negative pressure in the sample container (leakage, sample-to-sample variation) affect significantly the sampled volume.

Another source of variation in the sampled volume represents co-sampling of gas bubbles (air, nitrogen). As a consequence differences in sample volumes provoked by these changing process conditions are not recognized by current sampling devices and resultant metabolite concentrations are therefore afflicted with unknown uncertainty which eventually leads to false interpretation of results.

Furthermore as intracellular metabolite analysis is extremely expensive knowledge of the exact volume of sampled cell broth is therefore, from an economic point of view, essential to increase the number of reliable metabolite samples.

Based on this it was the intention to develop an automated rapid sampling device with which 1 mL (the typical volume used in current metabolite analysis) of cell broth can be selectively (little to no carry over from one to the next sample) withdrawn from any lab-scale reaction vessel in less than 1 sec and transferred into a flask containing an appropriate quenching solution with which the cell broth is mixed rapidly.

## 1.3 Quantification of the Volume

To improve the already known devices the volume of the sample should be quantified. Therefore a few options are discussed in this paragraph.

### Quantification of the volumetric flow rate

One option to quantify a volume ( $V$ ) would be the integration over its volumetric flow ( $\dot{V}(t)$ ).

$$V = \int_{t=0}^{t_{end}} \dot{V}(t) dt \quad (1)$$

To quantify the flow rate an optical sensor, a turbine or an ultrasonic sensor were discussed.

- **Optical Sensor:**

Optical determination of the flow rate is difficult due to the transparency of the sampled liquid. Furthermore, the occurrence of air-bubbles can severely corrupt the measurement.

- **Turbine:**

When using a turbine for the quantification the cleaning would be much more complex and contamination would pose an issue.

- **Ultrasonic:**

The sensors for determination of the flow-rate based on the Doppler-effect are very expensive for the needed flow rate range (approximately 1ml/sec). For example the Atrato Ultrasonic 2-500 ml/min flow sensor (Atrato, United Kingdom) costs EUR 803 at RS-Components. [45]

Due to these restrictions a direct measurement of the flow rate is not possible.

### Quantification of the volume based on the pressure difference

An other option to quantify the volume would be through the pressure difference in the tubes. According to Hagen-Poiseuilles law it is possible to calculate the flow-rate of a Newtonian liquid as follows:

$$\frac{dV}{dt} = \frac{\pi \cdot r^4 \cdot \Delta p}{8 \cdot \nu \cdot l} = \frac{\Delta p}{R} \quad (2)$$

To use this equation it is necessary to know the pressure difference  $\Delta p$ , the viscosity  $\nu$  of the liquid, the radius  $r$  and the length  $l$  of the tubes.

The radius is not constant over the whole system and therefore it is hard to calculate the flow rate by using the geometric dimensions. Furthermore, there is an extremely strong dependence on the radius of the tube ( $r^4$ ). Changes in the geometry will lead to strong variations of the flow.

Instead of calculating the Resistance  $R$  using the geometry, it is possible to determine it by drawing a sample. For this the pressure difference, the sampling time and the volume of the sample has to be measured and by using the following equation the resistance  $R$  can be calculated.

$$R = \frac{t \cdot \Delta p}{V} \quad (3)$$

With this empirically determined resistance it is possible to calculate the flow rate for future drawn samples, if the pressure difference is known.

This poses the issue, that the pressure at the entrance of the sampling system and at the end of the sampling system has to be measured. For the end it is quite easy to install a pressure sensor next to the sampling vessel, but for the entrance point a pressure sensor would have to be installed inside the bioreactor.

Also differences in the hydrostatic pressure (filling level of the bioreactor, position of the sampling vessel) have to be considered.

Furthermore the pressure sensor has to be exact and fast enough to monitor vacuum fluctuations generated by the pump.

Beside these issues, the sampled liquid contains cells and therefore the rheological properties of the liquid deviates from those of an the ideal Newtonian fluid. Due to the low cell density, this effect is negligible.

Furthermore this calculation works only for a steady state, which does not apply most of the time.

Despite these caveats the Hagen-Poiseuilles law is still used for some approximations and for identifying important factors for system optimization.

### **Quantification of the volume based on a volumetric cell**

Similar to the pipetting of a sample, the underlying idea of this method is to fill a defined volume in the system, which is then emptied into the sampling tube.

The challenge of this method is to guarantee a complete filling and draining of the volumetric cell. The second downside is the inability to easily change the amount of the sampled volume.

### **Quantification of the volume based on determination of mass**

Another approach is to allow for a variation of the sampled volume and to determine the real volume by a mass measurement.

To draw a sample, the sampling time is chosen according to the volume desired.

Given, that this method is very sensitive due to pressure changes and other factors, the mass after sampling is measured. Using this information it is possible to accept a higher variance of the sampled volume, which can be corrected for the analysis of the sample.

Assuming the liquid is nearly as dense as water, the water density is used for the volume calculation.

## **1.4 Requirements**

The device developed should fulfill the following requirements:

- For easy installation of the device, it should work with vacuum and withdraw the sample from top of the reactor.
- The reproducibility of the volume and mass should be lower than 1%, which is comparable to a manual sampling by means of a pipette.
- The carryover of solutes between subsequent samples should be lower than 5%. Therefore the dead volume of the device has to be small enough to allow the system to be cleaned.
- The sampling time should be lower than 1s.
- The amount of liquid required to prepare the system for the sampling ought to be minimized.
- The device should be user friendly.

- For every sample a time stamp should be created.
- The sampled volume should be monitored.
- It should be possible to vary the sampling volume within a range of 0.5ml to 10ml.

## 1.5 Design decision

For this master thesis two different designs were created and validated.

For both designs the approach with the tubing system was used. The reason for this decision is, the possibility to draw the sample from the top of the bioreactor, without any modification of the reactor. An other advantage of this setup is that vacuum can be used to draw the sample.

To get knowledge about the volume of the drawn sample two different methods for quantification of the sampled volume were used.

For the Version 1 a volumetric cell was used and for the Version 2 the sampled mass was measured using a weight-sensor.

## 1.6 Development Tools

To accomplish the goal of this master thesis following tools were used.

### 1.6.1 Electronic Circuit Simulation

LT-Spice (Linear Technology, Milpitas, USA) [54] is a freeware tool based on SPICE (University of California, Berkeley, USA) [42] for simulation of electronic circuits. The underlying SPICE simulator was devolved under the BSD-License.

This tool is capable of Transient Analysis, AC-Analysis, DC-sweep and other analysis. It is also possible to create a Montecarlo-Simulation to evaluate the drift or the systematic error through component tolerances.

Another advantage of this tool is the availability of different models. A lot of component sellers like Texas Instruments or Analog Devices offer simulation models of their components for PSpice and LTSpice.

### **1.6.2 PCB Design**

To draw the schematic and to design the PCB, Eagle 6.4 light (Cad-soft Computer GmbH, Pleiskirchen, Germany) [48] was used.

The freeware Version of this tool allows to designing PCBs with two layers and an area of 100 x 80 mm.

For complexer PCBs and the option for auto-routing the commercial version would have been required.

### **1.6.3 Firmware-Development**

To develop the firmware for the micro controller Eclipse 4.5 (Eclipse Foundation, Ottawa, Canada) [17] was used. It is an IDE published under the Eclipse Public License and supports a lot of programming languages like JAVA, C or C++. It is also possible to add modules for developing, compiling and flashing firmware for ARM processors like the STM32F4 series(STMMicroelectronics, Swiss) [53], which was used for this project.

Eclipse has the advantage of platform independency and offers, like many other IDEs, code highlighting, intelligent code completion and real time syntax check.

As compiler and Linker Sourcery Codebench Lite Edition (Mentor Graphics, Wilsonville, Oregon, USA) [20] was used. It allows to compile C and C++ code for many micro-controllers based on ARM-architecture like the used STM32F4.

With the "GNU ARM Eclipse Plug-in" it is achievable to link this compiler with Eclipse.

As last part of the toolchain a software for flashing the firmware to the microcontroller is needed. For this stlink (Stlink project) [49], which requires libusb [36], is used. This tool is distributed under the BSD License and can be linked with Eclipse.

The whole manual for setting up the toolchain can be found on [microcontroller.net](http://microcontroller.net) [39].

### **1.6.4 Software Development**

To create a software for the PC, which is capable to communicate over USB with the device, JAVA (Oracle Corporation, Santa Clara, USA) [6] was chosen as the programming language. The reason for this decision is its platform independency. It also offers a garbage

collector, which deletes unused objects, so that the developer does not have to worry about memory management.

With the Rxtx library [43] it is possible to communicate over a serial interface with an other device. This library is licensed under the LGPL.

For the-layout SWING was used, which is the default GUI-layout-description-language of JAVA. The elements of the SWING language are rendered like the JAVA code in the JAVA-Runtime-Environment.

As the development environment of the PC-Software NetBeans IDE 8.0.2 (Oracle Corporation, Santa Clara, USA) [7] was chosen because of its included GUI-Designer. It is licensed under the GPLv2 and CDDL, works with JAVA, is platform independent and offers, like many other IDEs, code highlighting, intelligent code completion and real time syntax check.

### **1.6.5 Matlab**

For simulating the model of the sampling devices Matlab (MathWorks, Natick, Massachusetts, USA) [37] was used. Through the possibility to gather data from a serial interface, it was also used to plot values from the weight and the pressure sensor in real-time to analyze them.

## 2 Methodes and materials

### 2.1 Materials

Components and tubes used to create the tubing system of the device are collected in Table 1. For the sampling device also different sampling tubes (Table 2) were used.

Part	Type	quantity	Supplier
Vacuum pump	vaccum: 1000Pascal	1	no specified
Vacuum bottle	volume 1L, PP, incl. cap with 3 connections	2	Bartelt, AT (21261000)
Tubing for vaccum	red natural rubber, IDm:6mm, ODM:16mm	1m	Bartelt, AT (9205806)
Tubing for sample	silicone tube talkumier, RAUSIL FG, IDm: 1 mm, ODM: 3 mm	1m	Bartelt, AT (9205222)
Pinch valve	12V, 300mA	5	unknown
Y-Connectors	ODm: 1.6mm	9	Bartelt, AT (9207831)
Docking seal	made of Klass 4 Dental Turbosil Dupli- ersilikon	1	ZPP, AT (13203080)
Needle	BD Microlance 3, ODm: 1.2mm, length: 40mm	2	Bartelt, AT (7660927)
Luer Lock	Luer Lock P336.1, ODm: 1.5mm	2	Bartelt, AT (7400904)
Volumetric pipette 1ml	IDm: 3.3mm length: 130mm, used for the volumetric cell	1	Bartelt, AT (9273259)
Rain-X			ITW Global Brans, USA
Silicon glue	UHU 46735, 80 ml		UHU GmbH and Co. KG, Germany

Table 1: List of material for the pipe system

Part	Type	Supplier
$ST_{ST275}$	Steel tube, IDm: 1.8 mm, ODm: 3 mm ,length: 275mm	unknown
$ST_{ST275-H}$	Steel tube, IDm: 1.8 mm, ODm: 3 mm ,length: 275mm, second inlet at the bot- tom on the side	unknown
$ST_{FEP270}$	Fluorinated ethylene propylene IDm:1.6mm, ODm:3.18mm, length: 270mm	Roth, DE
$ST_{FEP135}$	Fluorinated ethylene propylene, IDm:1.6mm, ODm:3.18mm, length: 135mm	Roth, DE

Table 2: List of the different sampling tubes used

Equipment and solutions used to verify the sampled mass and the carry over of the device are listed in tables 3 and 4.

Part	Type	Manufacturer
Spectrometer	DU800	Beckman Counter Inc, USA
Analytic balance	Kern 770	Kern und Sohn , Germany
Falcon-tubes	50ml	Sarstedt, Germany
Fermenter	LabForce 2	Infors HT, Swiss
Fermenter	LabForce 3	Infors HT, Swiss
Erlenmeyer flask	300ml	Schott DURAN Produktions GmbH & Co. KG, Germany
Pipette	Biomaster 1000 $\mu$ l	Eppendorf AG, Germany
Pipette tips	1000 $\mu$ l	Eppendorf AG, Germany
Vortex Shaker	Reax Top	Heidolph Instruments GmbH & Co. KG, Germany
Temperatur sensor	P0K1.232.3K.A.400-4.M.U.S	IST AG, Swiss
Multimeter	Keithley 2000	Keithley, USA
USB-GPIB Interface	82357B	Agilent Technologies Inc., USA
Soldering iron	20W Ersa Multi-Pro	ERSA, Germany

Table 3: List of equipment used for verification

Name	Components
<i>TP</i>	Tap water
<i>TP – CR</i>	60 mg of Congored solved in 1l of TP.
<i>PBB</i>	Potassium phosphate buffer (PBB) with 100 mM and a pH value of 7.0
<i>PBB – CR</i>	60 mg of Congored solved in 1l of PBB.

Table 4: List of the different solutions used to verify the device

For the verification with biological cells *Saccharomyces cerevisia* (CEN.PK 113 – 7D[59], supplied by the Institute of Biotechnology and Biochemical Engineering at TU-Graz), Agar-Agar (supplier: Carl Roth GmbH + Co. Kg, Germany) and the mineral medium as described in table 5 were used.

Solution	Component	$gL^{-1}$	
$A_1$	Glucose	20.0	
$B$	$KH_2PO_4$	14.4	
	$(NH_4)_2SO_4$	5	
	$Mg_2SO_4 \cdot xH_2O$	0.5	
$C$	Vitamins	D-Biotin	0.00005
		Ca-Pantothenate	0.001
		Thiamine-HCl	0.001
		Pyridoxine-HCl	0.001
		Nicotinic acid	0.001
		<i>p</i> -Aminobenzoic acid	0.002
		<i>m</i> -Inositol	0.025
$D$	Trace elements	$FeSO_4 \cdot 7H_2O$	0.003
		$ZnSO_4 \cdot 7H_2O$	0.0045
		$CaCl_2 \cdot 6H_2O$	0.0045
		$MnCl_2 \cdot 2H_2O$	0.00084
		$CoCl_2 \cdot 6H_2O$	0.0003
		$CuSO_4 \cdot 5H_2O$	0.0003
		$Na_2MoO_4 \cdot 2H_2O$	0.0004
		$H_3BO_3$	0.001
		KI	0.0001
		$Na_2EDTA$	0.015

Table 5: **Components of the mineral medium (provided by I.B.B.)** Concentrations relate to the final composition.

## 2.2 Basic device

Both approaches pursued were based on a common tubing system. A detailed description is depicted in figure 2. This basic system was composed of vacuum pump, 5 valves, a waste and a sample container, a sampling tube and the tubing. Additionally Version 1 has a volumetric cell for quantification of the sampled volume and Version 2 provides a weight sensor for measurement of the sampled mass.

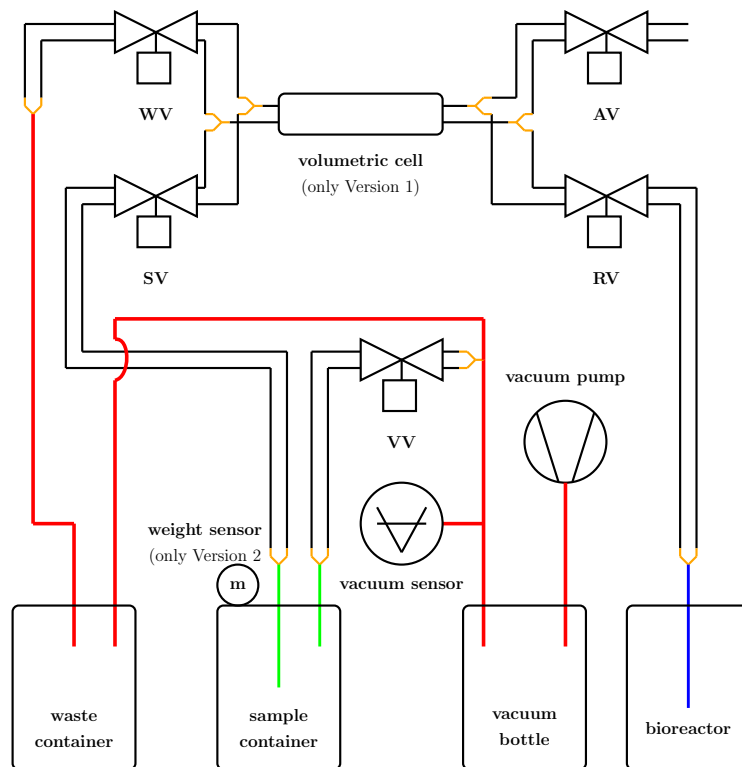


Figure 2: **Schematic of the tubing for Version 1 and Version 2.** blue...sampling tube, red... tubing for the vacuum, black...tubing for the sample, green...needle, orange...Y-Connectors, WV...Waste valve, AV...Air valve, SV...Sample valve, RV...Reactor valve, VV...Vacuum valve, Version 1 uses the volumetric cell and Version 2 measures the mass with the weight sensor.

To avoid contact between the sample and the valve, pinch valves were used. This avoids contamination of the valves and reduces the dead space.

To increase the flow-rate of the sample, silicon tubes with the largest diameter (ODm = 3mm), which is compatible with the pinch valves, are used. Also every connection is routed with two silicon tubes. For connecting the tubing only Y-connectors were used.

The vacuum for the system was generated by an old refrigerator compressor, which is capable of generating a vacuum of about 10,000 Pascal. To ensure a constant vacuum, vacuum bottles were used to buffer the vacuum.

The waste and the vacuum container are both vacuum bottles.

The sampling tube  $ST_{ST275}$  (Table 2) was used for the Version 1 of the device and for Version 2 different sampling tubes were tested.

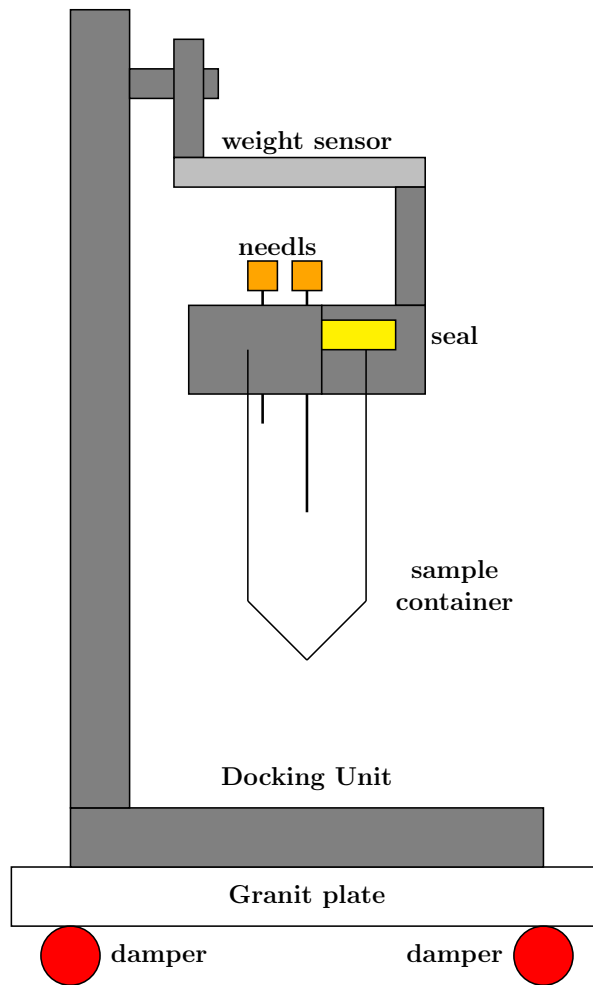


Figure 3: Docking unit

The docking unit (figure 3) consists of a housing made of hard plastic, a silicon seal and two needles. Through the right needle the sample is drawn into the sample container. The left ones is for creating a vacuum in the sample container. These needles are connected over Luer-Lock connectors to the tubing system. For Version 2 the docking unit stands on a granite plate and has a weight sensor.

## Volumetric cell



Figure 4: Volumetric cell

The volumetric cell is made of a 1ml volumetric pipette (Table 1), which was cut on both sides to a pipe with the length of 130mm and a diameter of 3.3mm (Figure 4). This results in a volume of 1.11 ml. To reduce friction for the liquid, the inner part of the tube was coated with Rain-Ex (Table 1). Then the volumetric cell was mounted with silicon glue (Table 1) to the tubing system.

### Setup for Version 2

For Version 2 of the sampling device the mass of the sample is measured and therefore the docking unit (Figure 3) has to be insusceptible against mechanical perturbations from the environment. Therefore a stone plate, lying on some vacuum pipes (Table 1), which work as springs, was used to reduce the mechanical coupling between the desk and the docking unit.

To avoid the transfer of mechanical perturbations over the pipes, the pipes are strain-relieved before entering the head. Also only one valve changes their state at the same time. If more than one valve has to be operating, a short delay (100ms) is used, to reduce the vibration on the pipes.

Due to the fact, that air has a mass, it is important, that the vacuum in the tube remains stable throughout the sampling sequence. To accomplish this a small vacuum buffer (approximately 10ml) is added next to the head.

## 2.3 Sampling procedure

A sample is drawn with the device through a list of handling steps shown in figure 5.

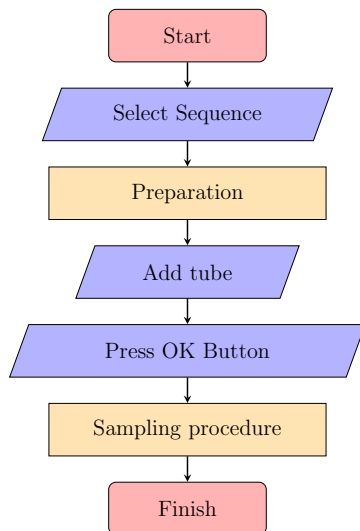


Figure 5: Handling of the sampling device. Blue rhombus ... user interaction, the orange rectangle ... Steps executed by the device, red rectangle ... start and stop state

### **Start:**

All valves are closed and the system is ready to be operate.

### **User select the sequence:**

The user selects the timing protocol on the device's GUI.

### **Preparation:**

The vacuum valve is opened to allow the user to docks a sample container to the docking unit.

### **Add tube:**

The user connects the sample container to the docking unit. The sample container is then kept in position due to the vacuum.

### **Press OK Button:**

The user presses the green (OK) button to start the sampling procedure.

### **Sampling procedure:**

This step is different for the two versions of the device. It contains the cleaning of the system and the sampling into into the sample container, but this is described later in detail (For Version 1 table 6 and for Version 2 table 7).

### **Finish:**

After the sampling is finished all valves are closed and the sample container can be removed.

## Sampling Procedure for Version 1

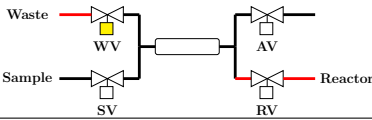
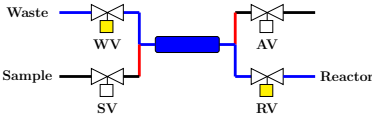
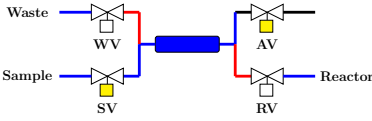
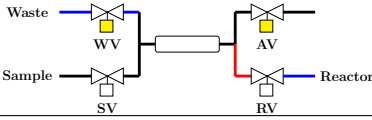
Step Number	Action	Valve state	Time ms	Remarks
1	Preparation		3000	Air is removed from the volumetric cell.
2	Cleaning		filling time 1000-5000	Tubing is cleaned and the volumetric cell is filled.
3	Filled 1	WV is closed	100	Filling stops.
4	Filled 2	RV is closed	100	The volumetric cell is loaded.
5	Sampling 1	SV is opened. AV stays closed.	100	
6	Sampling 2		release time 1000-5000	Sample is transferred from the volumetric cell to the sample container.
7	Empty	SV is closed. AV stays opened.	100	Volumetric cell is empty.
8	Air Cleaning		1000	Dead volume at WV is emptied
9	End 1	AV is closed.	100	
10	End 2	WV is closed.	100	

Table 6: **Timing protocol for Version 1** In the images the blue area marks the flow of the sample. The red are marks dead volumes and the yellow valves are opened. The white ones are closed.

## Sampling procedure in Version 2

Step No.	Action	Valve state	Time ms	Remarks
1	Preparation		3000	Waiting for the vacuum to get ready and the vibrations to decay.
2	DAQ 1		1500	Reference measurement of the mass.
3	Cleaning 1		cleaning time 750	Tubing is cleaned with liquid.
4	Cleaning 2	RV is closed	50	Delay for valve switching
5	Cleaning 3		200	Tubing is cleaned with air.
6	Delay 1	AV is closed	50	Delay for valve switching
7	Delay 2	WV is closed	50	Tubing is empty.
8	Sampling 1	RV is opened	50	Delay for valve switching
9	Sampling 2		sampling time 200-5000	Transfer of the sample into the sample container
10	Sampling 3	RV is closed.	50	Delay for valve switching
11	Sampling 4		200	Flushing the remaining fluid into the sample container with air
12	Waiting	SV is closed.	waiting time 1000	Waiting for vibrations to decay
13	DAQ 2	WV is opened.	1500	Mass measurement
14	End 1	AV is closed.	100	
15	End 2	WV is closed.	100	

Table 7: **Timing protocol for Version 2** In the images the blue area marks the flow of the sample. The red are marks dead volumes and the yellow valves are opened. The white ones are closed. DAQ... Data Acquisition

## 2.4 Electronical Hardware and Firmware

### 2.4.1 Overview

The hardware is divided into three main components, shown in figure 6. First there is the main module with the User Interface. It contains the power supply, the display, the keyboard and the STM32F4 Discovery board with the firmware. The two other modules are the sampling stand with the pressure and weight sensor and the valve box with the valves.

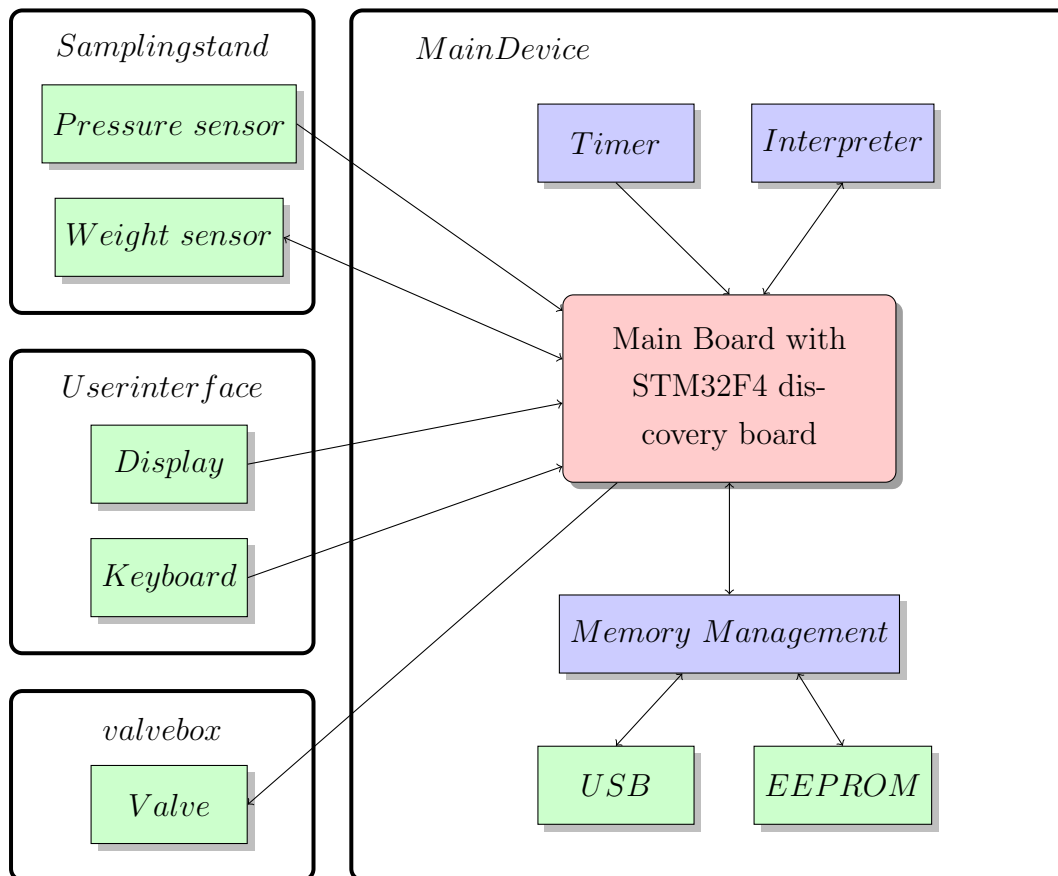


Figure 6: **Schematic of the firmware and hardware modules.** The green boxes are hardware parts with a firmware driver and the blue parts are firmware components. The red block symbolizes the main board with the STM32F4-Discovery board and the main function of the firmware, which includes a state machine.

Figure 6 shows the firm and hardware concept. The main board contains the STM32F4-Discovery board with a STM32F407VGT6 micro-controller, which operates on a clock-frequency of 168 MHz. All other hardware components are connected via the main board to this module.

The STM32F4-Discovery board is supplied with 5 V DC and generates a voltage of 3V DC with a line regulator for the micro-controller [51]. The Discovery board provides an USB Port for communication and one for flashing the micro-controller.

The firmware for the microcontroller is written in C and compiled with Sourcery CodeBench Lite Edition for ARM EABI.

**2.4.2 Power Supply**

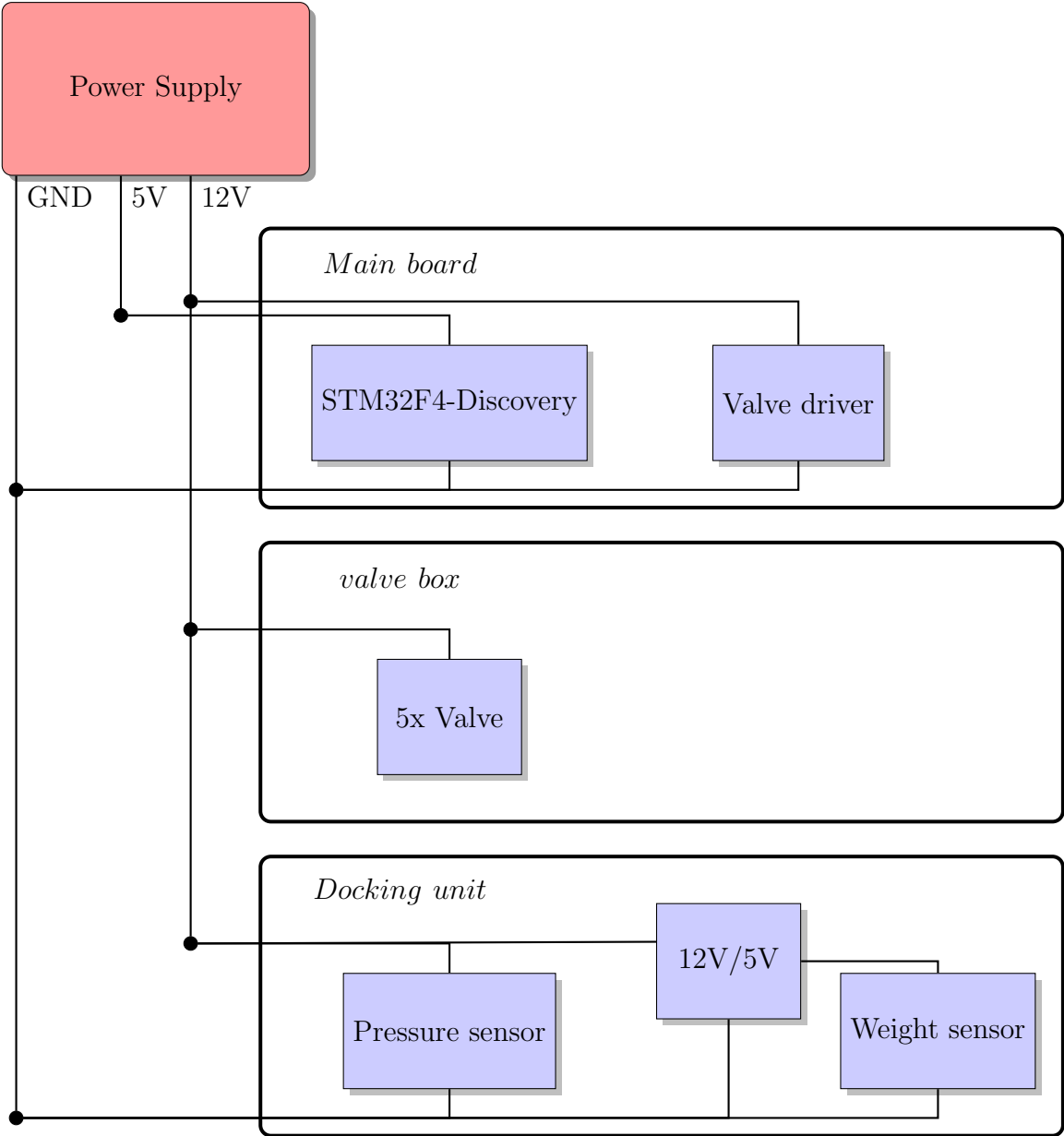


Figure 7: Schematic of the power supply

A PC-power supply is used to generate the 5V and the 12V needed for the electronic components (Figure 7). To enhance the stability of the outputted 12V two additional capacitors with  $100\mu F$  are added between the 12V supply and the ground line.

To improve the stability of the power supply for the weight sensor a linear regulator for 5V is added. For the mass measurement also 2 voltage references are used.

### 2.4.3 Valve and Valve Driver

The valves work with 12V DC and need a current of approximately 300mA in the closed state. In the opened state no power is consumed. During switching of the valve the peak current can be as high as 1.5A.

Through the fact, that the Micro-controller is only capable of outputting a voltage of 3.3 V and a current of 25mA, a driver is needed to activate the valves.

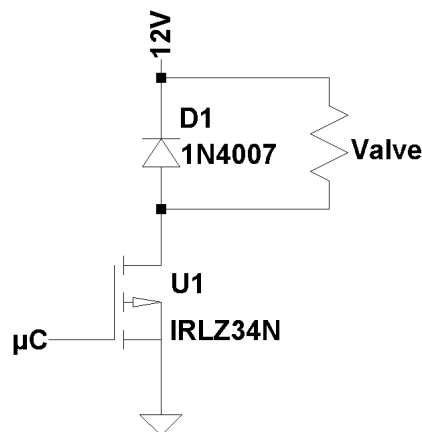


Figure 8: Low side switch as valve driver

Figure 8 shows the schematic for the valve driver. The component IRLZ34N (U1) is a N-Channel Power MosFET, which is capable of a drain-source voltage of 55 V and a drain-source current of 30 A [44]. If a gate-source voltage of 4V is applied to the component the resistance of the drain-source path is drops below 0.060 Ohm and a current can flow. According to the datasheet a voltage of 3V results into a possible current of 10A. So it is possible to toggle the valves with an output of 3.3V on the micro-controller.

Given the fact, that the pinch valve works like an electromagnet, it has not only a resistance but also an inductance. To prevent high voltage spikes after switching off, the freewheeling diode 1N4007 (D1) [60] is needed.

#### 2.4.4 Display

A LCD-Display (DEM 20485, Display Elektronik GmbH, Germany) with 4 rows and 20 symbols per row is used [19]. The display and the backlight LED are supplied with 5 V. The contrast level adjustment is done with a potentiometer with 10kOhm between VCC and GND (Figure 9).

For communication the display has eight data-lines, a read/write-Pin, a Register-select-Pin and an enable Pin. To communicate with the display it is possible to use all eight data-lines or only four data-lines. The method with four data-lines is chosen to reduce the amount of micro-controller pins needed. Also the Read/Write-Pin is hardwired to GND to set the display in permanent write-mode. The data lines are connected to Port PD0 to PD3, the register select pin to Port PD6 and the enable pin is connected to PD7.

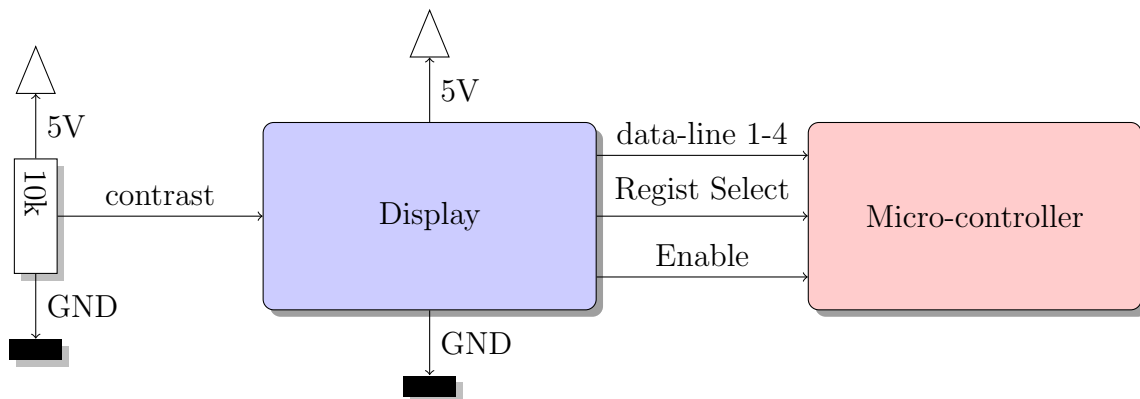


Figure 9: Connection of the display

The firmware configures the display on startup in four data-line mode and hides the cursor. To print a text on the display the firmware first sends the instruction to set the cursor to the correct position and after this the string is transferred using ASCII code.

### 2.4.5 Keyboard

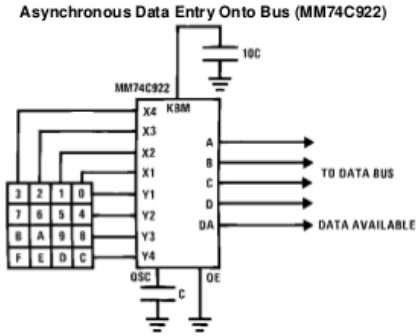


Figure 10: Keyboard schematic with MM74C922 [58].

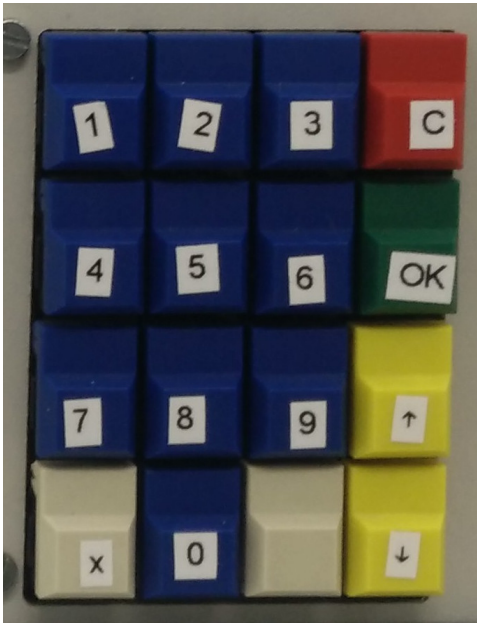


Figure 11: Keyboard Layout with the green OK-Button, a red cancel-Button, an up- and a downscroll button, 3 special buttons and the buttons 1-9.

The keyboard consists of 16 buttons as shown in figure 11. These buttons are connected over the driver IC MM74C922, to the micro-controller (Figure 10).

The driver IC works in asynchronous mode, that means if a valid key is pressed an interrupt on the data available line is triggered and the key number is outputted on the 4 data-lines immediately [16]. Another advantage of the MM74C922 is the fact, that the keys are debounced by the IC.

In the firmware the keyboard module checks the interrupt-line (GPIO Pin B15) and the 4 data-lines (GPIO Pins PB11-14) periodically and signals the state machine if a valid key-press has occurred.

## 2.4.6 Pressure sensor

For measuring the vacuum of the system a pressure sensor is needed. As sensor the 26PCC (Honeywell International Inc.,USA) was chosen. This sensor has a pressure-range of  $\pm 103421$  Pascal (15 PSI) in relation to the atmospheric pressure. Due to the fact, that the sensor is an unamplified wheatstone bridge, an amplifier is needed. Figure 12 shows the schematic of the amplification.

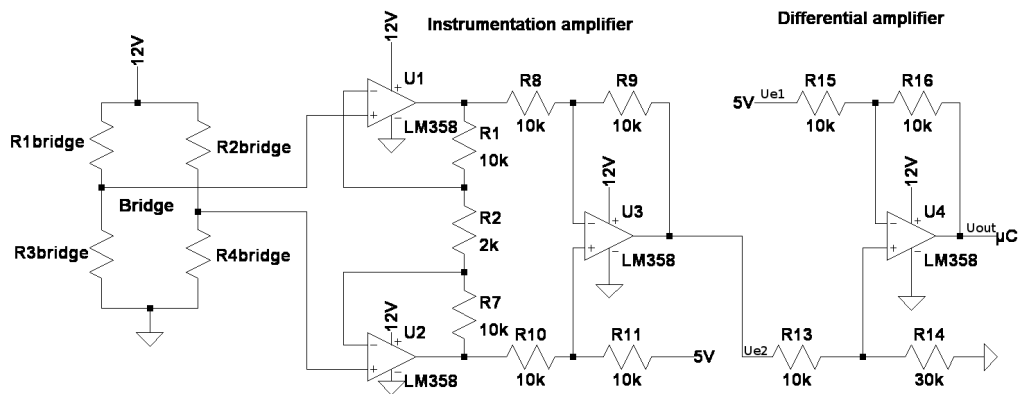


Figure 12: Pressure sensor

The first part, the wheatstone bridge, is the pressure sensor. The signal of the pressure sensor is then amplified with an instrumentation amplifier circuit. The output of the amplifier is inverted and relative to 5 V. With the amplifier U4 and the network R13 - R16, a differential amplifier, the offset is set to 2.5 V and the signal is amplified and inverted.

**The following components where used for the measurement:**

Pressure-sensor (26PCC [24]):

- Pressure-range:  $P_{Bridge;range} = 103421 Pa$
- Supply-Voltage:  $U_{Bridge;supply} = 12V$
- Maximum output span:  $U_{Bridge;span} = 100mV$
- Linearity:  $\Delta U_{Bridge;nonlinear} = 0.3mV$

- Span drift:  $\Delta U_{Bridge;span} = 0.9mV$
- Offset drift:  $\Delta U_{Bridge;offset} = \pm 0.5mV$

Amplifier (LM358 [26]):

- Supply-Voltage:  $U_{Amp;supply} = 12V$
- Offset-Voltage:  $U_{Amp;offset} = 2mV$
- Offset-Voltage drift:  $\Delta U_{Amp;drift} = 7\mu V/^{\circ}C$

ADC (internal ADC of STM32F407 [50]):

- Reference-Voltage:  $U_{ADC;ref} = 3V$
- Resolution:  $12bit$
- Dynamic Range:  $0 - 3V$

### Transfer-function:

First the amplification of the instrumentation amplifier consisting of  $U_1 - U_3$  is calculated.

The resistor  $R_2$  determines the gain. The resistors  $R_1, R_7, R_8, R_9, R_{10}$  and  $R_{11}$  are set to equal values to maximize the common mode rejection.

$$A_{inamp} = - \left( 1 + \frac{R_1 + R_7}{R_2} \right) = \left( 1 + \frac{10k + 10k}{1.5k} \right) = 14.33 \quad (4)$$

The 5V bias voltage at  $R_{11}$  shifts the output voltage of  $U_3$  at zero input to 5V. This level-shifting is necessary to allow negative bridge voltage to be amplified by only using a unipolar supply voltage for the amplifiers.

After the instrumentation amplifier the following signal is obtained:

$$U_{out} = U_{Bridge} \cdot A_{inamp} + 5V = U_{Bridge} \cdot 14.33 + 5V \quad (5)$$

This signal is applied by the differential amplifier  $U_4$ . Here a level-shifting by 5V is necessary to shift the amplified bridge voltage range to the dynamic range of the ADC (0 to 3V):

$$\begin{aligned}
U_{out} &= U_{e2} \cdot \frac{R_{15} + R_{16}}{R_{15}} \cdot \frac{R_{14}}{R_{13} + R_{14}} - U_{e1} \cdot \frac{R_{16}}{R_{15}} \\
&= (U_{Bridge} \cdot A_{inamp} + 5V) \cdot \frac{R_{15} + R_{16}}{R_{15}} \cdot \frac{R_{14}}{R_{13} + R_{14}} - 5V \cdot \frac{R_{16}}{R_{15}} \\
&= U_{Bridge} \cdot A_{inamp} \cdot \frac{(R_{15} + R_{16}) \cdot R_{14}}{R_{15} \cdot (R_{13} + R_{14})} + 5V \cdot \left( \frac{(R_{15} + R_{16}) \cdot R_{14}}{R_{15} \cdot (R_{13} + R_{14})} - \frac{R_{16}}{R_{15}} \right) \\
&= U_{Bridge} \cdot A_{inamp} \cdot \frac{(10k + 10k) \cdot 27.4k}{10k \cdot (10k + 27.4k)} + 5V \cdot \left( \frac{(10k + 10k) \cdot 27.4k}{10k \cdot (10k + 27.4k)} - \frac{10k}{10k} \right) \\
&= U_{Bridge} \cdot 21.00 + 2.32V
\end{aligned} \tag{6}$$

The bridge generates a voltage of 100 mV ( $U_{span}$ ) when the maximum pressure is applied. So it is possible to calculate the output voltage range for the amplifier.

For the minimum output the negative span is used:

$$U_{out;min} = -0.10V \cdot 21.00 + 2.32V = 0.22V \tag{7}$$

For the maximum output the positive span is used:

$$U_{out;max} = 0.10V \cdot 21.00 + 2.32V = 4.42V \tag{8}$$

The maximum output is higher than the dynamic range of the ADC, which has 3V, but since a vacuum should be measured, only the negative span matters. Also the maximum output is lower than the maximum input voltage allowed for the ADC pins, which is 5V. If no pressure is applied the ADC measures a voltage of 2.32V and so the microcontroller could detect if the amplifier is working correctly.

The internal ADC of the STM32F4 has a resolution of 12bit so the transfer-function of

the sensor with amplification and conversion can be calculated as followed:

$$\begin{aligned}
B_{adc} &= \frac{U_{out}}{U_{ADC;ref}} \cdot 2^{12} \\
&= (U_{Bridge} \cdot 21.00 + 2.32V) \frac{2^{12}}{U_{ADC;ref}} \\
&= \left( P \cdot \frac{U_{Bridge;span}}{P_{Bridge;range}} \cdot 21.00 + 2.32V \right) \frac{2^{12}}{U_{ADC;ref}} \\
&= \left( P \cdot \frac{-0.1V}{103421Pa} \cdot 21.00 + 2.32V \right) \frac{2^{12}}{3V} \\
&= P \cdot 0.0277Pa^{-1} + 3167.57
\end{aligned} \tag{9}$$

The transfer function describes a linear behavior with a gain of  $0.0277Pa^{-1}$  and a offset of 3167.57.

With the gain information it is now possible to calculate the minimal pressure resolution:

$$P_{min} = \frac{1}{0.0277Pa^{-1}} = 36.07Pa \tag{10}$$

This resolution is only theoretical. Due to nonlinearities and noise it may be worse.

In the firmware the ADC1 is used and the sampling-time for the ADC is set to  $1.7 \mu$  seconds without any averaging. When the function for getting the pressure is called, the micro-controller starts a conversion and waits for the result. The result is converted into a pressure value in Pascal and returned to the main function.

## 2.4.7 Weight sensor

### Components:

Voltage reference (AD586 [12]):

- Output-Voltage:  $U_{BRef} = 5V$
- Accuracy:  $\Delta U_{BRef} = 2.0mV$
- Temperature drift:  $\Delta U_{BRef;temp} = 2ppm/^{\circ}C$
- Noise:  $U_{BRef;Noise} = 4\mu V_{PP}$  (10 Hz Bandwidth)

Voltage reference (Ref5025 [28]):

- Output-Voltage:  $U_{ARef} = 2.5V$
- Accuracy:  $\Delta U_{ARef} = 0.05\%$
- Temperature drift:  $\Delta U_{Ref;temp} = 3ppm/^{\circ}C$
- Noise:  $U_{ARef;Noise} = 3\mu V_{PP}$  (10 Hz Bandwidth)

Bridge (Vishay Single Point Load Cell Model 1004 [59]):

- Maximum load:  $m_{max} = 300g$
- Voltage Sensitivity:  $1mV/V$
- Gain:  $A_{Bridge} = \frac{1V}{1000V} \cdot \frac{1}{300g}$
- Accuracy:  $\Delta V_{Bridge} = 0.0067\%$
- Output Impedance:  $R_{Bridge} = 350\Omega$

Instrumentation amplifier (LMP8358 [25]):

- Gain:  $A_{IAmp} = 50$  (set per SPI)
- Gain-Error:  $\Delta A_{IAmp} = 0.03\%$
- Input Offset-Voltage:  $U_{IAmp;Offset} = 1\mu V$
- Input Offset Voltage Temperature drift:  $\Delta U_{IAmp;Offset} = 50nV/^{\circ}C$
- Gain drift:  $\Delta A_{IAmp;Offset} = 3ppm/^{\circ}C$

- Input Noise:  $U_{IAmp;Noise} = 0.6\mu V_{PP}$  (10 Hz Bandwidth)

Amplifier (LMP7701 [27]):

- Gain:  $A_{Amp} = 1$
- Offset-Voltage:  $U_{Amp;Offset} = 37\mu V$
- Input Offset Voltage Temperature drift:  $\Delta U_{Amp;Offset} = 1\mu V/^{\circ}C$
- Input Noise:  $U_{Amp;Noise} = 9nV\sqrt{Hz}$

ADC (MCP3550 [38]):

- Resolution:  $n_{ADC} = 22bit$
- Accuracy:  $\Delta V_{ADC} = 2ppm$
- Offset-Voltage:  $U_{ADC;Offset} = 3\mu V$
- Temperature drift:  $\Delta U_{ADC;Offset} = 0.04ppm/^{\circ}C$
- Output-Noise:  $U_{ADC;noisen} = 2,5\mu V_{RMS}$

## Schematic



Figure 13 shows the schematic of the mass measurement circuit. The weight sensor is symbolized by the bridge with the four resistors. After the bridge the instrumentation amplifier increases the output by a gain of 50 and shifts the level to the reference voltage ( $U_{ARef}$ ) of 2.5V. This signal is smoothed by a Sallen-Key-Filter, which is a second order low pass filter with a bandwidth of 10.8Hz. Finally the analog signal is converted by the Sigma-Delta ADC into a digital signal and transmitted over SPI.

### Transfer-function

To calculate the transfer-function no noise and offset are assumed.

First of all the number of discretization steps per Volt of the ADC ( $V_{ADC}$ ) is calculated:

$$A_{ADC} = \frac{2^{n_{ADC}} - 1}{U_{ARef} - (-U_{ARef})} = \frac{2^{22} - 1}{2 \cdot 2.5V} = 838860.61/V \quad (11)$$

With this, the gain of the bridge and instrumentation amplifier the whole transfer function can be calculated.

$$\begin{aligned} B/m_{Weight} &= U_{Ref} \cdot A_{Bridge} \cdot A_{IAmp} \cdot A_{ADC} = \\ &= 5V \cdot \frac{1V}{1000V} \cdot \frac{1}{300g} \cdot 50 \cdot 838860.6 \cdot \frac{1}{V} \\ &= 699.05/g = 0.699/mg \end{aligned} \quad (12)$$

1mg equals 0.699 in integer units. So a theoretical resolution of  $1/0.699 = 1.43mg$  is achieved.

### Accuracy

For the calculation of the accuracy the method of error propagation is used. Also no noise is assumed.

First the potential influences are analyzed with the transfer function.

$$\begin{aligned} B/m_{Weight} &= U_{BRef} \cdot A_{Bridge} \cdot A_{IAmp} \cdot A_{ADC} \\ &= U_{BRef} \cdot A_{Bridge} \cdot A_{IAmp} \frac{2^{22} - 1}{2 \cdot U_{ARef}} \end{aligned} \quad (13)$$

Table 8 shows the potential influences:

Parameter	absolute accuracy	relative accuracy in %
$\Delta U_{BRef}$	$2.0mV$	$\frac{2.0mV}{5V} \cdot 100 = 0.04$
$\Delta U_{ARef}$		0.05
$\Delta A_{Bridge}$		0.0067
$\Delta U_{IAmp;Offset}$	$1\mu V$	$\frac{1.0\mu V}{5V} \cdot 100 = 2 \cdot 10^{-5}$
$\Delta A_{IAmp}$		0.03
$\Delta U_{Amp;Offset}$	$37\mu V$	$\frac{37.0\mu V}{2.5V} \cdot 100 = 1.480 \cdot 10^{-3}$
$\Delta U_{ADC;Offset}$	$3\mu V$	$\frac{3.0\mu V}{5V} \cdot 100 = 6 \cdot 10^{-5}$
$\Delta A_{ADC}$		0.0002

Table 8: Accuracy and offset of the components

The offset error ( $\Delta U_{IAmp;Offset}$ ) of the instrument amplifier is negligible to its gain error ( $\Delta V_{IAmp}$ ) so only the gain error is used for calculation.

Also the offset error of the amplifier ( $\Delta U_{Amp;Offset}$ ) and of the ADC ( $\Delta U_{ADC;Offset}$ ) are negligible to the accuracy of the voltage reference for the ADC ( $\Delta U_{ARef}$ )

Through this analysis it is possible to calculate the accuracy:

$$\begin{aligned}
\Delta B/m_{Weight} &= \left| \frac{\partial B/m_{Weight}}{\partial U_{BRef}} \cdot \Delta U_{BRef} \right| + \\
&+ \left| \frac{\partial B/m_{Weight}}{\partial A_{Bridge}} \cdot \Delta A_{Bridge} \right| + \\
&+ \left| \frac{\partial B/m_{Weight}}{\partial A_{IAmp}} \cdot \Delta A_{IAmp} \right| + \\
&+ \left| \frac{\partial B/m_{Weight}}{\partial A_{ADC}} \cdot \Delta A_{ADC} \right| + \\
&+ \left| \frac{\partial B/m_{Weight}}{\partial U_{ARef}} \cdot \Delta U_{ARef} \right| = \\
&= \left| A_{Bridge} \cdot A_{IAmp} \frac{2^{22} - 1}{2 \cdot U_{ARef}} \cdot \Delta U_{BRef} \right| + \\
&+ \left| U_{BRef} \cdot A_{IAmp} \frac{2^{22} - 1}{2 \cdot U_{ARef}} \cdot \Delta A_{Bridge} \right| + \\
&+ \left| U_{BRef} \cdot A_{Bridge} \frac{2^{22} - 1}{2 \cdot U_{ARef}} \cdot \Delta A_{IAmp} \right| + \\
&+ |U_{BRef} \cdot A_{Bridge} \cdot A_{IAmp} \cdot \Delta A_{ADC}| + \\
&+ \left| -U_{BRef} \cdot A_{Bridge} \cdot A_{IAmp} \frac{2^{22} - 1}{2 \cdot U_{ARef}^2} \Delta U_{ARef} \right|
\end{aligned} \tag{14}$$

$$\begin{aligned}
\Delta B/m_{Weight} &= \left| \frac{1}{1000} \cdot 50 \frac{2^{22} - 1}{2 \cdot 2.5} \cdot (5 \cdot 0.05\%) \right| + \\
&+ \left| 5 \cdot 50 \frac{2^{22} - 1}{2 \cdot 2.5} \cdot \left( \frac{1}{1000} \cdot 0.0067\% \right) \right| + \\
&+ \left| 5 \cdot \frac{1}{1000} \frac{2^{22} - 1}{2 \cdot 2.5} \cdot (50 \cdot 0.03\%) \right| + \\
&+ \left| 5 \cdot \frac{1}{1000} \cdot 50 \cdot \left( \frac{2^{22} - 1}{2 \cdot 2.5} 2ppm \right) \right| + \\
&+ \left| -5 \cdot \frac{1}{1000} \cdot 50 \frac{2^{22} - 1}{2 \cdot 2.5^2} (2.5 \cdot 0.05\%) \right| = \\
&= 104.86 + 14.05 + 62.91 + 0.42 + 20.97 \\
&= 203.21
\end{aligned} \tag{15}$$

Now this binary offset can be converted into a weight offset by using the transfer function:

$$m_{offset} = \frac{\Delta B/m_{Weight}}{B/m_{Weight}} = \frac{203.21}{0.699} mg = 290.41 mg \tag{16}$$

This shows, that a calibration is necessary.

### Noise analysis

The noise-level of the resistors is calculated, with the assumption of a temperature of  $20^\circ C$  (293 K) and a bandwidth of 10 Hz:

$$\begin{aligned}
U_{R1,Noise} = U_{R10,Noise} &= \sqrt{4k_B T R \Delta f} = \\
&= \sqrt{4 \cdot 1.380 \cdot 10^{-23} J/K \cdot 293 K \cdot 147 \cdot 10^3 \Omega 10 Hz} = \\
&= 154.2 nV
\end{aligned} \tag{17}$$

The noise of the bridge can be calculated similarly:

$$\begin{aligned}
U_{Bridge;Noise} &= \sqrt{4 \cdot k_B T R_{Bridge} \Delta f} = \\
&= \sqrt{4 \cdot 1.380 \cdot 10^{-23} J/K \cdot 293 K \cdot 350 \cdot 10 Hz} = \\
&7.53 nV
\end{aligned} \tag{18}$$

All noise sources are identified and listed in table 9. For calculating the RMS-Noise of the voltage references and the instrumentation amplifier Gaussian noise with a crest factor of 3.3 is assumed. [4] Taking into consideration that the values are given in peak to peak the factor is 6.6.

Parameter	peak to peak noise	RMS noise
$U_{BRef;Noise}$	$4\mu V_{PP}$	$0.61\mu V$
$U_{ARef;Noise}$	$3\mu V_{PP}$	$0.45\mu V$
$U_{Bridge;Noise}$		$7.53nV$
$U_{IAmp;Noise}$	$0.6\mu V_{PP}$	$91nV$
$U_{R1;Noise}$		$154.2nV$
$U_{R10;Noise}$		$154.2nV$
$U_{Amp;Noise}$		$28nV$
$U_{ADC;Noise}$		$2.5\mu V$

Table 9: Noise sources

As first part the digital noise of the signal path is calculated

The noise-level of the ADC is calculated as followed:

$$\begin{aligned}
B_{ADC,Noise} &= U_{ADC;Noise} \cdot A_{ADC} = \\
&= 2.5 \cdot 10^{-6}V \cdot \frac{2^{22} - 1}{5} 1/V = 2.097
\end{aligned} \tag{19}$$

The noise-level of the amplifier is calculated:

$$\begin{aligned}
B_{Amp,Noise} &= U_{Amp;Noise} \cdot A_{ADC} = \\
&= 28 \cdot 10^{-9}V \cdot \frac{2^{22} - 1}{5} 1/V = 0.023
\end{aligned} \tag{20}$$

The noise-level of the resistors  $R_1$  and  $R_{10}$  is calculated:

$$\begin{aligned}
B_{R1,Noise} &= B_{R10,Noise} = U_{R1;Noise} \cdot A_{ADC} = \\
&= 154 \cdot 10^{-9}V \cdot \frac{2^{22} - 1}{5} 1/V = 6.46
\end{aligned} \tag{21}$$

The noise-level of the instrument amplifier is calculated:

$$\begin{aligned}
B_{IAmp,Noise} &= U_{IAmp;noisen} \cdot V_{IAmp} \cdot V_{ADC} = \\
&= 91 \cdot 10^{-9}V \cdot 50 \cdot \frac{2^{22} - 1}{5} 1/V = 3.82
\end{aligned} \tag{22}$$

The noise-level of the bridge is calculated:

$$\begin{aligned} B_{Bridge,Noise} &= U_{Bridge;noisen} \cdot V_{IAmp} \cdot V_{ADC} = \\ &= 7.53 \cdot 10^{-9} V \cdot 50 \cdot \frac{2^{22} - 1}{5} 1/V = 0.32 \end{aligned} \quad (23)$$

The noise-level of the bridge reference is calculated by assuming the maximum load ( $m_{Weight} = 300g$ ):

$$\begin{aligned} B_{BRef,Noise} &= m_{Weight} \cdot U_{BRef;noisen} \cdot V_{Bridge} \cdot V_{IAmp} \cdot V_{ADC} = \\ &= 300 \cdot 0.61 \cdot 10^{-6} V \cdot \frac{1}{1000} \cdot \frac{1}{300} 1/g \cdot 50 \cdot \frac{2^{22} - 1}{5} 1/V = 0.026 \end{aligned} \quad (24)$$

Calculating the noise influence of the ADC-reference at a maximum load of 300g:

$$B = (U_{BRef} \cdot m_{Weight} \cdot V_{Bridge} \cdot V_{IAmp} + U_{ARef}) \frac{2^{22} - 1}{2 \cdot U_{ARef}} \quad (25)$$

$$\frac{\partial B}{\partial U_{ARef}} = -U_{BRef} \cdot m_{Weight} \cdot V_{Bridge} \cdot V_{IAmp} \cdot \frac{2^{22} - 1}{2 \cdot U_{ARef}^2} \quad (26)$$

$$\begin{aligned} B_{ARef,Noise} &= m_{Weight} \cdot (-U_{ARef;Noise}) \cdot U_{BRef} \cdot V_{Bridge} \cdot V_{IAmp} \cdot \frac{2^{22} - 1}{2 \cdot U_{ARef}^2} = \\ &= 300g \cdot (-0.45 \cdot 10^{-6} V) \cdot 5V \cdot \frac{1}{1000} \cdot \frac{1}{300g} \cdot 50 \cdot \frac{2^{22} - 1}{2 \cdot 2.5^2} 1/V^2 = -38 \cdot 10^{-3} \end{aligned} \quad (27)$$

The whole noise can be calculated as the square root of the quadratic sum.

$$B = \sqrt{\sum_{i=0}^n B_i^2} \quad (28)$$

The calculation shows, that only the noise of the instrumentation amplifier ( $B_{IAmp,Noise} = 3.82$ ), the noise of the resistors  $R_1$  and  $R_{10}$  ( $B_{R1,Noise} = B_{R10,Noise} = 6.45$ ) and the noise

of the ADC ( $B_{ADC,Noise} = 2.097$ ) are important. All other sources are negligible.

$$\begin{aligned} B_{whole,Noise} &= \sqrt{B_{IAmp,Noise}^2 + B_{R1,Noise}^2 + B_{R10,Noise}^2 + B_{ADC,Noise}^2} \\ &= \sqrt{3.82^2 + 6.45^2 + 6.45^2 + 2.097^2} = 10.11 \end{aligned} \quad (29)$$

To translate the calculated integer noise into the mass, it is possible to use the result of the Transfer-function:

$$m_{noise} = \frac{B_{Noise;total}}{B/m_{Weight}} = \frac{10.11}{0.699/mg} = 14.46mg \quad (30)$$

So a total noise level is 14.46mg.

To reduce the noise level 10 samples are averaged:

$$m_{noise;avg} = \frac{m_{noise}}{\sqrt{n}} = \frac{14.46mg}{\sqrt{10}} = 4.57mg \quad (31)$$

The noise level after averaging is 4.57mg.

**Temperature drift** The temperature drift is similar to the noise calculation. Instead of the noise the temperature drift is inserted.

Parameter	given drift	binary drift
$\Delta U_{BRef;temp}$	$2ppm/^{\circ}C$	$8.3 \cdot 10^{-7} \text{ }^{\circ}C$
$\Delta U_{ARef;temp}$	$3ppm/^{\circ}C$	$0.63^{\circ}C$
$\Delta U_{IAmp;Offset}$	$50nV/^{\circ}C$	$2.10^{\circ}C$
$\Delta U_{Amp;Offset}$	$1\mu V/^{\circ}C$	$0.84^{\circ}C$
$\Delta U_{ADC;Offset}$	$0.04ppm/^{\circ}C$	$0.03^{\circ}C$

Table 10: Termal drift

The main source of the drift is the instrument amplifier. The amplifier and the reference have a small influence.

The whole drift is the square root of the quadratic sum.

$$\begin{aligned}
\Delta B_{whole,temp} &= \sqrt{\Delta B_{IAmp,Offset}^2 + \Delta B_{Amp,Offset}^2 + \Delta B_{AREf,temp}^2} \\
&= \sqrt{2.10^2 + 0.84^2 + 0.63^2} \\
&= 2.35/^{\circ}C
\end{aligned} \tag{32}$$

To transfer the integer drift into a mass drift, the transfer function can be used:

$$\Delta m_{drift} = \frac{B_{Drift,total}}{B/m_{Weight}} = \frac{2.35/^{\circ}C}{0,699/mg} = 3.36mg/^{\circ}C \tag{33}$$

The drift can not be reduced through averaging, because it is a non stochastic signal.

## Noise+Drift

The calculation shows that the temperature drift and the noise are critical.

$$m_{total,error} = m_{noise,avg} + \Delta m_{drift} \cdot \Delta T = 4.57mg + 3.36mg/^{\circ}C \cdot \Delta T \tag{34}$$

A total mass error ( $m_{total,error}$ ) of 10mg is desired and therefore the maximum temperature change could be calculated as followed:

$$\begin{aligned}
\Delta T &= \frac{m_{total,error} - m_{noise,avg}}{\Delta m_{drift}} \\
&= \frac{10mg - 4.57mg}{3.36mg/^{\circ}C} \\
&= 1.62/^{\circ}C
\end{aligned} \tag{35}$$

To guarantee an error of maximum 10mg the temperature of the electronic must not change more than 1.62 $^{\circ}C$ .

## Firmware

The ADC and the instrumentation amplifier are connected to the micro-controller via SPI. On initializing the SPI communication is set to full duplex mode with 8 data bit and frequency is set to 656.25 kHz. The clock-line is set to high in sleep mode and the data are valid on the positive edge of the clock. The chip-select lines are not handled by the SPI controller and set manually.

After the SPI bus is initialized the gain of the instrumentation amplifier is set to 50. This is also done at the start of every sequence.

To get the mass value from the ADC the chip select line for the ADC is shortly set to low to start a conversion. After this the software checks every 10 ms, if a valid result is available. Typically the conversion should take 80 ms. If a valid result is available the result is stored in the result-buffer for the reference or the weight values.

Once the sequence is finished the mass is calculated by removing the maximum and the minimum values from the buffer, to reduce outliers. The remaining 8 values are then averaged. After this the averaged reference is subtracted from the averaged mass value. The result is then converted into the sampled mass by multiplying with a factor, which can be calibrated.

#### **2.4.8 Timer**

As timer only the timer number 3 is used. This timer runs with 10kHz, which equals a timebase time base of 0.1 ms. From this timer-clock every timing for the state-machine is derived.

If the timer exceeds 1ms the system-time is increased. This time is used for reading out the start timestamp for every started sequence.

For the mass measurement every 10 ms a flag is set. If this flag is set the state machine checks if a valid ADC value for the weight-measurement is available.

If a sequence is running the time between the states are given in ms and if this time is exceeded the timer sets a flag for signaling the state machine to load the next step of the sequence.

#### **2.4.9 Memory Management**

This module provides the functionality to store sequences and calibration data in the internal memory. Sending sequences and data for the measurement over USB to a PC is also one part of it.

As memory a part of the internal flash of the microcontroller is used. For accessing this memory the Virtual EEprom library from Uwe Becker was used.

The USB Driver is a modified version from Tilen of the Virtual COM Port driver from STM.

The memory is designed to store the calibration data and 9 sequences with 90 steps and a sequence name with a length of 10 characters.

Per USB it is possible to transfer new calibration data or a new sequence to the device. The protocol for transferring the sequence is shown in figure 14. It is the same protocol for transferring the sequence from the PC to the device and vice versa. If a new sequence is transferred to the device the PC should read it back and check if the transfer was valid. The transfer contains for every state of the timing protocol the exit condition, the stepname, the duration of the step, the state of the mass measurement and all the valve stats. For the PC it is enough to send only the informations which valves changes their state. On the other hand the device sends always the state of all valves.

For every executed sampling process carried-out a measurement protocol is generated. It consists of a sequence-number, a timestamp, the pressure at the execution time of operation and the mass of the sample. These data are transferred to the PC in CSV format using ASCII characters and semicolons. Between different sapling processes a carry return is inserted.

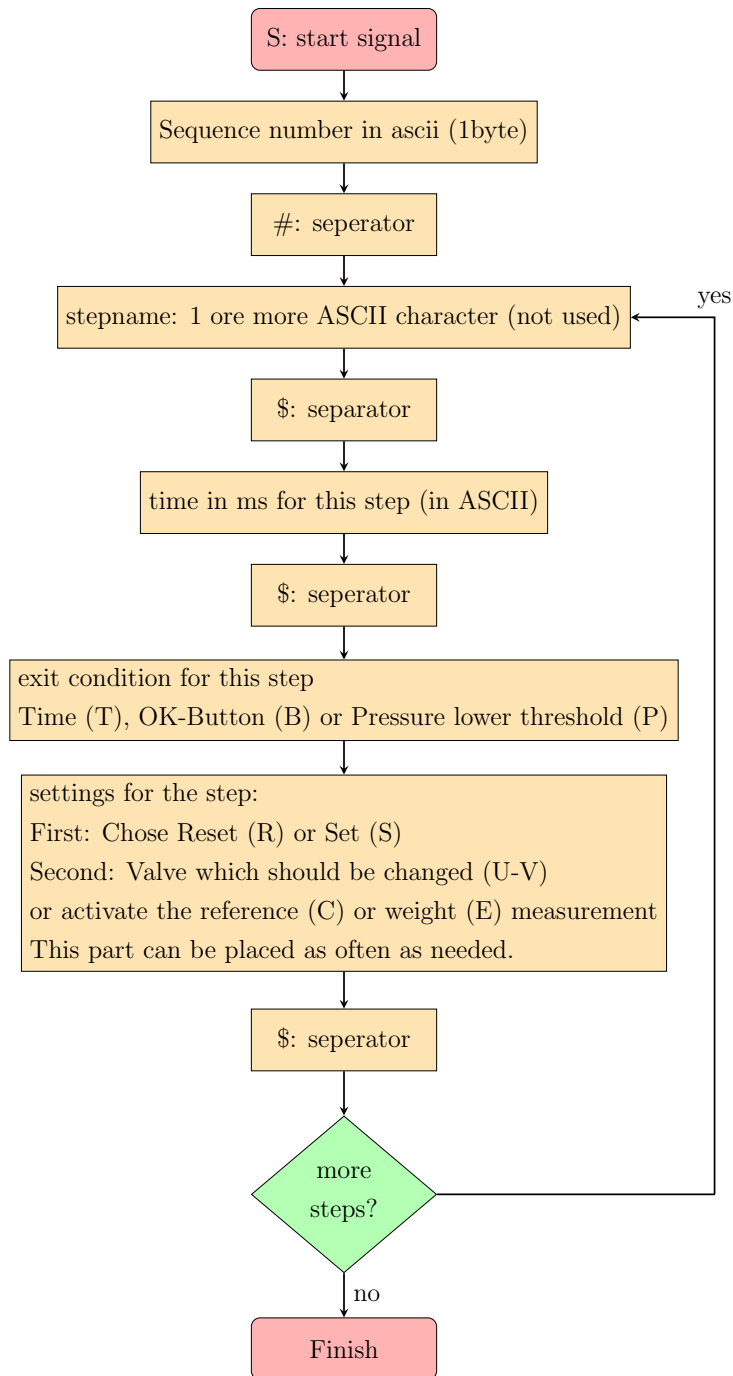


Figure 14: Transfer protocol for the sampling sequence between a PC and the device.

#### 2.4.10 Interpreter

If a sequence is loaded or a step changes, the interpreter gets the compressed data from the memory and sets the valves according to this data. If a mass measurement is desired

in this step, the mass measurement is activated. Also the exit condition for the new step is loaded and set.

### 2.4.11 Connectors

To connect the valve-box to the main device a 25 pin sub-D connector (Tyco Electronics, Swiss) with the pinning shown in table 11 was used. For the weight sensor a sub-D connector with 15 pins (Tyco Electronics, Swiss) was used. The pinning is described in table 12.

For the pressure sensor a 7 pin Din connector(Lumberg Holding, Germany) is used. The pinning is explained in table 13

Pin	Type	Port
1	n.c.	
2	Valve 1	PE10
3	Valve 2	PE11
4	Valve 3	PE12
5	Valve 4	PE13
6	Valve 5	PE14
7	Valve 6	PE15
8 -11	n.c.	
12	12V	
13 -25	n.c.	

Table 11: Pinning of the valve connector

Pin	Type	Port
1	12V	
2	AGND	
3	SCK	PB3
4	MISO	PB5
5	MOSI	PB4
6	CS Iamp	PD10
7	CS ADC	PD11
8	3,3V	
9	DGND	
10-13	n.c.	

Table 12: Pinning of the weight sensor connector

Pin	Type	Port
1	n.c.	
2	GND	
3	n.c.	
4	V-Pressure	
5	5V	
6	n.c.	
7	12V	

Table 13: Pinning of the pressure sensor connector

## 2.5 Software

For modifications of the timing protocol a software was written in JAVA. It allows the user to modify the timing and the switching order of the valves. With the software it is also possible to transfer the protocolled data of the drawn sample to the PC. The data includes the measured mass, the start time and the pressure during sampling.

## 2.6 Matlab model

To determine the bottlenecks of the tubing system a Matlab model, was developed. This model calculates the volume and the flow rate using the Hagen-Poiseuilles law. Therefore the tubing was partitioned in compartments, where the radius is constant (Figure 15).

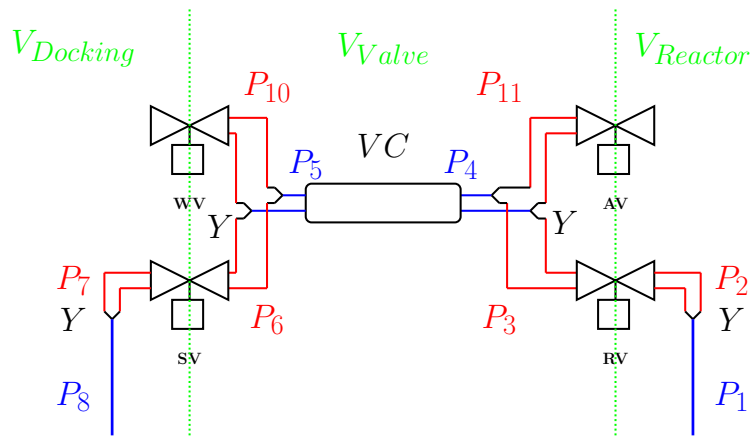


Figure 15: **Tubing system showing the different compartments.**  $P_1$ ...sampling tube,  $P_8$ ...needle,  $P_2 - P_7$  and  $P_{10} - P_{11}$ ...tubing parts,  $Y$  ... Y-Connectors,  $VC$  ... Volumetric cell (only version 1)

### Calculation of the volume

The Volume of the compartments ( $V_i$ ) was calculated as cylinder for  $P_8$ ,  $P_8$  and VC with the radius  $r_i$  and the length  $l_i$ :

$$V_i = r_i^2 \cdot l_i \quad (36)$$

For the parts  $P_2 - P_7$  and  $P_{10} - P_{11}$  the calculation were similar, but instead of one cylinder there were two parallel cylinders:

$$V_i = r_i^2 \cdot l_i \cdot 2 \quad (37)$$

The volumes for the reactor section, the valve section (Version 1 and Version 2) and the docking section can than be calculated as set out below:

$$V_{Reactor} = V_{P_1} + V_{P_2} \quad (38)$$

$$V_{Valve,version1} = V_{P_3} + V_{P_4} + V_{P_5} + V_{P_6} + V_{P_{10}} + V_{P_{11}} + V_{VC} \quad (39)$$

$$V_{Valve,version2} = V_{P_3} + V_{P_4} + V_{P_5} + V_{P_6} + V_{P_{10}} + V_{P_{11}} \quad (40)$$

$$V_{Docking} = V_{P_8} + V_{P_7} \quad (41)$$

Due to the small Volume of the Y-Connectors (ID=1mm, l=10mm, V=2.5 $\mu$ l) they are neglected.

### Calculation of the flow rate

To calculate the flow rate constant laminar flow and the fluid properties of water ( $\nu_{Water,20^\circ C} = 1.0087 mPa \cdot s$ ) are assumed.

Therefore the Flow-Resistances  $R_{flow,i}$  for the parts  $P_3$ ,  $P_8$  and VC are calculated for a cylinder geometry with the length  $l_i$  and radius  $r_i$ .

$$R_{flow,i} = \frac{8 \cdot \nu \cdot l_i}{\pi \cdot r_i^4} \quad (42)$$

The calculation for the parts  $P_2 - P_7$  and  $P_{10} - P_{11}$  is similar, but instead of one cylinder there are two parallel cylinders and therefore the resistance must be halved:

$$R_{flow,i} = \frac{8 \cdot \nu \cdot l_i}{\pi \cdot r_i^4} \cdot \frac{1}{2} \quad (43)$$

The total resistance is then calculated by adding the parts, where the sample flows, together

$$R_{flow,total,version1} = \sum_{i=1}^8 R_{flow,P_i} + R_{flow,VC} \quad (44)$$

$$R_{flow,total,version2} = \sum_{i=1}^8 R_{flow,P_i} \quad (45)$$

The Y connectors are neglected due to fact that the diameter is similar to the silicon tubes and the their short length (10mm) in comparison with the overall system.

The flow-rate can then be calculated by using the equation 2.

## 2.7 Verification of the sampling device

### 2.7.1 Setup for experiments

The device is placed next to the sample source and the tubing system is assembled like described in section 2.2.

For Version 2 it was necessary to reduce artifacts on the mass measurement. Therefore vibrations from the surroundings has to be reduced, by using a damped granite plate, which should not touch anything other than the damping elements below it. Additionally air flow can also act as a force onto the weight sensor, which will result in a disturbance of the measured mass. To prevent this carton wall was placed on the side and behind of the docking unit.

All experiments were carried out under room temperature. As sample container 50ml Falcon-tubes (Table 3) were used.

### 2.7.2 Accuracy of the mass

As mentioned in the requirements (Section 1.4) the sampled must be similar for all samples (Version 1) or the weight sensor must be able to measure the exact mass (Version 2).

To verify the accuracy of the sampled mass an analytical balance (Table 3), with an error margin of less than 1mg, was used. [35].

As test liquid TW (Table 4) was used, which has a density of approximately  $1kg/m^3$  ( $3.98^\circ C$ ) [23] .

To determine the sampled mass, the Falcon-tubes were measured before and after the sampling procedure. The difference is the mass ( $m_{scale}$ ) of the sampled liquid.

$$m_{scale} = m_{scale,after} - m_{scale,before} \quad (46)$$

For Version 1 the mass residuals were calculated as follows:

$$residue = m_{scale} - \mu(m_{scale}) \quad (47)$$

For Version 2 the relative mass residuals were calculated as follows:

$$residue = \frac{m_{device} - m_{scale}}{m_{scale}} \cdot 100\% \quad (48)$$

### 2.7.3 Carry over

To analyze the carry over two different solutions (Table 4) were sampled alternately. These liquids have different solute concentration and thus different absorption coefficient for optical reference measurements.

For Version 1 only the liquids TW and TW-CR were used.

For Version 2 first the un-buffered liquids TW and TW-CR were used and later than the pH buffered liquids PBB and PBB-CR.

The experiment was carried out according to the sequence described herinafter:

1. Depending on the experiment either TW or PBB was filled in flask 1
2. Furthermore TW-CR or TBB-CR was filled in flask 2
3. A magnetic stirrer was inserted into the flasks. (only Version 2)
4. Samples were drawn. This step differed between the two versions of the device and is described in the next paragraph.
5. For all samples the optical density was measured by the photometer DU800 (Beckman Coulter, Germany) at a wavelength of 491nm.

### **Drawing of the samples for Version 1**

1. One reference samples was drawn from flask 1 by using a pipette( $OD_1$ ).
2. A second reference sample was drawn from flask 2( $OD_2$ ).
3. The sampling tube was inserted into flask 1.
4. The sampling procedure was executed 2 times for preconditioning of the tubing.
5. The sampling tube was inserted into flask 2.
6. The sampling procedure was executed 6 times.
7. The sampling tube was inserted into flask 1.
8. The sampling procedure was executed 6 times(first experiment) or 2 times(second experiment).

### **Drawing of the samples for Version 2**

1. The sampling tube is inserted into flask 2.
2. 3 unused samples are drawn.
3. The sampling tube is inserted into flask 1.
4. With a pipette 2 reference samples are drawn from flask 1 ( $OD_1$ ).
5. The sampling procedure is executed 3 times
6. The sampling tube is inserted into flask 2 ( $OD_2$ ).
7. With a pipette 2 reference samples are drawn from flask 2.
8. The sampling procedure is executed 3 times
9. Steps 3-8 are repeated.

## Analyzing the samples

If the optical density of the liquid in flask 1 ( $OD_1$ ) and the optical density of solution in flask 2 ( $OD_2$ ) is known, the carry over for the sampled solution ( $OD_{sample}$ ) can then be calculated.

If there was a concentration step from flask 2 to flask 1 the calculation is as follows:

$$CO_{1,2} = \left(1 - \frac{OD_{sample} - OD_1}{OD_2 - OD_1}\right) \cdot 100\% \quad (49)$$

In case of the opposite concentration step the carry over is:

$$CO_{2,1} = \frac{OD_{sample} - OD_1}{OD_2 - OD_1} \cdot 100\% \quad (50)$$

The reference ODs ( $OD_1, OD_2$ ) were measured 1 time at the beginning (Version 1) or before every drawn sample (Version 2).

### 2.7.4 Sampling water from a bioreactor (only Version 1)

For Version 1 the device was mounted to a bioreactor filled with water. As bioreactor a LabForce 2 (Table 3) with a volume of 1l was used. This bioreactor is equipped with a pH-,  $pO_2$ - and a temperature sensor. The device was mounted by placing the sampling tube  $ST_{ST275}$  through a pipe inlet. The stirrer speed was set to 300rpm for the whole experiment.

30 Falcon-tubes were prepared and the mass was measured. Another 30 Falcon-tubes were filled with a 10ml (preload) of water and the mass was measured.

Then samples were drawn according to this schema:

- Nitrogenflow was set to 0.2l/min.
- 10 samples were drawn into the Falcon-tubes without preload.
- Nitrogenflow was set to 0.1l/min.
- 10 samples were drawn into the Falcon-tubes without preload.
- Nitrogenflow was set to 0.0l/min.

- 10 samples were drawn into the Falcon-tubes without preload.
- Nitrogenflow was set to 0.2l/min.
- 10 samples were drawn into the Falcon-tubes with the preload.
- Nitrogenflow was set to 0.1l/min.
- 10 samples were drawn into the Falcon-tubes with the preload
- Nitrogenflow was set to 0.0l/min.
- 10 samples were drawn into the Falcon-tubes with the preload.

The Falcon-tubes were measured again and the mass is calculated as in section 2.7.2 described.

### **2.7.5 Sampling cultivation broth from a bioreactor (only Version 2)**

For this experiment a cell culture was grown by the Institute of Biotechnology and Biochemical Engineering at TU Graz.

#### **Preculture**

As preculture a *Saccharomyces cerevisiae* (CEN.PK 113-7D) stock was incubated in petri dishes, containing a mineral medium and 1.6% agar agar, over a timespan of 2 days at 30°C.

A loopful of this preculture was inserted into a 300ml shake flask (Table 3) containing 30ml mineral medium (Table 5) and 0.015g/L antifoam 204 (Sigma Aldrich, USA). The cultures were cultivated overnight at 120 rpm and at 30°C. Resultant cells were used to inoculate the bioreactor.

#### **Preparation**

A Labfors 3 bioreactor (3) was used to cultivate *S. cerevisiae*. The working volume was 2 L and the cultivation was initiated by the addition of cells to a final optical density of 0.15. The bioreactor was equipped with pH, pO<sub>2</sub> and temperature sensor. The pH value is PID controlled to a value of 6.5, while pO<sub>2</sub> was PID controlled by applying a cascade involving mass flow and stirrer speed.

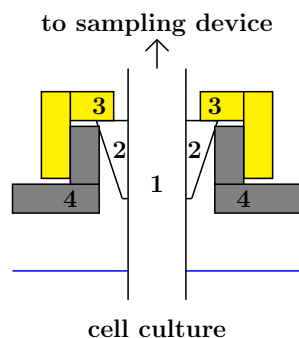


Figure 16: **Cross section of the mounted sample tube.** The sampling tube (1) is mounted into the reactor(4) and kept in place by a conus (2) and the screw joint (3).

The rapid sampler was connected to the reactor by mounting the sampling tube through an inlet into the reactor (Figure 16).

Two sets of Falcon-tubes were prepared and their mass was measured by an analytic balance (Table 3):

- **F1:** These Falcon-tubes were prepared with a preload of 10ml methanol and were later cooled in two boxes with 5kg carbon dioxide snow.
- **F2:** These Falcon-tubes did not contain any preload.

## Sampling

- First the nitrogen flow rate was set to 2l/min and the stirrer speed was set to 300rpm, which was increased to 3l/min and 1000rpms after 2 hours and 15 minutes.
- 6 of the F1-tubes were inserted into the carbon dioxide snow box to cool them down.
- After 30min the sampling was procedure started.
- Every 15 min 3 samples were transferred into the cooled F1-tubes. For this 1 tube was taken out of the carbon dioxide snow box and was cleaned from condensed water by using a paper towel. After this the tube was connected to the docking port of the sampling device and the sample was transferred.
- After the withdrawal of 3 samples the box was filled with 3 of the remaining tubes.
- Every 20 min 1 sample was drawn into a F2-tube.

## **Analysis**

The mass was analyzed, when the temperature of the Falcon tubes returned to room temperature. After this the tubes were shortly opened to equalize the air pressure inside of the tubes with the pressure of the environment. Otherwise this difference can lead to an invalid mass value. The Falcon tubes were measured and their value before the sampling was subtracted as described in section 2.7.2.

### **2.7.6 Step response of the mass measurement (only Version 2)**

To analyze the dynamic behavior of the mass measurement a step response experiment was carried out. Therefore the rapid sampler was connected per USB to a PC. The firmware was set to a modus, where all unfiltered mass values were transferred over USB.

As sample source a flask with TW was used and the sampling tube  $ST_{ST275}$  (Table 2) was inserted into the flask. Then the samples were drawn for different sampling times and the mass data were acquired with Matlab.

### **2.7.7 Temperature drift of the mass measurement (only Version 2)**

To analyze the influence of temperature on the readout of the weight sensor a PT100 sensor (Table 3) was mounted with heatsink paste in the middle on the top of the bending beam of the weight sensor. The PT100 sensor was then connected to a Keithley 2000 multimeter (Table 3).

The whole device was put into a box with 1x1x1m and the unfiltered data from the weight sensor were transmitted per USB to a PC running Matlab. The temperature values were also transmitted over GPIB to the same PC.

Both data were then synchronized and analyzed with Matlab. The acquisition interval was 1s.

For the first experiment there was no heat-source added and data were acquired over a duration of 30min.

For the second experiment a 20W soldering iron (Table 3) was placed with the tip in a distance of 30cm directly under the weight sensor. During the data acquisition the soldering iron was switched on for 30min and after this time switched off for another 30min. Therefore it was possible to generate a positive and negative heat gradient.

### 2.7.8 Calibration of the mass measurement

For the calibration of the mass measurement the procedure was similar to the verification of the mass (Section 2.7.2).

To execute this calibration 10 samples are drawn and measured by an analytic balance. These masses ( $m_{scale}$ ) are then averaged ( $\mu_{m_{scale}}$ ). Also the masses ( $m_{device}$ ) measured by the device are averaged ( $\mu_{m_{device}}$ ). Then the PC is connected to the device and the software is started. The averaged masses are entered into the software and the PC calculates the quotient (factor):

$$factor = \frac{\mu_{m_{scale}}}{\mu_{m_{device}}} \quad (51)$$

This factor is then send via USB to the device, which then multiplies this factor to the current calibration. After this the device is calibrated.

## 3 Results

### 3.1 Results of the simulation using the Matlab model of the tubing systems

For optimization of the tubing system a Matlab model was developed as described in section 2.6. With this model it was possible to determine bottlenecks for the flow speed and dead volumes of the system. The construction parameter and the resulting volumes and flow resistances can be seen in table 14 for Version 1 and table 15 for Version 2. Table 16 shows the differences in the volumes for the different grouped compartments of the tubing system.

Compartment of the tubing	l mm	d mm	V $\mu l$	$R_{flow}$ $kPa \cdot s/ml$
P1	1.8	275	699	0.95
P2	1.0	500	785	9.07
P3	1.0	30	47	0.54
P4	1.0	10	16	0.18
VC	3.3	130	1112	0.04
P5	1.0	10	16	0.18
P6	1.0	80	126	1.45
P7	1.0	350	550	6.34
P8	0.7	70	27	10.57
P10	1.0	80	126	1.45
P11	1.0	30	47	0.54

Table 14: Volume and flow resistance of the tubing system for Version 1

Part of the tubing	l mm	d mm	V $\mu l$	$R_{flow}$ $kPa \cdot s/ml$
P1	1.6	275	543	1.49
P2	1.0	420	660	7.62
P3	1.0	15	24	0.27
P4+P5	1.0	25	39	0.45
P6	1.0	15	24	0.27
P7	1.0	350	550	6.34
P8	0.7	70	27	10.57
P10	1.0	15	24	0.27
P11	1.0	15	24	0.27

Table 15: Volume and flow resistance of the tubing system for Version 2

	Volume of Version 1 $\mu l$	Volume of Version 2 $\mu l$
$V_{Reactor}$	1484	1203
$V_{Valve}$	1490	135
$V_{Head}$	577	577
$V_{total}$	3551	1915

Table 16: The grouped volume of the tubing system

Table 16 shows that the volume of the valve section  $V_{Valve}$  for Version 2 is much smaller (1490 $\mu l$  vs 135 $\mu l$ ) than for Version 1, which is a result of the missing volumetric cell and the reduced volumes for  $P_3$ ,  $P_4$ ,  $P_5$ ,  $P_6$ ,  $P_{10}$  and  $P_{11}$ .

The simulation results for the flow resistance and flow rate are shown in Table 17. The flow rate of Version 2 is higher (2.90 ml/s vs. 3.14 ml/s), due to the improved tubing.

Version	$R_{flow,total}$ $kPa \cdot s/ml$	$I_{flow}$ $ml/s$
Version 1	29.3	2.90
Version 2	27.0	3.14

Table 17: Simulation Results for flow resistance and flow rate

## 3.2 Verification Version 1

### 3.2.1 Verification of the volumetric cell

As the first step the variation of the sampled mass ( $m_{scale}$ ) was analyzed in respect to the filling ( $t_{fill}$ ) and release time ( $t_{release}$ ). For this the filling and release time were varied.

First the filling time was set to 1,2,3,4 and 5s with a fixed release time of 5 seconds. For every time step 15 samples were drawn. The dependency between filling time and the sampled mass are plotted in figure 17. The lowest variance of the mass ( $\sigma_{m_{scale}} = 11.0mg$ ) can be estimated at a filling time of 2 seconds, but there is only a small difference compared to the other filling times (Table 18). Also the mean value of the mass changes with the filling time between 1198.0mg (at 4s) and 1207.8mg (at 3s).

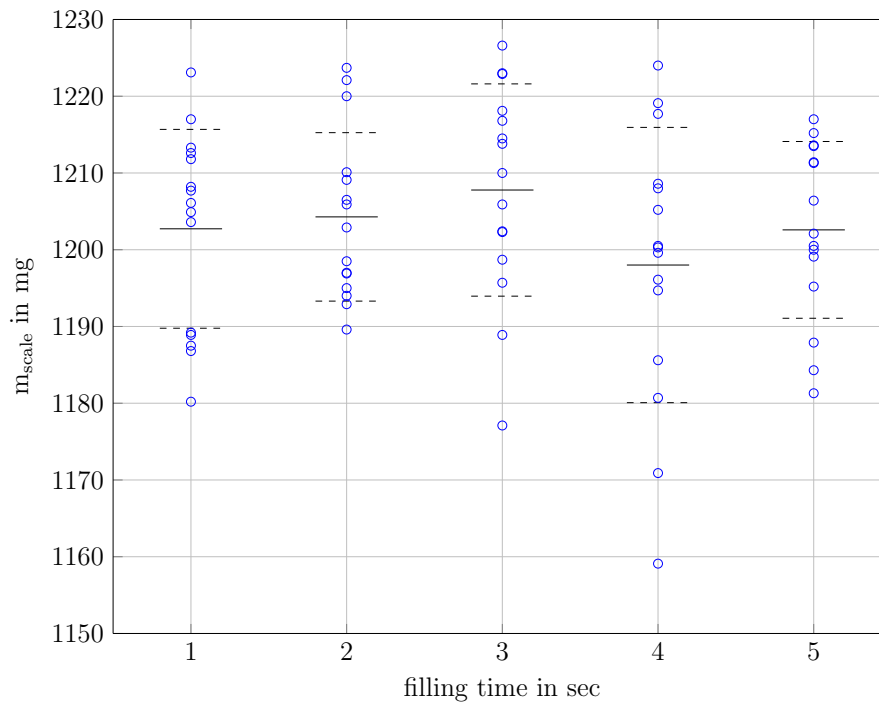


Figure 17: **Dependency between sampled mass and filling time.** Solid lines...mean value, dashed lines... $\pm$  one standard deviation

filling time	$\mu_{m_{scale}}$	$\sigma_{m_{scale}}$
s	mg	mg
1	1202.7	13.0
2	1204.3	11.0
3	1207.8	13.8
4	1198.0	18.0
5	1202.6	11.5

Table 18: Standard deviation and mean value of the sampled mass for different filling times.

After this the release time was varied and the filling time was fixed to 5s. The variation of the sampled mass for different release times is shown in figure 18. The lowest variance ( $\sigma_{m_{scale}} = 9.3mg$ ) occurred at a release time of 2 seconds (Table 19). The mean value does not changed as much as for the previous experiment, the range is between 1202.4mg (at 4s) and 1204.9mg (at 3s).

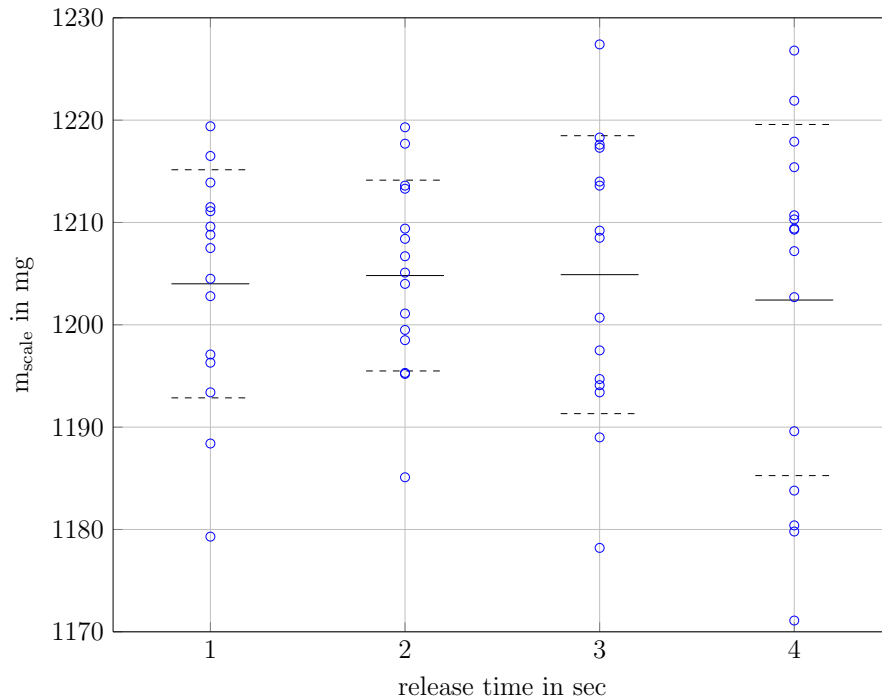


Figure 18: **Dependency between sampled mass and discharge time.** Solid lines...mean value, dashed lines... $\pm$  one standard deviation

release time	$\mu_{m_{scale}}$	$\sigma_{m_{scale}}$
sec	mg	mg
1	1204.0	11.1
2	1204.8	9.3
3	1204.9	13.58
4	1202.4	17.2

Table 19: Standard deviation and mean value of the sampled mass for different release times

Finally a combination of the filling and release time was tested. For this experiment the times, where the lowest variance occurred were used ( $t_{fill} = 2s$ ,  $t_{release} = 2s$ ). With this setting 20 samples were drawn and plotted in figure 19. The mean value (1210.9 mg) is higher than in the previous experiments and the standard deviation is 13.3 mg (Table 20). Also the plot indicates, that the variance of the sampled mass increases with the increase of the absolute vacuum pressure.

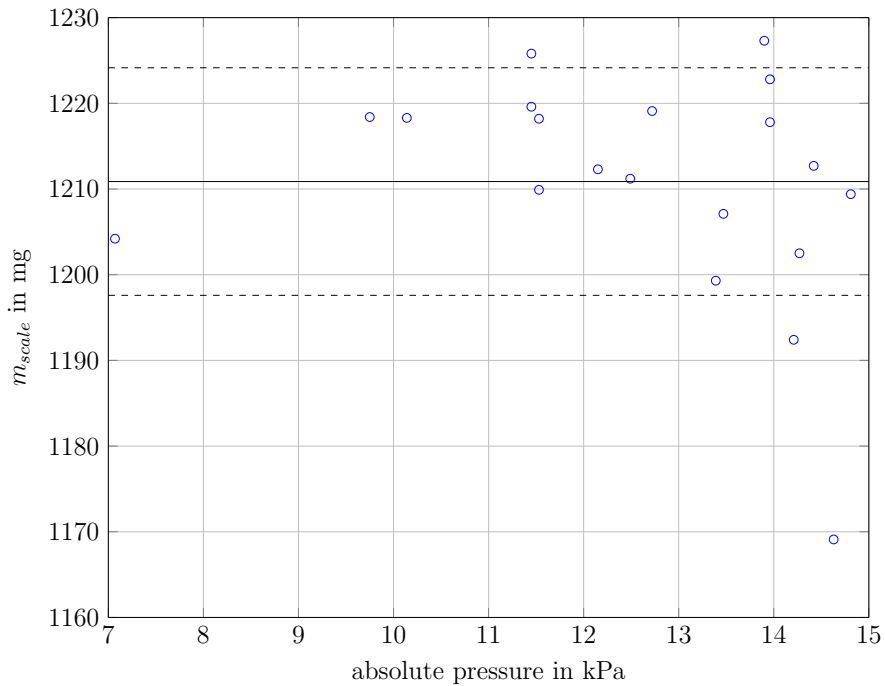


Figure 19: Mass in relation to the residual pressure after evacuation. Solid lines...mean value, dashed lines... $\pm$  one standard deviation

$\mu_{m_{scale}}$	$\sigma_{m_{scale}}$
<i>mg</i>	<i>mg</i>
1210.9	13.2

Table 20: Standard deviation and mean value of the sampled mass for the combination with  $t_{fill} = 2sec$  and  $t_{release} = 2sec$

### 3.2.2 Verification of the carry over

To analyze the carry over two different solutions were sampled alternately as explained in section 2.7.3. The filling and the release time were kept at 2s. In addition to the carry over the mass was analyzed.

For the first experiment the sample source (reactor) was an open flask. After this samples were drawn and different treatments were tested to improve the carry over (Figure 20). Following treatments were tested:

1. **default:** No special treatment, only the liquid has been changed.
2. **air-cleaning:** Between each switch from one solution to the other the sampling tube was removed from the flask and a sampling procedure was carried out. Thereby air was drawn through the sampling tube and the volumetric cell into a Falcon-tube, which was not used for further analysis.
3. **longer filling:** The filling time for the sample after the change of the liquid was extended to 3 seconds.

Furthermore the sampled mass was also analyzed during this experiment (Figure 21).

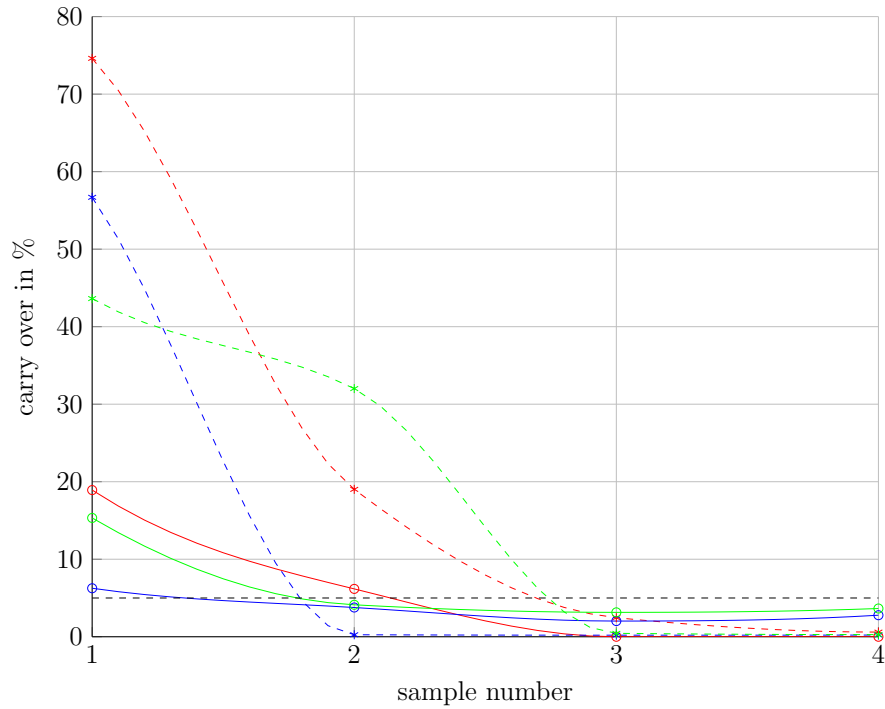


Figure 20: **The carry over for the different treatments** Red dataset...default treatment on sample number 2, blue dataset...with air-cleaning procedure, green dataset...longer filling time, circles...switch from TW to TW-CR, stars...switch from TW-CR to TW. Solid lines... cubic interpolation for the switch from TW to TW-CR Dashed colored lines... cubic interpolation for the switch from TW-CR, dashed black line...required 5% threshold, The interpolations is only for a better visual representation and there is no concrete physical model behind them.

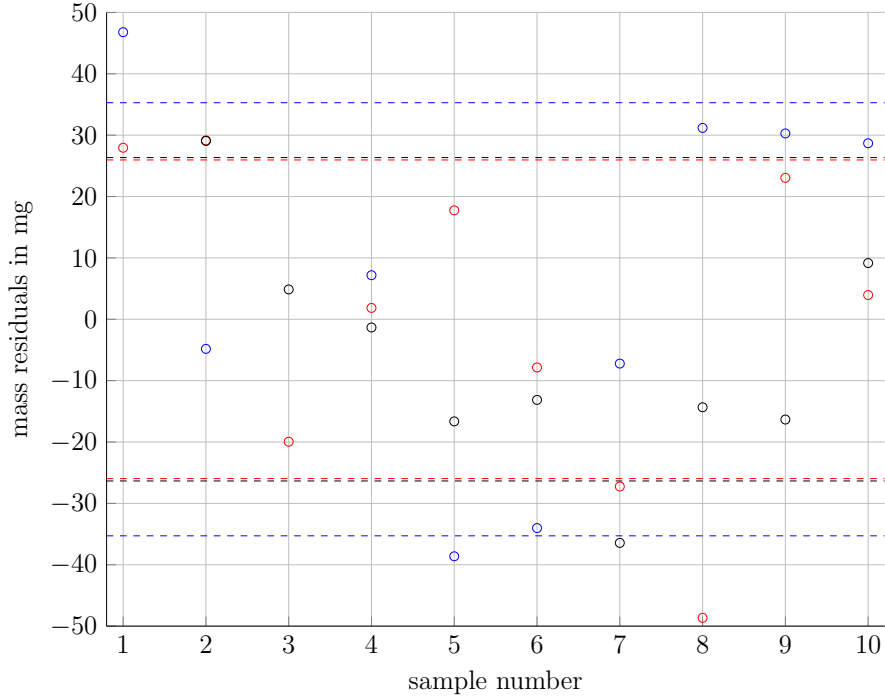


Figure 21: **The sampled mass during the carry over analysis.** Red dataset ... default treatment after the switch, blue dataset... with air-cleaning procedure, black... longer filling time, Dashed lines...  $\pm 1$  standard deviation of the data-points. For a better comparison both data series were subtracted from their mean value. The mean value and the standard deviation is shown in table 21.

treatment	$\mu_{m_{scale}}$ mg	$\sigma_{m_{scale}}$ mg
default	1192.2	25.9
air-cleaning	1100.0	35.3
longer filling	1184.8	26.3

Table 21: Standard deviation and mean value of the sampled mass for the different treatments

Figure 20 illustrates that the switch from TW to TW-CR results in a lower carry over than the other direction and that the air cleaning procedure results in a lower carry over (under 5% ) on sample number 2, than the other procedures. The mean value for the sampled mass (1100mg) is also lower, than for the other 2 treatments (1192mg and 1185mg) as shown in figure 21 and table 21. The standard deviation of the mass by using the air

cleaning procedure results in a higher standard deviation (35.3mg) compared to the other treatments (25.9 ms and 26.3mg).

As a second carry over experiment the difference between sampling from an opened conical flask and a closed flask was researched. This was done to test, if the sampling procedure requires a pressure equalization with the environment to work properly. The results are displayed in figure 22. During the liquid was changed, the sampling system was cleaned with air like in the previous experiment.

During this experiment the sampled mass was also measured. The difference between the two setups is shown in figure 23.

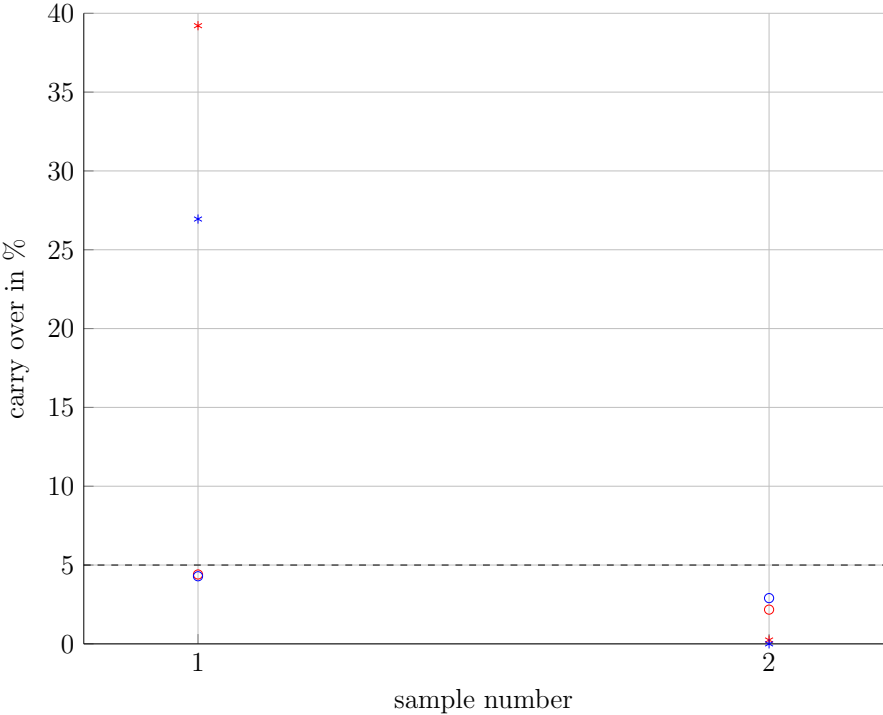


Figure 22: **The carry over during the second sample switch experiment.** Red circles...opened flask with switch from TW to TW-CR, red stars...opened flask with switch from TW-CR to TW, blue circles...closed flask with switch from TW to TW-CR, blue stars...closed flask with switch from TW-CR to TW, black dashed line... required 5% threshold

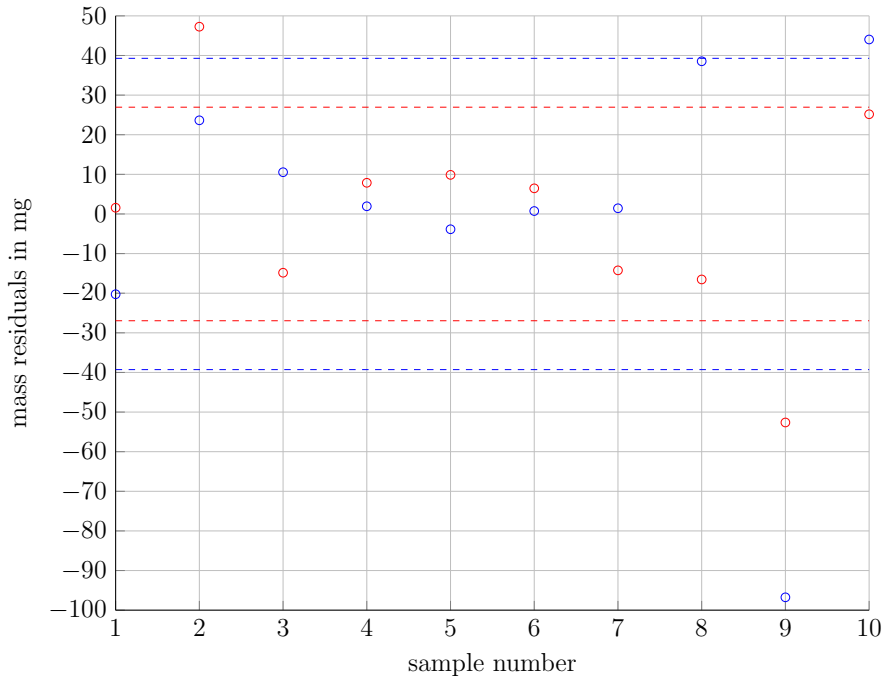


Figure 23: The sampled mass for the two different sample source. red datapoints...opened flask and blue datapoints...closed flask, Dashed lines...+/-one standard deviation. For a better comparison both data series were subtracted from their mean value. The mean value and the standard deviation is shown in table 22. The switching of the liquid and air cleaning occurred between sample 1 and 2 and between 8 and 9.

source	$\mu$ <i>mg</i>	$\sigma$ <i>mg</i>
opened flask	1167	27
closed flask	1173	39

Table 22: Standard deviation and mean value of the mass of the samples

Figure 22 shows that the carry over is similar to the previous experiments for the opened and the closed flask. The mean value of the mass of the open flask (1167mg) and of the closed (1173mg) flask are very similar but the standard deviation is higher for the closed flask(39mg) in comparison to the opened flask(27mg) (Table 22). This indicates that a pressure equalization is needed for future experiments.

### 3.2.3 Verification with a bioreactor

To test the device under process conditions an experiment with a bioreactor was carried out. For this experiment the bioreactor was filled with water and samples were drawn like described in section 2.7.2 To analyze the influence of the nitrogen flow on the performance of the sampling device, the flow rate was set to to 0.0l/min, 0.1l/min and 0.2l/min. For the different flow rates 10 samples were drawn and the masses (residuals in 24) were measured.

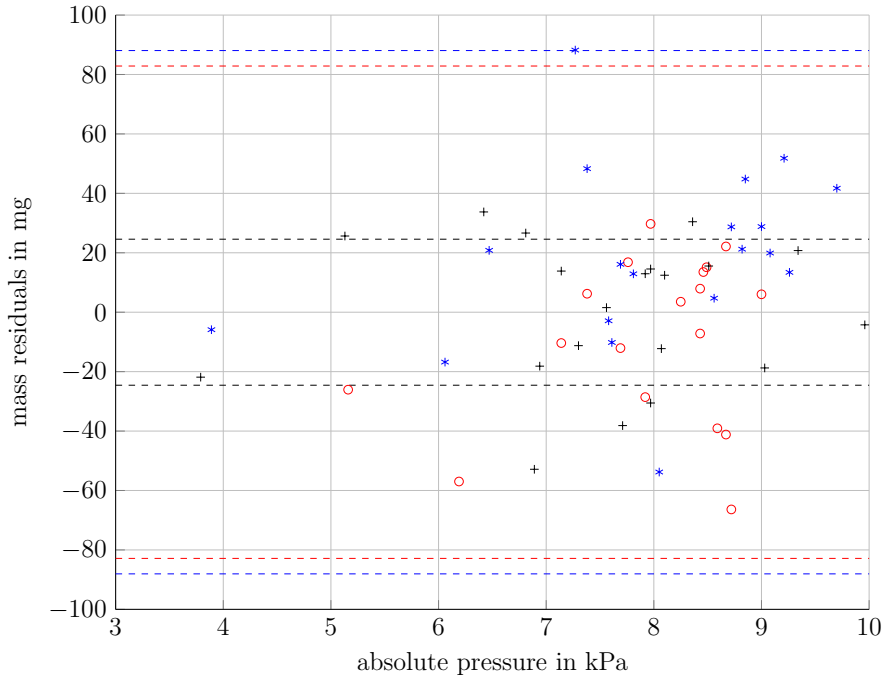


Figure 24: **Mass residuals for different nitrogen flow rates.** Red dataset...nitrogen flow of 0.2 l/min, blue datapoints...nitrogen flow of 0.1 l/min, black data-points... no nitrogen flow, dashed lines...one standard deviation. The mean value and the standard deviation for this data is shown in table 23.

flowrate <i>l/min</i>	$\mu$ <i>mg</i>	$\sigma$ <i>mg</i>
0.2	1209	83
0.1	1184	88
0.0	1174	25

Table 23: Standard deviation and mean value of the mass for the different flow rates

As shown in figure 24 and table 23 the standard deviation of the mass is significantly smaller (25mg) if the nitrogen flow is deactivated. The mean value of the sampled mass is between 1174mg and 1209mg for the different flow rates.

### 3.3 Verification Version 2

#### 3.3.1 Analyzes of the dynamic behavior of the weight sensor

In Version 2 the sampled mass depends on the sampling time. To determine the required sampling time (Table 7) for a specific mass, the sampling time was varied between 100ms and 1s. The sampled mass was measured and these data were analyzed by calculating a linear fit. Figure 25 shows the datapoints and the corresponding linear fit.

The linear fit ( $R^2 = 0.997$ ) was calculated with Matlab over the dataset from 200ms to 1000ms and produced the following solution:

$$m = 2.011mg/ms \cdot t + 195.7mg \quad (52)$$

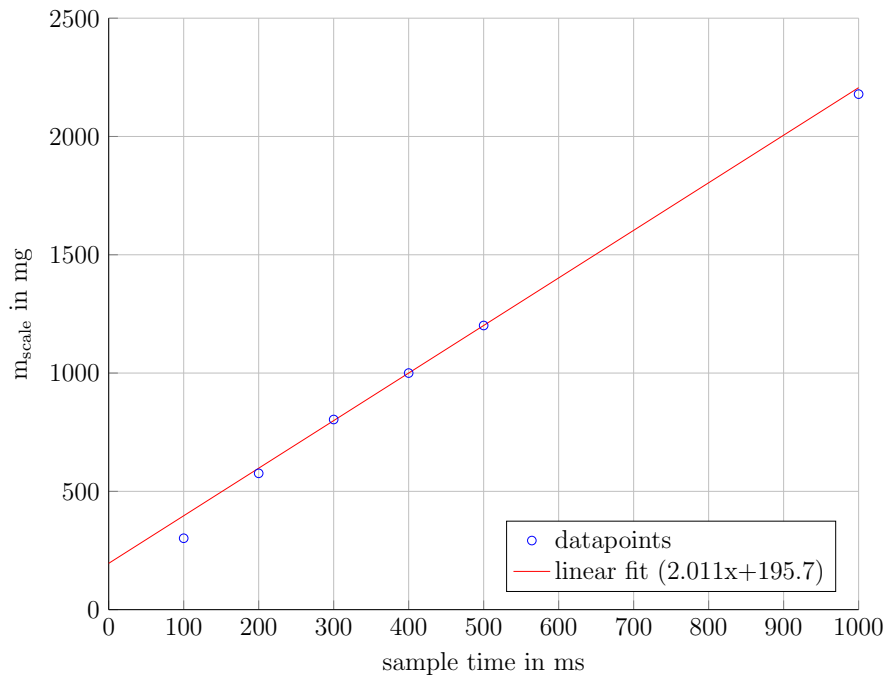


Figure 25: Mass in relation to the sample time

As shown in figure 25 the datapoints at 300, 400 and 500ms are on the curve of the linear fit. The datapoints at 100ms, 200ms and 1000ms differ from the curve.

In the next instance the step response of the system was analyzed (Section 2.7.6). This is necessary to obtain a better understanding of the dynamic behavior of the weight measurement.

During the injection of the fluid into the sampling container a strong transient acceleration acts on the container, which results in mechanical oscillations of the weight sensor and consequently to oscillating mass readings (Figure 26).

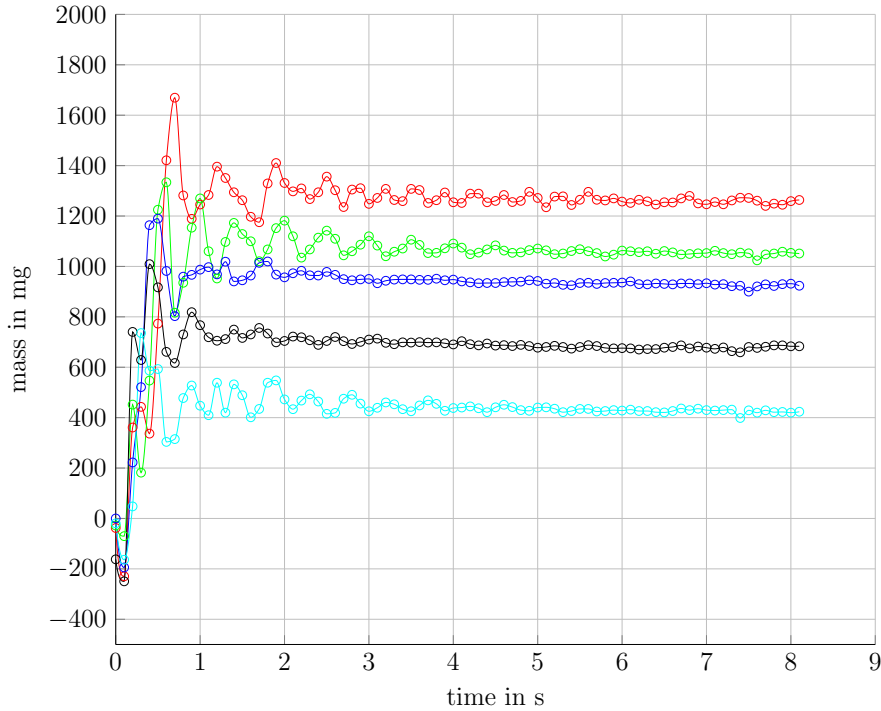


Figure 26: **Step response of the mass readings** red datapoints... $t_{sample} = 500ms$ , green datapoints... $t_{sample} = 400ms$ , blue datapoints... $t_{sample} = 300ms$ , black datapoints... $t_{sample} = 200ms$ , cyan datapoints... $t_{sample} = 100ms$ , solid lines...cubic interpolation for the corresponding dataset

Due to the oscillation there is a difference in the result, when the measurement occurs. This is shown in figure 27. The difference between the sampled and measured mass is the lowest for the calibration point (waiting time =1s, sampled mass= 1200mg)

Data were fitted (linear fit over whole dataset) using Matlab:

$$m_{5sec} = 0.044mg/ms \cdot t_{sampling} + 49.499mg \quad (53)$$

$$m_{1sec} = 0.047mg/ms \cdot t_{sampling} + 57.615mg \quad (54)$$

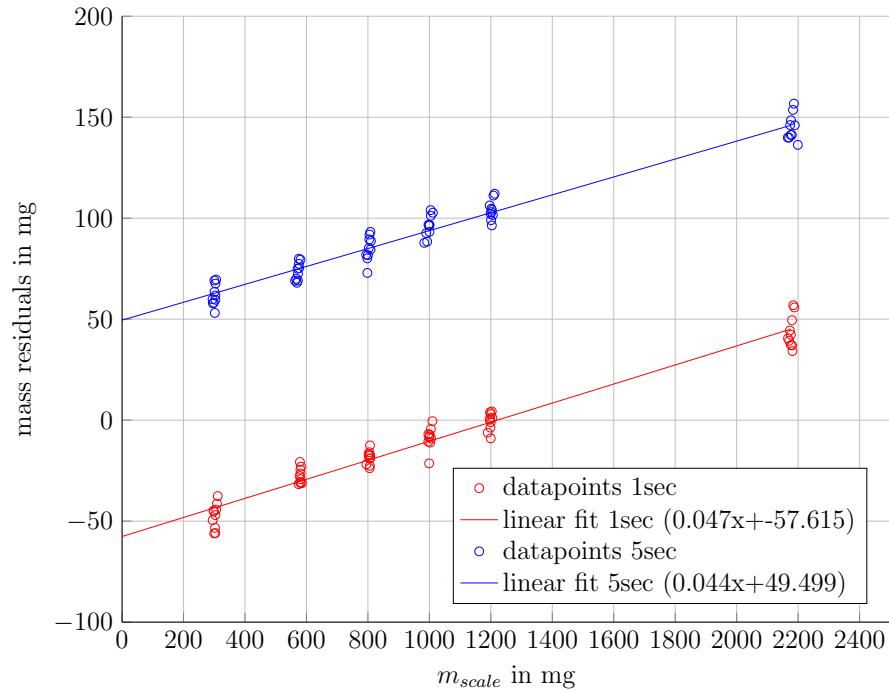


Figure 27: **Mass residuals for different waiting times.** The red dataset...waiting time=1s, blue dataset...waiting time=5s, Solid lines... linear fit of the corresponding dataset.

### 3.3.2 Temperature drift

For the verification of the thermal drift the device was put into a closed environment containing a heat source, as described in section 2.7.7).

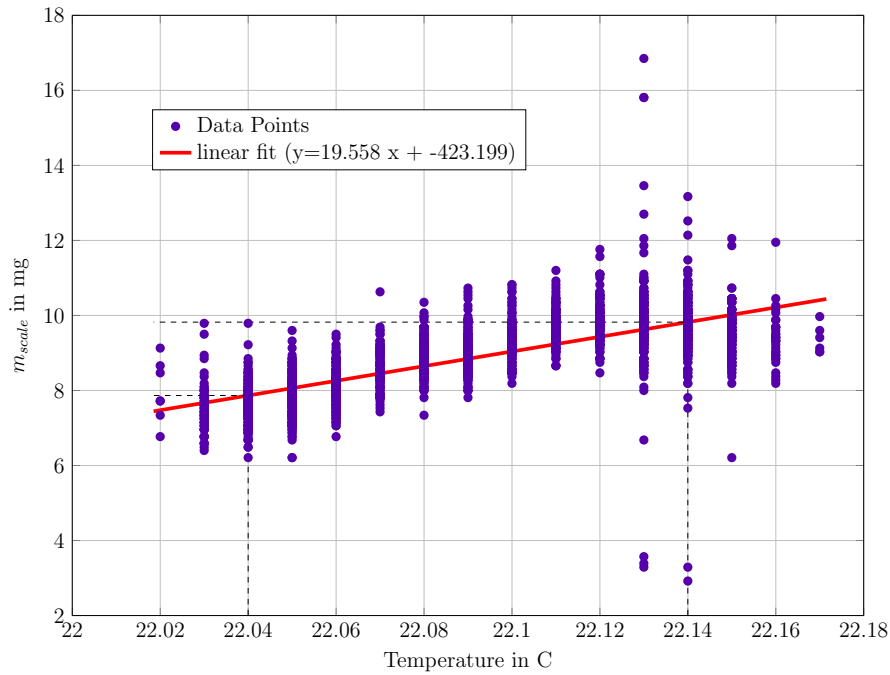


Figure 28: **The relation of the weight sensor output in relation to the ambient temperature in a closed environment.**

Figure 28 shows the drift of the sensor without an additional heat source. Only the own heat of the device was used, therefore the temperature range of this experiment was only from  $22.02^{\circ}C$  to  $22.18^{\circ}C$ .

From the data a linear fit with Matlab was calculated:

$$m = 20mg/^{\circ}C \cdot T - 423mg \quad (55)$$

For the second experiment a heat source was used to get a higher temperature range ( $19.5^{\circ}C$  to  $24.0^{\circ}C$ ) as shown in figure 29.

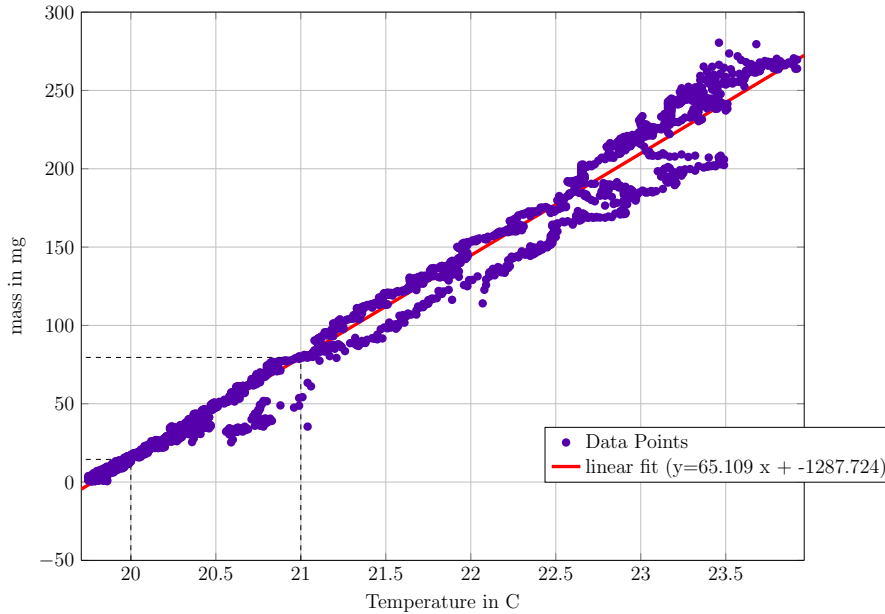


Figure 29: The weight-sensor output in relation to the ambient temperature with a heat source below the sensor

For this experiment the linear fit looks like:

$$m = 65mg/^{\circ}C \cdot T - 1288mg \quad (56)$$

The 2 calculated linear fits differ. The linear fit of the second experiment with the heat source has a higher gain (65mg vs 24mg) and a higher negative offset (-1288mg vs -423 mg). Both experiments show that the temperature change during future experiments have to be kept as low as possible.

### 3.3.3 Verification of the mass measurement

To verify the accuracy of the weight sensor the following experiment was carried out as described in section 2.7.2. For this purpose 192 samples were drawn over a timespan of two days (96 samples per day). The sampling time ( $t_{sample}$ ) was set to 500ms and the mass ( $m_{scale}$ ) was measured with an analytic balance and by the device ( $m_{device}$ ). The relative residuals occurring were calculated and plotted in figure 30.

To obtain accurate values, 10 samples were drawn by the device for calibration, before carrying out the experiment on the first day.

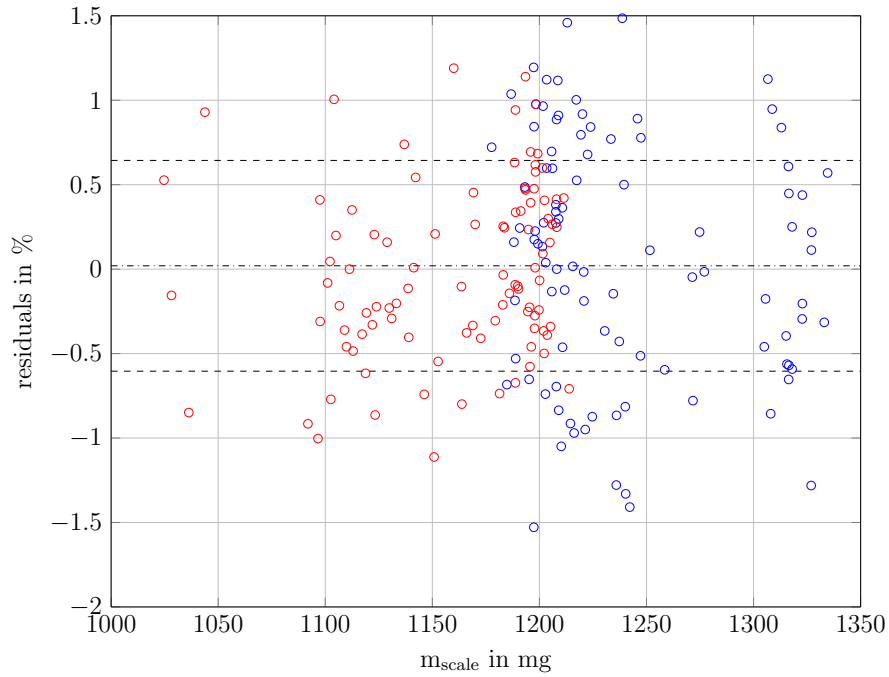


Figure 30: **Relative mass residuals in relation to the mass  $m_{scale}$ .** red circles...data of the day 1, blue circles...datapoints of day 2, solid black line... mean value, black dashed line...  $\pm$  one standard deviation

$\mu$	$\sigma$
%	%
0.01	0.62

Table 24: Standard deviation and mean value of the mass residuals

Figure 30 shows that 99% of the datapoints are between  $\pm 1.5\%$ . The mean value of the residuals is at 0.01 which shows, that the calibration is very accurate. The standard deviation of the residuals is under 1%.

The residuals are also plotted in relation to pressure as shown in figure 31. It shows two clusters which relates to the day the samples were drawn.

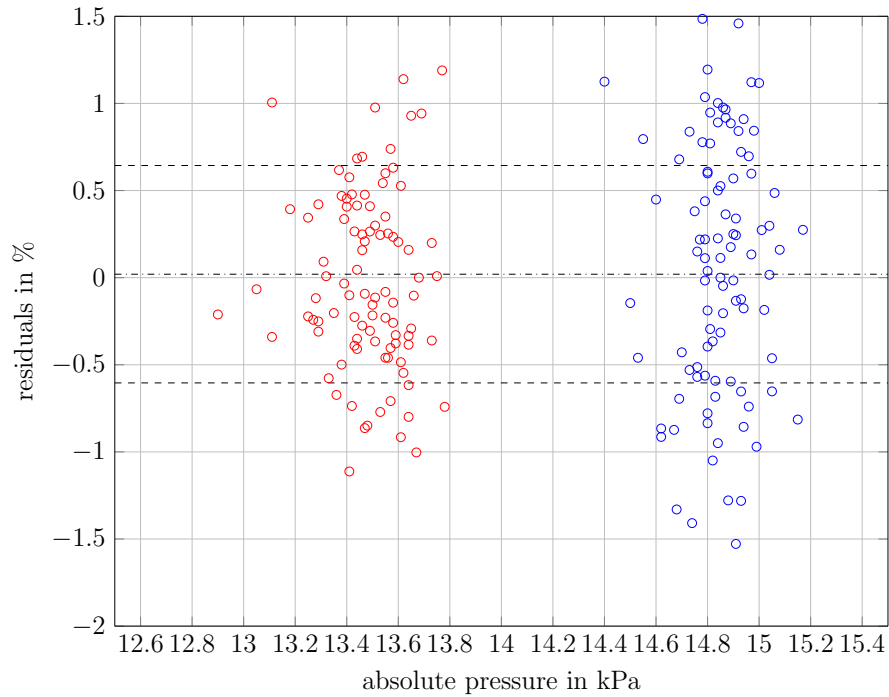


Figure 31: **Mass residuals in relation to the residual pressure after evacuation.**  
 red circles...data of the day 1, blue circles...datapoints of day 2, solid black  
 line... mean value, black dashed line...  $\pm$  one standard deviation

To show the dependency of the mass in relation to the residual pressure after evacuation the same data were plotted in figure 32. It shows two clusters corresponding with the day the sample was drawn. The cluster with the higher residual pressure after evacuation leads to a higher mass  $m_{scale}$

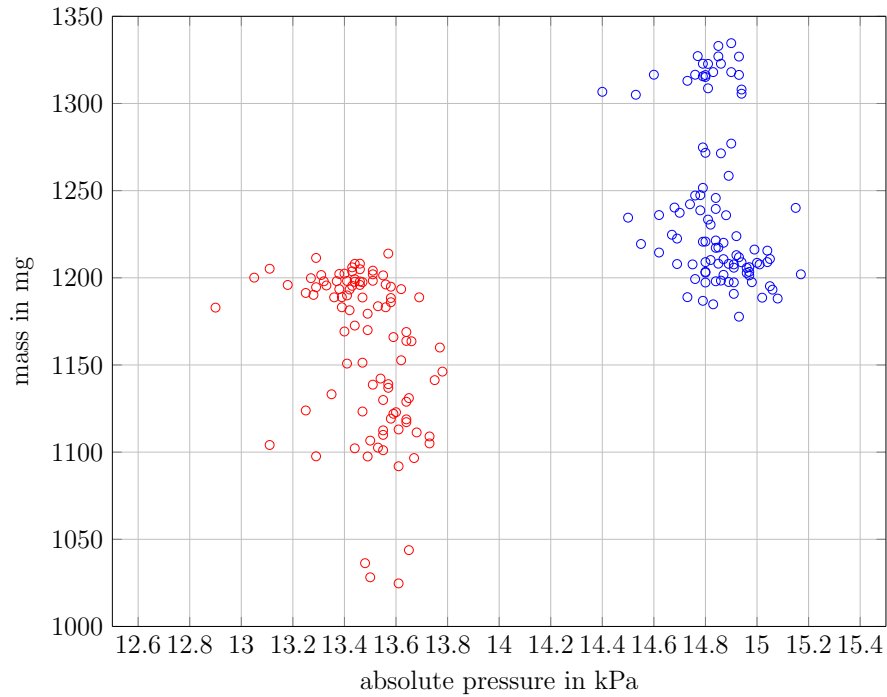


Figure 32: Mass in relation to the residual pressure after evacuation. red circles...data of the day 1, blue circles...datapoints of day 2

### 3.3.4 Verification of the carry over

To estimate the cleaning volume needed for a carry over lower than 5%, the experiment was carried out as described in section 2.7.3.

For the first experiment as sampling tube  $ST_{ST275}$  (Table 2) was used and the results are shown in figure 33. There are two datasets for the repeated experiments with unbuffered solutions (TW, TW-CR) and one with buffered solutions (PBB, PBB-CR) (Table 4).

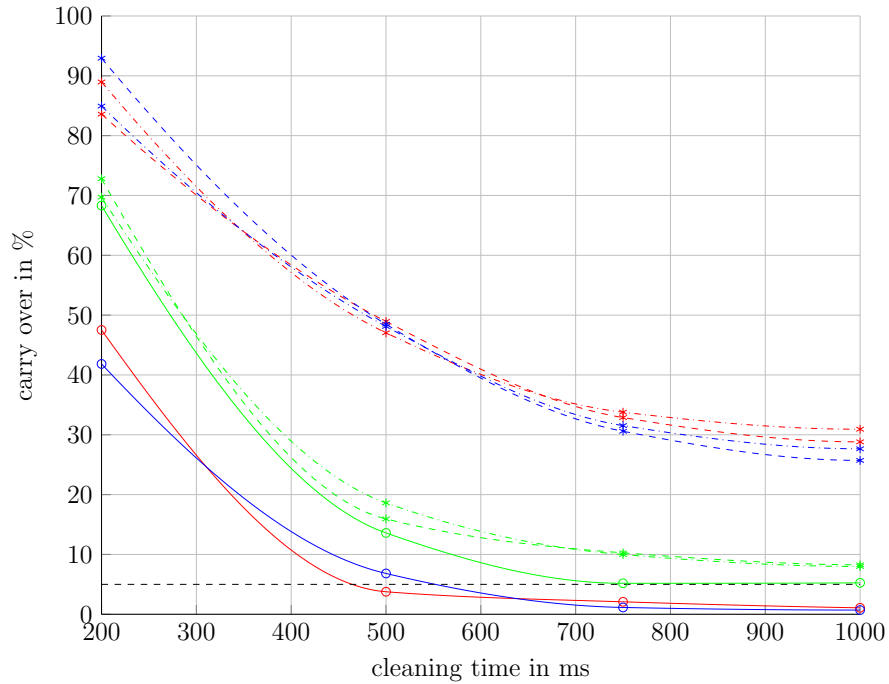


Figure 33: **Carry over in relation to the cleaning time.** red circle...first dataset for switch from TW-CR to TW, red stars...first dataset for switch from TW to TW-CR, blue circle...second dataset for switch from TW-CR to TW, blue stars...second dataset for switch from TW to TW-CR, green circle...dataset for switch from PBB to PBB-CR, green stars...dataset for switch from PBB-CR to PBB, colored solid lines..cubic interpolation for the corresponding dataset(circles) colored dashed lines..cubic interpolation for the corresponding dataset(stars), black dashed line...required 5% threshold

By using the data from the buffered solutions, the carry over reached a value between 5% and 10% for a cleaning time of 750ms. (figure 33) The experiment also showed that the curves with the buffered solutions were more similar than the curves of the unbuffered solutions. The reason for this could be a change in pH of the unbuffered solutions during the experiments. Therefore only the buffered solutions were used in the following experiments and the cleaning time was fixed to 750ms.

Next different sampling tubes (Table 2) were tested to improve the carry over. For this purpose the different sampling tubes were installed and the experiment carried out as described in section 2.7.3. The cleaning time was set to 750ms. The results for the different sampling tubes are shown in figure 34.

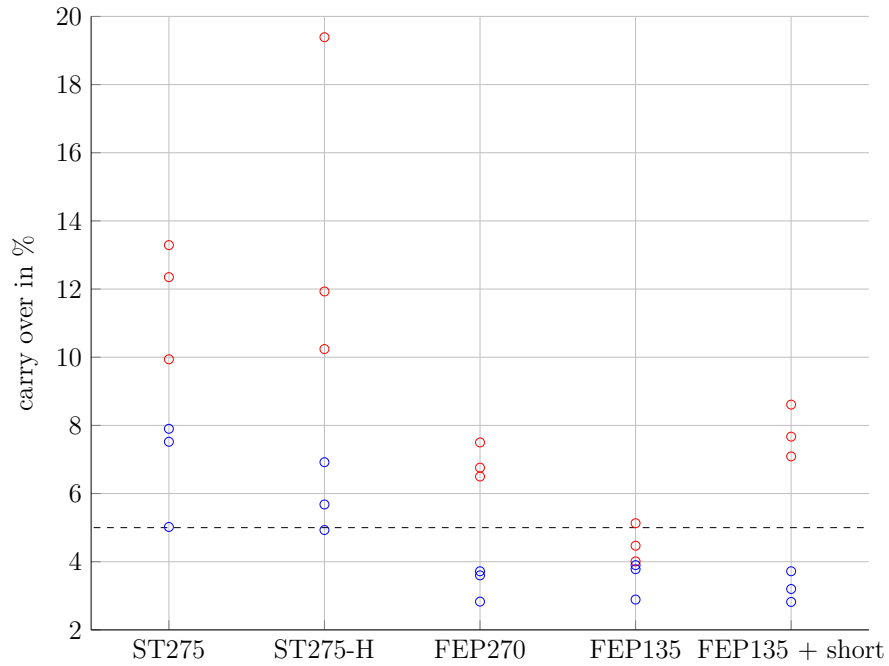


Figure 34: **Carry over of different sampling tubes (Table 2).** red circle...dataset for switch from PBB to PBB-CR, blue circle...dataset for switch from PBB-CR to PBB, black dashed line...required 5% threshold

Figure 34 shows that the hydrophobic sampling tube ( $ST_{FEP270}$ ) reduces the carry over from ( $ST_{ST275}$ ) to under 8%.

To estimate the improvement of using the hydrophobic sampling tube  $ST_{FEP270}$  an other switch experiment was carried out. Therefore the sampling tube  $ST_{FEP270}$  was used and the cleaning time was varied between 200 and 1000 ms. The carry over of this experiment was then compared to the data of the sampling tube  $ST_{ST275}$ . The result is shown in figure 35.

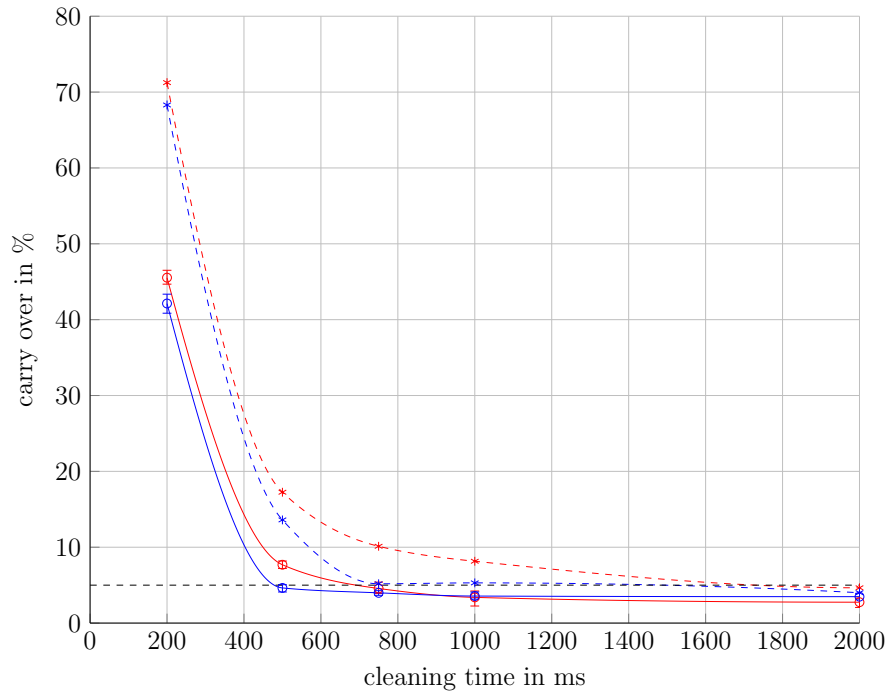


Figure 35: **Carry over of the sampling tube  $ST_{ST275}$  and  $ST_{FEP270}$ .** red circle...switch from PBB to PBB-CR with  $ST_{ST275}$ , red stars...switch from PBB-CR to PBB with  $ST_{ST275}$ , blue circle...switch from PBB to PBB-CR with  $ST_{FEP270}$ , blue stars...switch from PBB-CR to PBB with  $ST_{FEP270}$ , solid lines..cubic interpolation for the corresponding dataset(circles) dashed lines..cubic interpolation for the corresponding dataset(stars), black dashed line...required 5% threshold

As shown in figure 35 the carry over using the  $ST_{FEP270}$  sampling tube is lower than the the carry over using  $ST_{ST275}$ . For  $ST_{FEP270}$  a carry over lower than 5% is reached after a cleaning time of 750ms. This is better than in the previous experiment (Figure 33) but not significant.

### 3.3.5 Verification with biological samples

Finally the system was tested within a bioreactor using biological samples to show that the system delivers reliable data for the sampled mass under a realistic laboratory environment.

For that reason samples were drawn into Falcon-tubes containing 10ml methanol (described in section 2.7.5). After approximately 8500 seconds the nitrogen flow was increased from 2l/min to 3l/min and the rotor speed was increased from 300rpm to 1000rpm.

In figure 36 the sampled mass is plotted in relation to the time when the sample was drawn. It is obvious that most of the samples are between 1300mg and 1400mg. After the changing of the nitrogen flow and stirrer speed the sampled mass decreases and an outlier occurs (at  $t=10628s$ ).

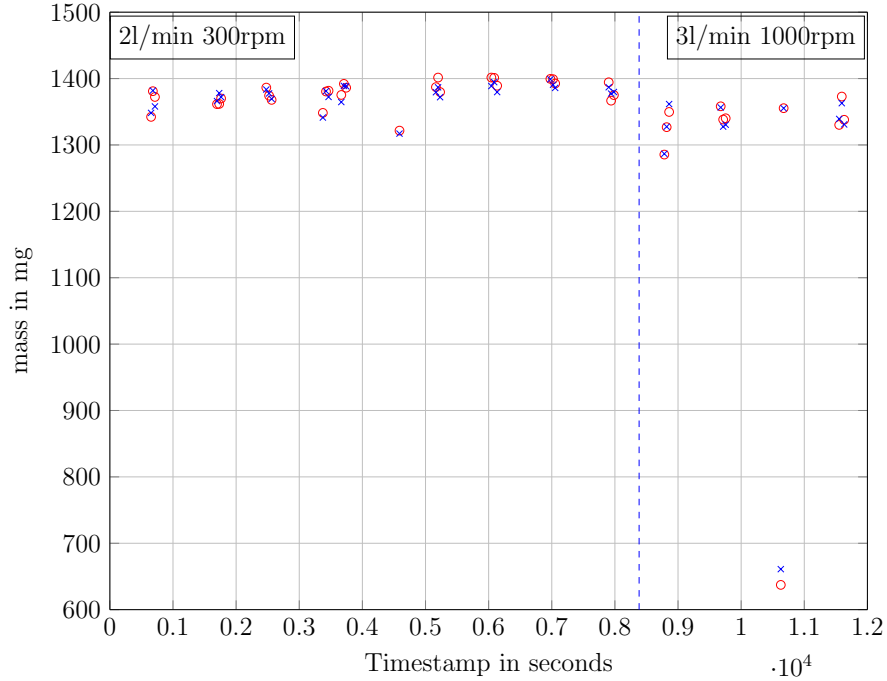


Figure 36: **Sampled mass over time with a change in the nitrogen flow and stirring speed.** blue stars... $m_{device}$ , red circles... $m_{scale}$ . The switch of the flow rate and stirrer speed is shown by a vertical blue dashed line.

$\mu$	$\sigma$
%	%
0.08	0.83

Table 25: Standard deviation and mean value of the residuals of the sample in the Falcon-tubes with 10ml methanol prelaod. (F1)

The residuals during this experiment are shown in figure 37. Despite of the outlier all datapoints are between  $\pm 1.5\%$  and the standard deviation is at  $0.83\%$ .

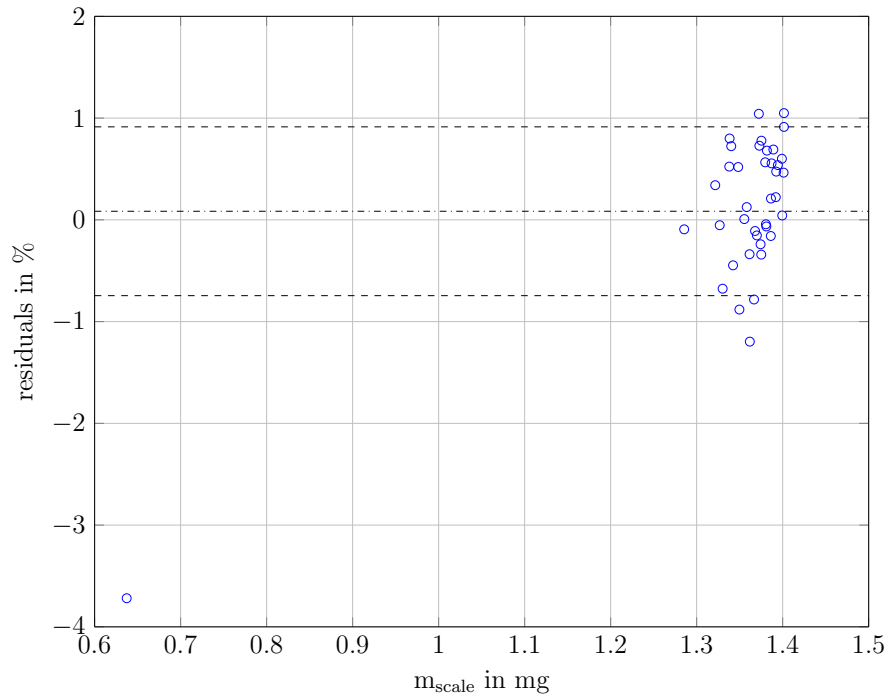


Figure 37: residuals of the sample in the Falcon-tubes with 10ml methanol prelaod. (F1) blue circles...datapoints, green dashed line...mean value of the residuals, red dashed line...  $\pm$  one standard deviation

To show the accuracy of the device outside of the calibrated range the Falcon-tubes without preload (F2) were used (residuals in figure 38) The mean value is lower ( $-2.54$ ) as in the calibrated range. All data are between  $\pm 0.6\%$ .

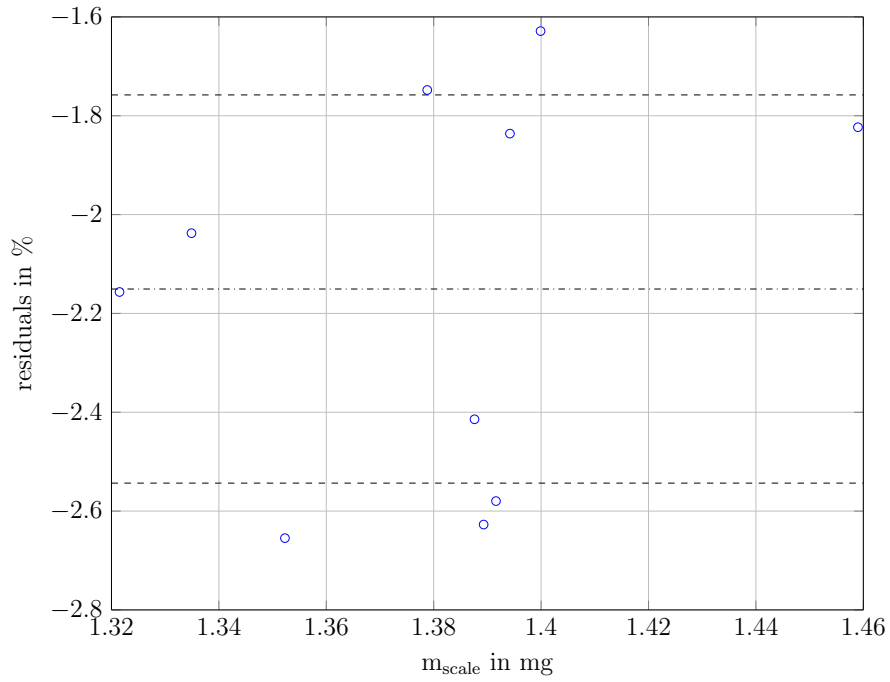


Figure 38: residuals of the sample in the Falcon-tubes without preload (F2) blue circles...datapoints, green dashed line...mean value of the residuals, red dashed line...  $\pm$  one standard deviation

$\mu$	$\sigma$
%	%
-2.54	0.39

Table 26: Standard deviation and mean value of the residuals of the sample in the Falcon-tubes without preload. (F2)

## 4 Discussion

The purpose of this master thesis was to develop a rapid sampler, which is capable of drawing a reproducible amount of liquid ( $1ml...10ml \pm 1\%$ ) from a bioreactor and transferring it into a sample container. The carry over should be better than 5% and the transfer of the sample should take less than 1s. To fulfill this conditions two devices were developed and assessed. The first one uses a volumetric cell (Version 1) and the second one measures the sampled mass (Version 2)

### 4.1 Technical requirements

#### 4.1.1 General

For the electrical design of both of the devices some issues had to be considered.

The valves have a 5 times higher switching current, as during the closed phase (0.5A). Due to this fact it is important to limit the maximal load for the power supply by avoiding to change the state of more then one valve at the same time. If more valves have change their state a small (50ms) delay has to be inserted.

To enhance the stability of the power supply, during this event, two additional  $1\mu F$  capacitors (MKT 1822-510-255, Vishay,USA) were added next to the connector off the valve box and the weight-sensor.

Also during the switching of the valves the mass measurement was disturbed. To enhance the stability of the mass measurement, the weight-sensor PCB has its own 5V power supply with a liner regulator. Also the digital and the analog ground are separately routed to the main device and connected to the power supply too.

#### 4.1.2 Pressure sensor

The experiments (Figure 19) indicate that a pressure measurement for the vacuum is necessary. Consequently a pressure sensor was added with a small amplifier. This amplifier consists of a discrete build instrumentation amplifier and a differential amplifier. The amplifier was build discrete to get the option to tweak every resistor of the designed pcb. But for improvement of the performance an instrumentation amplifier ICs can be used. It is necessary, that the instrumentation amplifier can be supplied asymmetrically ( $V_{++} = 12V$  and  $V_{--} = 0V$ ), otherwise a charge pump would be required.

### 4.1.3 Weight sensor (Only Version 2)

Due to the requirement, that the sampled mass should be monitored with an accuracy of 10mg, a precise mass measurement was developed for Version 2.

#### Resolution

To accomplish a resolution better than 2mg a sigma delta ADC with 22bit (MCP3550) was chosen. The 22bits are distributed between  $\pm U_{Ref}$ . The signal has to be amplified to this range to get an optimal resolution. To fulfill this an instrument amplifier with a gain of 50 was used.

#### Linearity

To allow for an easy calibration of the weight-sensor, by only using gain and offset, the components used, should have a negligible non-linearity. This was accomplished by using an instrument amplifier with a non-linearity of 3.3ppm and the ADC with a non-linearity of 2ppm.

#### Noise

Moreover the noise of the weight-sensor was important. For a practicable measurement the noise should be as low as possible. Due to this issue all components were chosen for their very low noise level. As reference voltage for the ADC and instrument amplifier a low noise voltage reference was used, and also for the bridge a separate low noise voltage reference was used. To reduce noise coupling over the power supply of the PCB, the weight-sensor is supplied by a separate 5V voltage, which is generated by a voltage reference (LT1431). Also the digital and analog ground are separated and routed over 2 different wires to the ground of the power supply.

The calculation (Equation 29) shows that the most important sources of noise are the resistors  $R_1$  and  $R_{10}$  ( $B_{R1,Noise} = B_{R10,Noise} = 6.45$ ) and the instrument amplifier ( $B_{IAmp,Noise} = 3.82$ ). If the quality of the mass measurement has to be improved the following options should be considered:

- The values of the resistors ( $R_1$  and  $R_{10}$ ) for the Sallen-key filter have to be decreased ( $U_{Noise,R} \propto \sqrt{R}$ ). To keep the filter frequency constant, the values of the capacitors ( $C_3$  and  $C_{11}$ ) has to be adapted.

- Using an instrumentation amplifier with a lower input voltage noise (currently  $0.6\mu V_{pp}$  for a bandwidth of 10Hz). For example AD8229HDZ with an input noise of  $1nV\sqrt{Hz}$  and an output noise of  $45nV\sqrt{Hz}$ . [13]

### Temperature drift

An other important parameter is the temperature drift. A thermal drift can lead to invalid mass values, if the temperature changes during the measurement. So, if there was the choice between two or more components with the same noise, the one with the lowest temperature drift was chosen. To reduce the thermal effects of the anti aliasing filter between the ADC and the instrumentation amplifier C0G Capacitors (GRM31C5C1E104JA01L, Murata, Japan) and  $5ppm/^{\circ}C$  resistors (Vishay, USA) were used for the Sallen-Key filter. The capacities of C0G capacitors have a low relationship between capacity and temperature ( $\delta C \leq 1\%$  between  $0^{\circ}C$  and  $50^{\circ}C$ ) or voltage ( $\delta C \leq 5\%$  at 5V). By using this capacitors and resistors the filters cut off frequency changes less than 5% over the temperature and voltage range.

The calculation shows that the instrument amplifier (LMP7701) has an offset drift of  $2.10/^{\circ}C$  and is responsible for the high thermal drift of  $2.35/^{\circ}C$  (Table 10).

It is important to point out, that due to the differential measurement of the mass, the offset drift of the instrument amplifier only poses an issue for the temperature change between the reference measurement DAQ1 and mass measurement DAQ2 (Table 7). For example if the temperature stays constant it will result in the same error in the reference and in the mass measurement. Due to the subtraction of the two results the offset is compensated. If the temperature changes only the difference in the offset between these two measurements will not be compensated. The timespan between this DAQ1 and DAQ2 is 6 seconds for a sample volume of 1ml and as the results shows the occurred temperature change during the experiments did not pose an issue.

To improve the thermal behavior there would be four options:

- Replace the instrument amplifier for example AD8229HDZ [13]
- Keep the instrument amplifier at a constant temperature by using for example a peltie control.
- Measure the temperature of the instrument amplifier and calibrate the weight-sensor for the required temperature span.

- Implementation of a lock-in amplifier, where the bridge would be supplied with a carrier wave. The bridge will then modulate the amplitude of the signal according to the applied mass. This signal is then amplified by the instrument amplifier and digitalized by the ADC. The firmware has to demodulate the signal to calculate the applied mass. Due to the alternating current (AC) measurement the offset drift of the instrument amplifier is compensated.

### **Offset and gain accuracy**

The offset and the gain accuracy of the components were not so important through the possibility of a calibration and the differential measurement of the mass.

### **Conversion rate of the adc**

The current ADC needs 80ms for one conversion. If a faster one is used more samples could be averaged to reduce the noise. Due to the low conversion rate a fitting for the step response, was not tried for the currently obtained data but with a higher conversion rate a fitting should be considered.

#### **4.1.4 Thermal verification of the mass measurement**

To verify if the weight sensor could be used the thermal drift has to be validated.

For the thermal drift two experiments with a closed environment and a heat source were carried out as described in section 2.7.7.

The results in section 3.3.2 indicates that the drift may be much higher, than calculated. Without using a heat source (figure 28 ) the drift is approximately 6 times higher ( $20mg/^\circ C$ ) than calculated ( $3.36mg/^\circ C$ ). By using a heat source (figure 29) the drift is 20 times higher ( $65mg/^\circ C$ ).

The calculation of the thermal drift does not include the drift of the weight-sensors load cell, therefore the calculation is too low. But also both experiments are not very significant since these setups imply a few challenges:

- The temperature range of the first experiment is very low ( $0.12^\circ C$ ).
- The activation of a heat source leads to an airflow. If this airflow is obstructed by the weight sensor, it will result in a force, which will lead to disturbed data. This hypothesis was not tested during this master thesis.

To obtain more reliable data other measurement options would be possible.

- The device could be placed in a temperature chamber, which generates a nearly homogeneous heat distribution over the whole chamber. This device also uses ventilators to distribute the heat, therefore there are still air fluctuations and vibrations from the ventilators.
- An other option would be to directly heat the bending beam, but it also poses the challenge to avoid the transmission of vibrations onto the sensor.

The execution of these options would be beyond the scope of this master thesis.

#### 4.1.5 Analysis of the dynamic behavior of the system for Version 2

##### Relation between sampling time and sampled mass

To understand the dynamic behavior of the system the relation between sampling time and sampled mass had to be analyzed. Also the step response of the weight sensor is important to determine a good delay for the mass measurement.

Figure 25 shows a nearly linear relation between sampling time (Table 7) and sampled mass. If we assume that the flow rate is constant the relation between sampling time and mass has to be linear.

But the mass of the sample, at a sampling time of 100ms, is lower than the linear fit predicts. The reason for this effect could be the acceleration of the liquid. At the beginning of the sampling process (step Sampling 2 in table 7) the flow will first be accelerated until it reaches a constant flow speed. This effect will lead to a lower volume than by assuming a constant flow. This effect is stronger for small sampling times, because the timespan of the acceleration stays constant, but the timespan, with the constant flow rate is reduced.

An other indicator for this effect is that the calculated flowrate ( $I_{flow} = 3.14ml/ms$ , Table 17) is larger than the one calculated by the linear fit (2.011ml/s), but this could be also due to simplifications of the model. These simplifications are the neglect of the Y connectors, compression of the tubes and pressure variations in the tubes.

Also the linear fit shows an offset of 195.75  $\mu$ l. This offset could arise due to emptying of the docking unit section ( $V_{Docking}$ ) during the step Sampling 4 (Table 7) which takes 200ms.

The instrument shows a stable correlation between sampling time and sampled mass for masses larger than 400 mg (sampling time >200ms). This is an important feature as the mass to be sampled is scaleable and can be calculated upfront (Equation 52).

### Step response of the mass measurement

During the sampling process, the liquid is bursted into the Falcon-tube and is then decelerated through the liquid in the Falcon-tube or the bottom, if the tube is empty. This results in a force, which leads to an oscillating step response (Figure 26). To obtain reliable data it is important to wait long enough until the system reaches a steady state again. This will occur after 5-7 seconds. Due to the fact, that this is a long time in comparison with the sampling time, this time has to be reduced. It also poses the issue, that the mass measurement of the weight-sensor may drift away due to thermal changes. Therefore it is better to reduce this time.

To fulfill this it is assumed that the system reacts similarly to a spring mass system. For that reason the frequency of the oscillation is similar for similar masses ( $\omega = \sqrt{\frac{k}{m}}$  where k is the modulus of the spring and according to this constant). It is also assumed, that the decay of the baseline after the sampling is akin for similar masses.

To get a valid mass value the system waits for a fixed waiting time (table 7), which is between 1-5s, before the measurement is executed. After this delay 10 values were taken. From this 10 the minimum and maximum are rejected (to remove outliers) and the other values are averaged. This results in a value, which has to be multiplied by a calibration factor to obtain the real mass value. This calibration factor has to be obtained by comparison of the masses measured by the device ( $m_{device}$ ) and the masses measured by the analytic scale ( $m_{scale}$ ). Under the assumption of Gaussian noise and a standard deviation of the mass measurement of 0.83% (Table 23), the accuracy of the calibration can be calculated as followed:

$$accuracy = \frac{standarddeviation}{\sqrt{calibrationpoints}} \quad (57)$$

Therefore by using 10 samples for calibration the accuracy of the calibration is 0.26%.

This method was then verified for different sample volumes and waiting times (figure 27). It shows that the error is linear with the sampled mass. Both lines for 1s and for 5s are nearly parallel. If it is assumed that the steady state is reached after 5s, then the error should be independent of the sampled mass. But both fits have nearly the same slope. Through this there must be an other still unknown reason.

This reason could be the non-linearity of the mass measurement. The components used for enhancing and converting the signal have a non-linearity of 3ppm to 2.5ppm and are therefore too weak to result in such a non-linearity, but the linearity of the bridge and the mechanical construction is unknown and can thus be the reason for the non-linearity.

An other reason could be the calibration of the mass measurement itself. It is only a factor which is multiplied with the measurement value. This means a lower value results in a lower mass. This could result in such a curve if the correct compensation should be an offset. With an offset the lower values would be relatively higher than the higher ones and the curve would start approaching a horizontal line. On the other hand due the differential weight measurement an offset compensation is automatically applied.

## 4.2 Knowledge of the mass

To get reliable informations about the metabolite concentration, it is important to know the volume of the sample. Therefore the sampled volume must not vary for different samples drawn (Version 1) or the volume of the sample has to be measured (Version 2). The goal was a accuracy of 1% which is comparable with uncertainties reported for commercial high precision single channel volume adjustable pipettes (e.g. from Eppendorf: model  $1mL - 10mL$  : 0.6% to 3% [2]).

### 4.2.1 Version 1

The obtain of a reproducible mass poses a few challenges:

- **The volumetric cell has to be equally filled for every drawn sample.**

Otherwise the sampled mass would vary. The experiment with the different filling times (figure 17) shows that a longer filling time does not necessarily lead to a higher mass reproducibility. The reason for this could be dead volumes which are not equally filled ore emptied during the experiments. For example the volumetric cell has corners at the connecting points to the tubing system. Also the tubing system itself has dead volumes ( $P_6$  and  $P_{11}$ ) shown as red area in table 6 step 2 (Cleaning). This dead volumes may get better filled if the filling time increases. Due to small differences in the vacuum this dead volumes may not get filled equally for every sample. Therefore the standard deviation of the sampled mass can increase with the filling time.

- **The volumetric cell has to be completely emptied.**

Otherwise the remaining liquid in the volumetric cell lead to a higher carry over and a variation in the sampled mass. The experiment with different releasing times shows that a longer releasing time does not result in a better discharge of the system (Figure 18). The mean value indicates that in general the sampled volume is nearly the same for the different releasing times, but the standard deviation of the sampled mass is higher for a release time of 3 and 4 sec (13.58mg, 17.2mg) than as it is for 2 seconds (9.3mg). The reason for this could be dead volumes of the volumetric cell and of the tubing system. The dead volumes ( $P_3$  and  $P_{10}$ ) shown as red area in table 6 step 6 are getting completely filled during the cleaning procedure, but during the sampling process they are not emptied completely. An increasing of the releasing time could lead to better emptying of this section, but due to vacuum fluctuations this area may not be emptied reproducibly.

- **The sampled volume is affected by the pressure difference.**

The vacuum has to be below 13 kPa absolute pressure to obtain a reliable mass of approximately  $1220 \text{ mg} \pm 10 \text{ mg}$  (figure 19 ). With increasing absolute pressure, the relative pressure decreases and the sampled mass varies more. This increase may increase the variation of the filling degree of the volumetric cell. This sensitivity to pressure differences also imposes a challenge if the air pressure changes. To compensate for this issue for every experiment additional samples have to be drawn to obtain the information how much liquid is sampled and if the sampled mass is reliable.

Additionally as shown in figure 23 it is necessary to open the cultivation vessel, to allow a pressure equalization with the environment, otherwise the variance of mass of the drawn samples increases (27mg to 39mg).

- **Gas bubbles affects the sampled volume.**

Under process conditions by using a bioreactor with nitrogen flow the variation of the mass increases (Figure 24, table 23). If the nitrogen flow is disabled the standard deviation is the same as for the opened flask (25mg), but with the activation of the nitrogen flow the deviation increases to 83mg at a flowrate of 0.2l/min. The reason for this are gas bubbles, which are created by the nitrogen flow. If the device draws a bubble into the volumetric cell, it will occupy space and the sampled mass will be too low. Therefore the nitrogen flow has to be deactivated to enhance the reproducibility of the drawn volume, but this is not an option if the cultivation environment should stay in a steady state.

In conclusion the best filling and emptying time was determined to be 2 seconds and due to the pressure dependency it is required to draw additional samples to determine if the sampled mass is reliable. Furthermore the sample source has to be opened.

#### 4.2.2 Version 2

For Version 2 it was important that the difference between the mass measured by an analytic balance ( $m_{scale}$ ) and the mass measured by the device ( $m_{device}$ ) is lower than 1%. As already discussed (section 4.1.5) the rapid sampler has to be calibrated for the needed mass, but there are still a few other challenges:

- **Independence of the residuals from the sampled mass**

As shown in figure 30 there is no relation between the sampled mass and the variance of the residuals. The mean value of the residuals is 0.02% and the standard deviation is 0.63%. This means the mass measurement of the sampling device is better than the required 1%. Also there is no significant difference in the distribution of the samples with lower and higher mass.

- **Independence of the mass measurement from the applied vacuum**

Figure 31 shows that the reliability of the mass measurement is independent from the applied pressure difference.

- **Reliable mass measurement at different air pressure**

There is a correlation between the mass and the day the samples were drawn (Figure 32). Furthermore with the same sampling time applied, the mass values are distributed over a range of 350mg. This means that it is necessary to use a mass measurement to determine the mass of the sample. It is not possible to predict the sampled mass only via the sampling time and the applied vacuum.

According to the Hagen-Poiseuille equation a higher pressure difference should lead to higher mass values. The mass values in figure 32 indicates the opposite. But the atmospheric pressure in Graz can change for more than 3kPa (Figure 39). This indicates that the air pressure has changed more than the difference in vacuum during these two days. To estimate the volume of a drawn sample it would have been also necessary to measure the air pressure in the bioreactor. This was not done during this master thesis but it should be considered for future developments.

- **Vibrations, air flow fluctuation and condensation have to be avoided**

Under process conditions the standard deviation of the mass measurement error

increases to 0.8% (Figure 37). This is higher than under the ideal environment for verifying the mass measurement (Figure 30). The sensitivity of the measurement to vibrations from the surrounding and air flow fluctuation imposes an challenge for the measurement. Also the falcon tubes were cooled with carbon dioxide snow. Due to this low temperature, water humidity from the ambient air will inevitably condensate and will change the mass measured by the weight sensor. To avoid this, condensed water at the tube wall was removed before connecting the falcon tube to the docking unit. To obtain a correct reference measurement with the analytic balance the samples had to return to room temperature and had to be shortly opened to equalize the air pressure inside the tube with the ambient pressure, otherwise the differences in the air densities would affect the measurement. For example the density of air is approximately  $1.20\text{kg}/\text{m}^3$  at a temperature of  $20^\circ\text{C}$  and  $1.42\text{kg}/\text{m}^3$  at a temperature of  $-25^\circ\text{C}$  (airpressure=1013hPa) [32]. For the range of  $20^\circ\text{C}$  to  $-25^\circ\text{C}$  the difference in density is  $\delta\rho = 0.22\text{kg}/\text{m}^3 = 0.22\text{mg}/\text{ml}$ . After the sampling 40ml of the Falcon-tube are still filled with air, therefore the mass difference would be 8.8mg. Due to the fact that dry ice has a temperature below  $-78.5^\circ\text{C}$ , this effect could be even worse.

- **Nitrogen flow in the bioreactor shall not effect the mass measurement**

With an increase of the nitrogen flow rate the amount of gas in the liquid increases and therefore the likelihood to draw gas bubbles increases. This is shown in figure 36, where the sampled mass decreased slightly (for all samples except one less than 0.1g) after increasing of the nitrogen flow rate. But the mass measurement still works properly, which shows that the nitrogen flow does not pose an issue anymore. But if the amount of drawn gas, results in a sampled mass outside of the calibrated range, the accuracy of 1% is not given anymore. But despite this issue the mass measurement is still capable of detecting such an event (Figure 37). For example the drawing of a gas bubble with a volume of more than 0.5ml leads to a measurement error of  $-3.7\%$ .

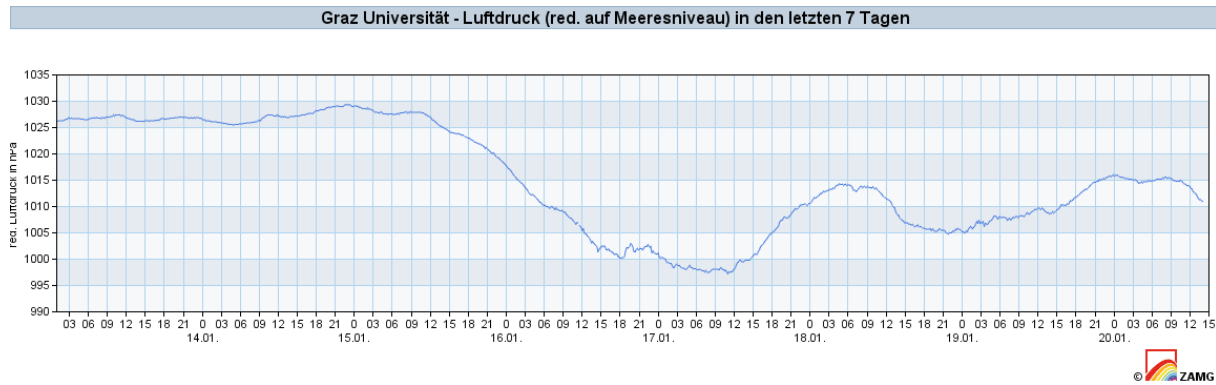


Figure 39: Air pressure measured in Graz at KFU [63]

### 4.2.3 Comparison of the two versions with other published devices

With the exception of [9,40], where a high-precision peristaltic pump was used to maintain constant fluid flow, transfer of a sample from the bioreactor to the sample container is driven by the pressure difference between the bioreactor and the sample container.

The flow rate will therefore depend on the pressure difference. Due to the fact, that the pressure conditions can change (pressure in bioreactor, air pressure, vacuum pressure) the flow rate will also change. This results in the necessity to measure some of the samples to obtain information about the drawn volume as experienced during the validation and already mentioned by other authors [8,56,57]. For Version 1 additional samples have to be drawn to determine the mass. Therefore there is no improvement to the already known devices. For Version 2 the mass is measured during sampling, therefore no additional samples have to be drawn and there is no need to determine the mass manually afterwards, which is a huge advantage in comparison to the already known devices.

Also all published devices [1,3,5,8–11,15,18,22,29–31,33,34,40,41,46,47,56,57,62] would not detect the occurrence of air bubbles or sample variations, without determining the mass afterwards. For Version 1 this is still an issue, but due to the integrated mass measurement in Version 2 this issue can be overcome.

## 4.3 Carry over

To analyze the metabolic activity over time, every sample drawn should only contain cells, which are taken from the reactor during the same interval (sample transfer time).

The part of older cells (carry over) in the sample has to be minimized. 5% is a factor widely accepted in the scientific community [22]. To analyze the carry over 2 solutions with different optical density were sampled alternately (Section 2.7.3).

Due to the optical measurement of the carry over experiments, it is important, that the absorption spectrum of the solution does not change during the transfer of the sample. If the spectrum changes the measured carry over will not be similar for a switch from TW to TW-CR and a switch from TW-CR to TW. (Figure 20) In this case the switch from TW-CR to TW led to a lower carry over (between 5% and 10% for a cleaning time of 500ms) than a switch from TW to TW-CR (approximately 50% for a cleaning time of 500ms). A possible reason for this could be a change in the pH value during the sample transfer. To compensate for this effect the carry over experiments for Version 2 were made with pH-buffered solutions (PBB and PBB-CR). With this buffered solutions, the carry over differs less than 10% between the two directions. The reason for the remaining difference could still be a slight pH dependency or an other still unknown effect. For Version 1 this effect was not corrected, because this effect was only understood later during the verification of Version 2.

### 4.3.1 Version 1

To improve the carry over of Version 1 different cleaning procedures were tested (figure 21):

- **Default:** As the starting point no special cleaning procedure was used. The filling time, during which the system was also cleaned, was set to 2s. The first sample drawn after changing the liquid results in a carry over of 19% to 75%
- **Air-Cleaning** To improve this behavior during the sample change the sample tube was pulled from the sample source and a sample was drawn from the air. This resulted in a better carry over (6% to 57%).
- **Longer filling time** An other experiment was to increase the filling time to 3s for the first sample after the sample source changed. This resulted in an carry over between 15% and 44%.

Each of the options tested are affected by the issue, that the carry over after the first sample is more than 5%. This means the first sample after a change in the liquid can not be used. The second sample after the change may be used, if the system is previously

cleaned with air (carry over below 5% for both directions). But this would also require that there is no change of the metabolite profile between the withdraw of this two samples.

This experiment also shows (table 21) that the air-cleaning procedure results in a smaller mass (1100mg vs 1192mg). This indicates that the volumetric cell is not completely emptied during the releasing step of the sequence (Table 6). This remaining amount of liquid is mixed with the next sample and results in the high carry over.

To improve this the dead volumes has to be reduced, which is very challenging for this approach.

### 4.3.2 Version 2

To improve the carry-over different sampling tubes were tested for a cleaning time of 750ms. (figure 34):

- $ST_{ST275}$  was the steel tube, which was also used for Version 1. The carry over by using this tube is between 5% and 14%
- For the  $ST_{ST275-H}$  a hole was made in the wall of the steel tube  $ST_{ST275}$ . The idea was to generate a turbulent flow. But the carry over was not improved.
- For the next tube a hydrophobic material was used ( $ST_{FEP270}$ ). The carry over was improved to 3% to 7%
- As next step the hydrophobic tube was cut half in length ( $ST_{FEP135}$ ) without changing the cleaning time. This resulted in a slightly better, but probably insignificant, cleaning of the sampling tube (carry over between 3% and 5%).
- If the cleaning time for the shorter hydrophobic tube ( $ST_{FEP135}$ ) is also adapted to the shorter tube length (cleaning time=375ms) the carry over is comparable with the one from the longer hydrophobic tube ( $ST_{FEP270}$ )

The reason for the improvement with  $ST_{FEP135}$  is that  $ST_{ST275}$  generates a laminar flow profile and  $ST_{FEP135}$  produces a more flatter flow profile.

For the steel tube ( $ST_{ST275}$ ) laminar flow dominates due to the small diameter and the adhesion between the wall and the water molecules. This will result in a high flow rate in the center of the tube and a much slower flow rate at the wall. Therefore most of the liquid used for cleaning flows through the center of the tube therefore the cleaning in the center is good but next to the wall the cleaning is not so efficient.

If hydrophobic material ( $ST_{FEP270}$ ) is used the adhesion between the water molecules and the wall is weaker and for that reason the flow profile becomes more turbulent. This results in a flatter flow profile than for laminar flow. Therefore the distribution of the liquid used for cleaning is more equal over the cross section of the tube, which results in a better cleaning in the area next to the wall.

To show this difference the carry over in relation to the cleaning time for the steel ( $ST_{ST275}$ ) and the hydrophobic ( $ST_{FEP270}$ ) tube was tested (figure 35). With a cleaning time of 750ms it is possible to obtain a carry over better than the required 5% by using the hydrophobic tube. By using the steel tube the carry over is only better than 10%.

### 4.3.3 Comparison of the two Versions with published devices

None of the published devices [1, 3, 5, 8–11, 15, 18, 22, 29–31, 33, 34, 40, 41, 46, 47, 56, 57, 62] specifies a carry over. They only specify the dead volume, which should be avoided or at least minimized to improve the carry over of the sample content from one to the next sample. Dead volumes are also a potential source for deposits and microbial contamination.

Version 1 of the device has a volume (Figure 15 compartment:  $P_6 P_7 P_{11}$ ) of  $723\mu l$  (Table 14), which can not be cleaned with liquid, but this section is emptied by air during the transfer of the sample into the sample container. This section is a potential source of carry over due to the issue, that liquid can remain in this section by sticking to the wall.

To improve this Version 2 has a little smaller volume ( $598\mu l$ , Table 14) due to geometric optimization. But the improved carry over ( $< 14\%$  vs  $< 75\%$ ) mainly results from the absence of the volumetric cell ( $1112\mu l$ ).

Both volumes are large in comparison to the sampling devices with little to no dead volumes ( $200\mu l$  [57]) but the two developed devices uses a cleaning procedure to compensate for this.

Also the published devices, which remove stagnant fluid by evacuation [18, 22] or flushing with cell broth, sterile air, and disinfection solution [5, 22, 62] have a smaller not flushed dead volume ( $50\mu l$  [22],  $50\mu l$  [62]).

Due to optimization of the tubing (for example smaller valve box mounted on top of the bioreactor) it could be possible to reduce the dead volume for both versions, but this would have exceeded the scope of this master thesis.

But as the experiments showed the carry over does not only depend on the dead volume. In addition the flow profile, as previously described, is also important. Only some of the published devices consider this [9, 46, 47], but the carry over was not assessed.

## 4.4 Sample transfer time

Due to the high turnover rates (for ATP 1.5 to 2s) a short transfer time of the sample is necessary. [9] In this master thesis the goal was a transfer time lower than 1s.

### 4.4.1 Version 1

For Version 1 of the device a volumetric cell is filled, with the whole sample and this sample is then transferred in the next step to the sample container (Table 6). The timing parameters for these steps were optimized for obtaining a reproducible mass and consequently the parameter times are quite long (filling time 2s, releasing time 2s). This results in a transfer time of 4.3s which does not fulfill the requirement. An improvement of this time to 1s is not possible due to the concept of the volumetric cell.

### 4.4.2 Version 2

In this version the tubing is first cleaned and thereafter the sample is directly drawn into the sample container (Table 7). After the cleaning phase the reactor side of the tubing ( $V_{Reactor} = 1203\mu l$ ) and the dead volume next to the valve RV ( $V_{P3} = 24\mu l$ ) contains the first part of the sample. This volume is altogether  $1227\mu l$ . Assuming a flow rate of  $2.011ml/\mu s$  (Equation 52) it takes 610ms to fill this section. After this the system waits for 400ms to clean the middle part and to switch different valves. After this the sample is transferred into the sample container (500ms for 1ml). Altogether this approach needs 1510ms to transfer a sample of 1.2ml. This is larger than the goal but it could be improved by considering a few different options:

- Reducing of the switching delays of the valves (currently 4x50ms)
- Developing a valve section with a smaller volume (currently  $V_{valve} = 100\mu l$ ) would result in a lower air cleaning time (currently 200ms).

- Developing a valve section, which can be mounted on top of the reactor would result in a reduced volume of the connection between the sampling tube and the valve section (currently  $V_{P1} = 660\mu l$ ).
- Also an increase in pressure difference would increase the sample transfer time.

With this improvements it would be possible to obtain a sample transfer time under 1s.

#### 4.4.3 Comparison of the two Versions and the literature

Most of the published devices have a transfer time lower than 1s (<500ms [9], 150ms [57], 640ms [15], 700ms [62], 200ms [46], 250ms [31], <1000ms [41], 100ms [22]).

But to achieve this property some of the devices need either a peristaltic pump [9] or over pressure [62] to enhance the flow rate. Some other devices need a special installation [31, 41, 57] and due to this installation the sample transfer time can be increased for example by reducing the volume of the sampling tube. The most similar device, which also operates with vacuum, has a transfer time of 100ms [22], but this device is mounted to the wall of the bioreactor. Due to this type of connection the volume of the sample tube is highly decreased and therefore the sample transfer time reduced. The developed device would be theoretical capable of such an installation but due to the need of modification of the bioreactor this was not tested. With the previously mentioned optimizations the transfer time will be strongly decreased but for such a low value the volume of the sampling tube ( $V_{P1} = 660\mu l$ ) has to be reduced, because it takes 330ms to fill this compartment under the assumption of a flowrate of 2ml/s.

#### 4.5 Amount of cleaning liquid

An other requirement is to minimize the amount of liquid needed for cleaning. A smaller amount of cleaning liquid means a more efficient use of the liquid from the bioreactor and therefore for drawing the same number of samples a smaller cultivation vessel can be used.

### **4.5.1 Version 1**

For Version 1 the whole volume of the tubing system is approximately 3.6 ml (Table 14) and 1.1ml of this volume is made up by the volumetric cell (Table 14). Due to the filling time (Table 6) of 2sec the volumetric cell is filled and the system is cleaned. Assuming a flowrate of 2ml/sec the amount of consumed liquid during this phase is 4ml. Only the volume in the volumetric cell is then sampled into the sample container. Therefore it requires 4ml of liquid to draw a 1.1ml sample.

Additionally the carry over requires the first sample to be dismissed. This results in additional 4ml, which are wasted.

Furthermore this approach requires that additional samples have to be drawn, where the mass is measured by an user. This results in additionally wasted liquid. Also it must be assumed that the system is stable in the volume of the transferred samples.

Together this system needs more than 8ml to obtain a sample of 1.1ml.

### **4.5.2 Version 2**

For Version 2 the whole volume is smaller. Here the volume is 1.9 ml (Table 14) only. The cleaning time is 750ms and if a flowrate of 2ml/s is estimated the amount of liquid needed to clean the system is 1.5ml.

In this case no additional liquid is wasted and the system needs 2.6ml of liquid to obtain a sample of 1.1ml.

## **4.6 Modification of the sample volume**

An other requirement is the possibility to change the sample volume in the range from 0.5ml to 10ml

### **4.6.1 Version 1**

For Version 1 the sample volume is related to the volume of the volumetric cell. Therefore the volumetric cell has to be changed for each required sample volume. Due to the change in the tubing system the cleaning and releasing time has to be optimized again and the carry over has to be validated again.

### **4.6.2 Version 2**

By using Version 2 the amount of liquid sampled can be easily adapted by a change of the sampling time (figure 25). The non linearity of the signal chain of the mass measurement requires a calibration (section 2.7.8) for the sampled liquid.

The volume can be adapted between 0.5ml (sampling time =200ms) and 100ml (sampling time=approximately 50s) in theory, but the withdraw was only tested between 0.5ml and 2ml (sampling time= 1s).

### **4.6.3 Comparison of the two versions**

For Version 1 the adaption of the sampling volume is quite difficult, but for Version 2 it is easily programmable. Due to this feature different volumes can be sampled ranging from 1 ml to 100 ml.

## **4.7 Installation**

Both of the devices (Version 1 and Version 2) can be connected at the head plate of a bioreactor [1, 3, 8, 29, 34]. Other published sampling devices are connected via special installation at the bottom [10, 11] or the sidewall of a bioreactor [ [5, 9, 10, 18, 22, 30, 33, 40, 41, 46, 47, 56, 57].

The connection to the head plate has the advantage that the cultivation vessel does not need to be modified to mount the rapid sampling device. This is especially a advantage for cultivation vessels made of glass, because for this type of mounting no modification of the bioreactor is necessary.

## **4.8 Other features**

Both versions of the device operate as required with vacuum. This bears the advantage that the reactor can be opened during sampling and it is not necessary to applying overpressure to the reactor.

None of the published devices [1, 3, 5, 8–11, 15, 18, 22, 29–31, 33, 34, 40, 41, 46, 47, 56, 57, 62] monitors any parameters during sampling. The developed device protocols the exact time the sample is drawn, the applied pressure and the measured mass (Version 2 only). This

information can be used to detect possible failures of the device (for example insufficient vacuum). The exact time and the measured mass can be used to compensate variances in the mass or execution time on the metabolite profile.

The timing protocol of both versions can be adapted by connecting the device per USB to a PC and 9 different timing protocols can be stored on the device. With this option a user can optimize the system, without knowledge about the firm- and hardware.

## 4.9 Conclusion

Version 1 is no mayor improvement to the already published devices, but Version 2 has the considerable advantage of the direct mass measurement, which detects variations in the sampled volume, without the need to measure the mass afterwards. But this device is also subject to a drawback; the dead volume is larger ( $598\mu l$  vs.  $50\mu l$  [22]) and sample transfer time ( $1510ms$  vs.  $100ms$  [22]). In future developments these drawbacks can be overcome.

The performance and the operating conditions for both devices are listed in the table 27 and below:

Parameter	Version 1	Version 2
Volume measurement	volumetric cell	mass measurement
Sample volume	1.2ml	0.5-100ml
standard deviation of the sampled volume	2%	0.63%
Transfer time	4.3sec	1.5sec
Cleaning volume	6.8ml	1.5ml
Carry over on the first Sample	< 57%	< 5%
Carry over on the second Sample	< 5%	< 5%
maximum air flow in the bioreactor	0.0l/sec	3l/sec
Installation position in the bioreactor	top	top

Table 27: Datasheet of the two different Versions

### Operation requirements for Version 1

- The pressure difference between the reactor and sample container has be kept constant.
- To determine the exact volume which is sampled, additional samples have to be drawn and measured.
- The whole system has to be cleaned after a change of the sample.
- The first sample after a change of the sampling liquid must not be used, due to the high carry over.

## **Operation requirements for Version 2**

- The weight sensor has to be calibrated for the required sampling mass.
- For a correct operation of the mass sensor, the Falcon-tube has to be cleaned from condensed water before inserting it into the device.
- The docking unit has to be fixed on a vibration free decoupled plate. For this purpose a granite plate on some vacuum tubes is sufficient.
- To avoid the impact of additional force on the sensor due to air flow the sensor should be shielded from the environment.

## 5 Literature

### References

- [1] Aragon AD, Allen C Quinones GA, Thomas J, Roy S, Davidson GS, Wentzell PD, Millier B, Jaetao JE, Rodriguez AL, and Werner-Washburne M. An automated, pressure-driven sampling device for harvesting from liquid cultures for genomic and biochemical analyses. *J Microbiol Methods*, 65:357–360, 2006.
- [2] Eppendorf AG. Eppendorf sop. 2013.
- [3] Schwaiger B, Hiller J, and Weuster-Botz D. Probenahmesystem für fluide proben. DE10314512A1:München TU., 2004.
- [4] Bonnie C. Baker. Matching the noise performance of the operational amplifier to the adc. *Analog Applications Journal*, 2Q, 2006.
- [5] Cannizzaro C. Device for automated bioreactor sampling. EP 1508791 A1:Ismatec SA L., 2003.
- [6] Oracle Corporation. Java. <http://www.java.com/>, 2012. [Online; accessed 23-03-2017].
- [7] Oracle Corporation. Netbeans. <http://netbeans.org/>, 2012. [Online; accessed 23-03-2017].
- [8] McCloskey D, Gangoiti JA, King ZA, Naviaux RK, Barshop BA, Palsson BO, and Feist AM. A model-driven quantitative metabolomics analysis of aerobic and anaerobic metabolism in e. coli k-12 mg1655 that is biochemically and thermodynamically consistent. *Biotechnol Bioeng*, 111:803–815, 2014.
- [9] Visser D, van Zuylen GA, van Dam JC, Oudshoorn A, Eman MR, Ras C, van Gulik WM, Frank J, van Dedem GW, and Heijnen JJ. Rapid sampling for analysis of in vivo kinetics using the bioscope: a system for continuous-pulse experiments. *Biotechnol Bioeng*, 79:674–681, 2002.
- [10] Weuster-Botz D. Sampling tube device for monitoring intracellular metabolite dynamics. *Anal Biochem*, 246:225–233, 1997.
- [11] Harrison DE and Maitra PK. Control of respiration and metabolism in growing klebsiella aerogenes. the role of adenine nucleotides. *Biochem J*, 112:647–656, 1969.

- [12] Analog Devices. Ad586 high precision 5v reference. <http://www.analog.com/media/en/technical-documentation/data-sheets/AD586.pdf>, 2005.
- [13] Analog Devices. Ad8229 1nv low noise instrumentation amplifier. <http://www.analog.com/media/en/technical-documentation/data-sheets/AD8229.pdf>, 2011.
- [14] Franco-Lara E and Weuster-Botz D. Estimation of optimal feeding strategies for fed-batch bioprocesses. *Biopro Biosys Eng*, 27:255–262, 2005.
- [15] Schädel F and Franco-Lara E. Rapid sampling devices for metabolic engineering applications. *Appl Microbiol Biotechnol*, 83:199–208, 2009.
- [16] Fairchild. Mm74c922; mm74c923; 16-key encoder; 20-key encoder. <http://www.mouser.com/ds/2/149/MM74C922-889663.pdf>, 2011.
- [17] Eclipse Foundation. Eclipse. <https://www.eclipse.org/downloads/>, 2012. [Online; accessed 23-03-2017].
- [18] Larsson G and Tornkvist M. Rapid sampling, cell inactivation and evaluation of low extracellular glucose concentrations during fed-batch cultivation. *J Biotechnol*, 49:69–82, 1996.
- [19] Display Elektronik GmbH. Dem 20485 syh-ly. <http://www.serandour.com/datasheets/DEM20485SYH-LY.pdf>, 2007.
- [20] Mentor Graphics. Sourcery codebench lite edition. <https://www.mentor.com/embedded-software/sourcery-tools/sourcery-codebench/editions/lite-edition/>, 2012. [Online; accessed 23-03-2017].
- [21] Hajjaj H, Blanc BJ, Goma G, and Francois J. Sampling techniques and comparative extraction procedures for quantitative determinations of intra- and extracellular metabolites in filamentous fungi. *FEMS Microbiol Lett*, 164:195–200, 1998.
- [22] Lange HC, Eman M, van Zuijlen G, Visser D, van Dam JC, Frank J, de Mattos MJ, and Heijnen JJ. Improved rapid sampling for in vivo kinetics of intracellular metabolites in *saccharomyces cerevisiae*. *Biotechnol Bioeng*, 75:406–415, 2001.
- [23] Uni Heidelberg. Dichte des wassers. [http://www.iup.uni-heidelberg.de/institut/studium/lehre/AquaPhys/docMVEEnv3\\_12/AqSysSkript\\_Kap2.pdf](http://www.iup.uni-heidelberg.de/institut/studium/lehre/AquaPhys/docMVEEnv3_12/AqSysSkript_Kap2.pdf), 2018. [Online; accessed 20-01-2018].

- [24] Honeywell. Pressure sensors 26pc series. <http://www.farnell.com/datasheets/17371.pdf>.
- [25] Texas Instruments. Lmp8358 zero-drift, programmable instrumentation amplifier with diagnostics. <http://www.ti.com/lit/ds/symlink/lmp8358.pdf>, 2013.
- [26] Texas Instruments. Lmx58-n low-power, dual-operational amplifiers. <http://www.ti.com/lit/ds/symlink/lm158-n.pdf>, 2014.
- [27] Texas Instruments. Lmp770x precision, cmos input, rrio, wide supply range amplifiers. <http://www.ti.com/lit/ds/symlink/lmp7702.pdf>, 2015.
- [28] Texas Instruments. Ref50xx low-noise, very low drift, precision voltage reference. <http://www.ti.com/lit/ds/symlink/ref5025.pdf>, 2016.
- [29] Hiller J, Franco-Lara E, Papaioannou V, and Weuster-Botz D. Fast sampling and quenching procedures for microbial metabolic profiling. *Biotechnol Lett*, 29:1161–1167, 2007.
- [30] Schaub J, Schiesling C, Reuss M, and Dauner M. Integrated sampling procedure for metabolome analysis. *Biotechnol Prog*, 22:1434–1442, 2006.
- [31] Lønsmann Iversen JJ. A rapid sampling valve with minimal dead space for laboratory scale fermenters. *Biotechnol Bioengin*, 23:437–440, 1981.
- [32] Junk. Rechner  $f\tilde{A}\frac{1}{4}r$  die luftdichte. <https://rechneronline.de/barometer/luftdichte.php>, 2018. [Online; accessed 20-01-2018].
- [33] Grönke K. *Dissertation. Metabolische  $^{13}C$ -Stoffflussanalyse - vom isotopisch stationären zum instationären Fall*. PhD thesis, Universität Siegen, Institut für Systemtechnik, Forschungszentrum Jülich, 2010.
- [34] Weibel KE, Mor JR, and Fiechter A. Rapid sampling of yeast cells and automated assays of adenylate, citrate, pyruvate and glucose-6-phosphate pools. *Anal Biochem*, 59:208–216, 1974.
- [35] KERN and Sohn GmbH. Operating instruction analytical and precision balances kern 770. <http://www.kern-sohn.com/manuals/files/English/770-GS-GJ-BA-e-0023.pdf>, 2000.
- [36] libusb. Libusb project. <http://libusb.info/>, 2012. [Online; accessed 23-03-2017].
- [37] Mathworks. Matlab. <https://de.mathworks.com/products/matlab.html>, 2012. [Online; accessed 23-03-2017].

- [38] Microchip. Mcp3550/1/3 low-power, single-channel 22-bit delta-sigma adcs. <http://ww1.microchip.com/downloads/en/devicedoc/21950c.pdf>, 2005.
- [39] Microcontroller.net. Stm32f4 discovery development in eclipse. <https://www.mikrocontroller.net/articles/STM32F4-Discovery>, 2012. [Online; accessed 23-03-2017].
- [40] Mashego MR, van Gulik WM, Vinke JL, Visser D, and Heijnen JJ. In vivo kinetics with rapid perturbation experiments in *saccharomyces cerevisiae* using a second-generation bioscope. *Metab Eng*, 8:370–383, 2006.
- [41] Jensen NB, Jokumsen KV, and Villadsen J. Determination of the phosphorylated sugars of the embden-meyerhoff-parnas pathway in *lactococcus lactis* using a fast sampling technique and solid phase extraction. *Biotechnol Bioeng*, 63:356–362, 1999.
- [42] EECS Department of the University of California at Berkeley. Spice. <http://bwrcs.eecs.berkeley.edu/Classes/IcBook/SPICE/>, 2012. [Online; accessed 23-03-2017].
- [43] RXTX Project. Rxtx. <http://rxtx.qbang.org/>, 2012. [Online; accessed 23-03-2017].
- [44] International Rectifier. Irlz34n. <http://www.irf.com/product-info/datasheets/data/irlz34n.pdf>, 1997.
- [45] RS-Components. Atrato ultrasonic 2-500 ml/min flowmeter. <http://at.rs-online.com/web/p/durchfluss-sensor-und-schalter/1366374/>, 2017. [Online; accessed 23-03-2017].
- [46] Buziol S, Schädel F, and van Gulik WM. Probenentnahmevorrichtung und verfahren zur entnahme einer probe aus einem bioreaktor. DE102012003113A1:GmbH FJ., 2013.
- [47] Buziol S, Bashir I, Baumeister A, Claassen W, Noisommit-Rizzi N, Mailinger W, and Reuss M. New bioreactor-coupled rapid stopped-flow sampling technique for measurements of metabolite dynamics on a subsecond time scale. *Biotechnology and Bioengineering*, 80:632–636, 2002.
- [48] Cad soft Computer GmbH. Eagle. <http://www.autodesk.com/products/eagle/free-download>, 2012. [Online; accessed 23-03-2017].
- [49] stlink. Stlink project. <https://github.com/texane/stlink>, 2012. [Online; accessed 23-03-2017].

- [50] STMicroelectronics. Stm32f405xx stm32f407xx. <http://www.st.com/content/ccc/resource/technical/document/datasheet/ef/92/76/6d/bb/c2/4f/f7/DM00037051.pdf/files/DM00037051.pdf/jcr:content/translations/en.DM00037051.pdf>, 2016.
- [51] STMicroelectronics. User manual discovery kit with stm32f407vg mcu. [http://www.st.com/content/ccc/resource/technical/document/user\\_manual/70/fe/4a/3f/e7/e1/4f/7d/DM00039084.pdf/files/DM00039084.pdf/jcr:content/translations/en.DM00039084.pdf](http://www.st.com/content/ccc/resource/technical/document/user_manual/70/fe/4a/3f/e7/e1/4f/7d/DM00039084.pdf/files/DM00039084.pdf/jcr:content/translations/en.DM00039084.pdf), 2016.
- [52] STMicrosystems. Stm-driver. [http://www.st.com/content/st\\_com/en/products/embedded-software/development-tool-software/stsw-link009.html](http://www.st.com/content/st_com/en/products/embedded-software/development-tool-software/stsw-link009.html), 2012. [Online; accessed 23-03-2017].
- [53] STMicrosystems. Stm32f4 serie. <http://www.st.com/en/microcontrollers/stm32f4-series.html?querycriteria=productId=SS1577>, 2012. [Online; accessed 23-03-2017].
- [54] Linear Technologies. Ltspice. <http://www.linear.com/designtools/software/>, 2012. [Online; accessed 23-03-2017].
- [55] TotaraLearn. Fluid flow. <https://www.myodesie.com/wiki/index/returnEntry/id/3006>, 2018. [Online; accessed 20-01-2018].
- [56] Schaefer U, Boos W, Takors R, and Weuster-Botz D. Automated sampling device for monitoring intracellular metabolite dynamics. *Anal Biochem*, 270:88–96, 1999.
- [57] Theobald U, Mailinger W, Reuss M, and Rizzi M. In vivo analysis of glucose-induced fast changes in yeast adenine nucleotide pool applying a rapid sampling technique. *Anal Biochem*, 214:31–37, 1993.
- [58] Ignacio Vazquez-Abrams. Asynchronous data entry onto bus mm74c922. <http://electronics.stackexchange.com/questions/95162/seeking-4x3-keypad-for-atmel-uc3-microprocessor>, 2014. [Online; accessed 23-03-2017].
- [59] Vishay. Model 1004 single point load cells. <http://docs-europe.electrocomponents.com/webdocs/010f/0900766b8010f46a.pdf>.
- [60] VISHAY. 1n4001. <http://www.vishay.com/docs/88503/1n4001.pdf>, 2016.

- [61] De Koning W and van Dam K. A method for the determination of changes of glycolytic metabolites in yeast on a subsecond time scale using extraction at neutral ph. *Anal Biochem*, 204:118–123, 1992.
- [62] Van Gulik WM, Canelas AB, Taymaz-Nikerel H, Douma RD, de Jonge LP, and Heijnen JJ. Fast sampling of the cellular metabolome. *Methods Mol Biol*, 881:279–306, 2012.
- [63] ZAMG. Graz universität-luftdruck. [https://www.zamg.ac.at/cms/de/wetter/wetterwerte-analysen/tawes-verlaufsgraphiken/graz\\_universitaet/luftdruck/](https://www.zamg.ac.at/cms/de/wetter/wetterwerte-analysen/tawes-verlaufsgraphiken/graz_universitaet/luftdruck/), 2018. [Online; accessed 20-01-2018].

## 6 Appendix

### 7 Manual

#### 7.1 Parts of the Device

In this section all parts of the sampling device are shown in the images 40 to 46.



Figure 40: Main Device with user interface



Figure 41: Docking unit with sensors

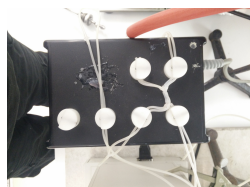


Figure 42: Valve box



Figure 43: Vacuum pump



Figure 44: Vacuum flask, waste flask



Figure 45: Sampling tube



Figure 46: Seal

## 7.2 Sampling Device

### 7.2.1 Set-Up

First of all set up the electrical connections. For this purpose make sure, that the device is switched off. If the device is not switched off, some of the components may take harm, if they are plugged into the main device. The valve box is connected with one connector and the docking unit with two connectors. For the power supply an IEC cord is needed.

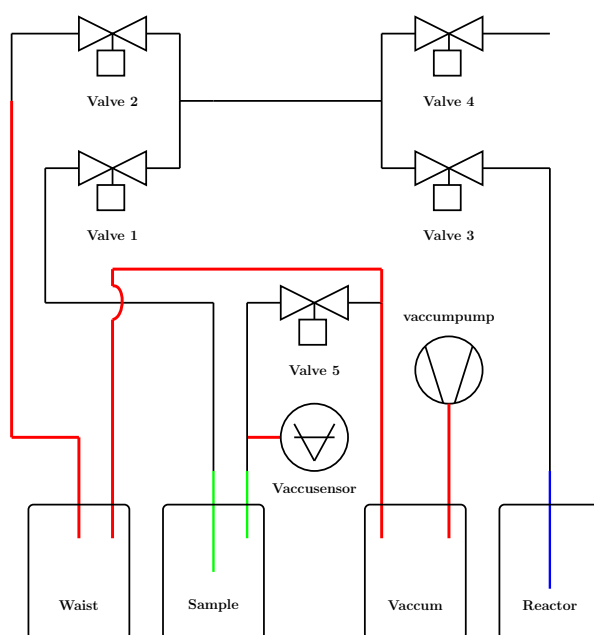


Figure 47: Pipe system

The pipe system should be assembled as shown in figure 47. The red lines symbolizes the vacuum pipes and the black lines the transparent tubing, which should be routed in

duplicate as long as possible. The green lines are the needles and the blue one represents the sampling tube. The arrangement of the valves is displayed in Figure 42.

To assemble the tube system the user connects the vacuum pump with the vacuum flask. From the vacuum flask a connection is made to the valve box and to the waste flask.

The vacuum pipes should be fixated with a stand to relieve traction force from the valve box.

The valve box has to be located at the level of the reactor outlet, to reduce the length of the tubing and therefore the amount of necessary cleaning volume. In every valve there should be 2 sampling pipes and the distance between the sampling valve and the reactor valve should be as short as possible.

The sampling tube should be sterile and connected to the valve box. For the sampling of the liquid the tube is then inserted into the reactor.

For the docking unit a granite plate (or something comparably heavy) is placed on 2 vacuum pipes (as shock absorbing material) to reduce mechanical forces on it. To increase the stiffness of the docking unit a laboratory stand which also stands on the granite plate could be used.

The inner sampling needle and the outer vacuum needle of the sampling head are connected to the valve box. The pipes of this needles must not touch the weight sensor and have to be fixated above the head to reduce vibrations coming from the pipes.

After setting up the device it is recommended to check:

- Only the docking unit must be on the granite plate and no other part must touch the granite plate.
- Nothing touches the weight sensor.
- There are no stress forces on the pipes.
- The pipes to the docking unit are fixated above the docking port.
- All parts of the device must be connected electrically. If one is missing switch off the device and establish the connection.

After this switch on the device and the vacuum pump. Select the Program 1 and add a Falcon-tube to the docking unit. If the tube holds, the pipes are connected correctly. It is recommended to run a whole sequence with water or ethanol to check the function of the whole system.

## 7.2.2 User Interface



Figure 48: User interface

1-9 : Different sampling sequences

0 : Shows the current pressure, weight and calibration factor.

\* : Shows the protocol with time, pressure, weight and sequence number.

# : does currently nothing (only used for debugging)

OK : Start the sequence

Cancel : Abort the sequence

up : Scrolls the screen up

down : Scrolls the screen down

## 7.2.3 Sampling

1. Take care that the system is cleaned, otherwise clean it if necessary.
2. Take care that the system is calibrated, otherwise calibrate it.
3. Insert the sampling tube into the reactor
4. Check if the sampling tube is deep enough in the liquid. This means, the inlet of the tube should be below the surface of the liquid throughout the whole sampling sequence.
5. Select a sequence

6. Insert a Falcon-tube into the docking unit and let the vacuum hold it.
7. Press the green OK button
8. Wait until the device has completed the sequence and do not touch any part of the sampling device. If the sequence has to be aborted press the red button.
9. If finished, remove the Falcon-tube softly. It is recommended to hold the Falcon-tube and press your thumb against the docking unit to remove it.

#### **7.2.4 Cleaning**

For the cleaning the normal sampling procedure is used, but instead of the sampling liquid distilled water and ethanol are used. First run the sampling procedure with distilled water, then with ethanol, then again with distilled water and at last with ethanol. After this empty the waste flask and clean it.

### **7.3 Software**

With the JAVA-Software Rapidsampler it is possible to calibrate, extracting the measurement protocol and modify the sequence.

#### **7.3.1 Installation**

To run the software the following components are needed:

- USB-Driver for the STM32F4
- Oracle Java Runtime Environment (tested with Version 8) or an alternative environment like Open-JDK.
- RXTXComm

In the following section the installation instructions for Microsoft Windows and Debian based Linux are provided.

**Windows** To install the driver, go to the webpage of STM and download the driver for the STSW-LINK009 <sup>1</sup> and start the installation.

After the installation is finished, switch on the device and plug it into the PC. The driver installation should start automatically.

As the next step go to Workspace → Settings → DeviceManager and check if a STMicroelectronics STLink Virtual COM Port is displayed.

The driver is now successfully installed. As next step the JAVA-RTE has to be installed. The installation-files can be downloaded from the Oracle webpage <sup>2</sup>.

The last step is to install the RXTXComm for the correct operating system. The files can be found on the RXTX webpage <sup>3</sup>.

After the installation is completed it should be possible to run the software by double-clicking on the Rapidsampler.jar file.

**Debian based Linux** If the software should run on a Debian based Linux derivate like Ubuntu, Mint or Knoppix it is only necessary to install the openjdk RTE and the RXTX-Com library. For the communication with the device the generic USB-Driver from Linux is enough, and so there is no need to install a specific driver.

To install the required parts an internet connection and the super user password is needed. Then open the terminal and enter the following commands:

```
sudo apt-get install openjdk-9-jre
sudo apt-get install librxtx-java
```

After completing these steps the software can be started by typing this command:

```
java -jar rapidsampler.jar
```

---

<sup>1</sup>[http://www.st.com/content/st\\_com/en/products/embedded-software/development-tool-software/stsw-link009.html](http://www.st.com/content/st_com/en/products/embedded-software/development-tool-software/stsw-link009.html)

<sup>2</sup><https://www.java.com/en/download/>

<sup>3</sup><http://rxtx.qbang.org/wiki/index.php/Download>

## 7.3.2 Overview

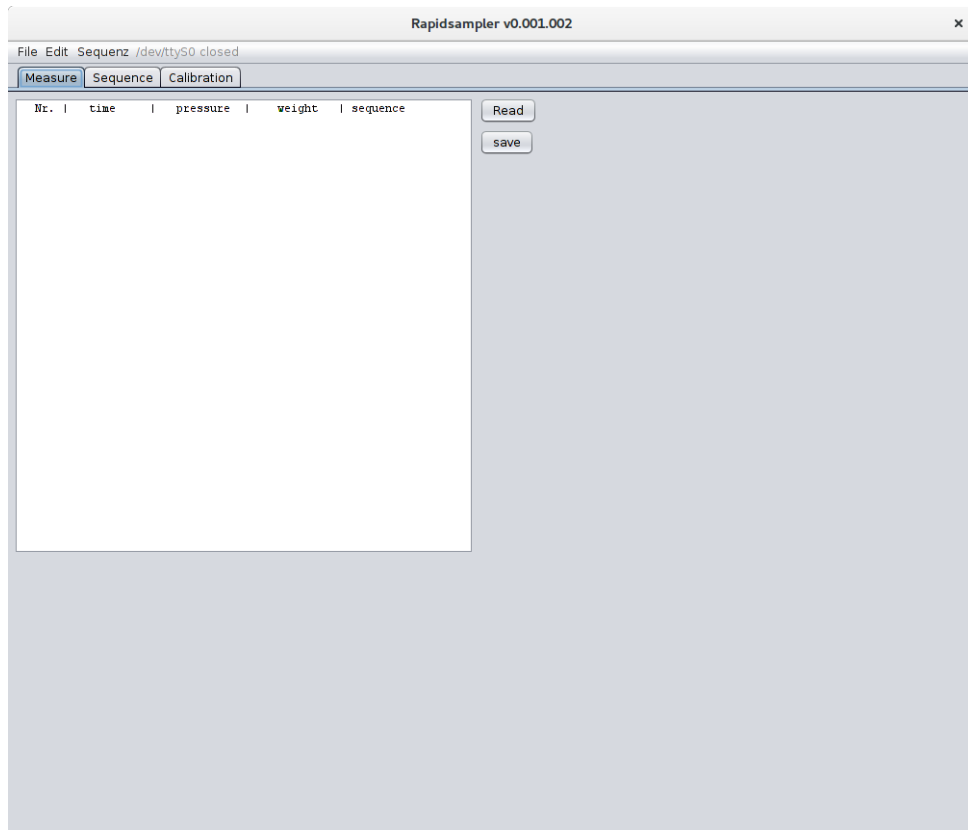


Figure 49: Software GUI

The image 49 shows the software. There are 3 tabs where the different functions can be chosen. The functions are:

**Measure Values** for getting the protocol data.

**Sequence** for modifying the sequence.

**Calibration** for calibration of the device.

## 7.3.3 Establishing a connection

Before connecting the main-device with the PC, switch on the device. After the device is successfully powered up, it can be connected via an USB-Cable (Type A to Mini B). The plug for the USB-cable is on the back of the main device.

Once the physical connection is established, it is necessary to obtain the information which COM-Port is used. In most cases only one COM-Port will be available and this is the sampling device.

On Windows this can be done in the Device-Manager Go to STM32F4 there and check which COM-PORT stands next to it.

In Linux it should be `/dev/ttyACM0` or something similar.

Now start the software and go to Edit → Configuration (Figure 50). Then chose the correct Port in the new window and click Apply (Figure 51).

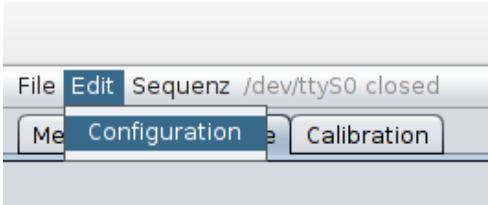


Figure 50: Opening Configuration window

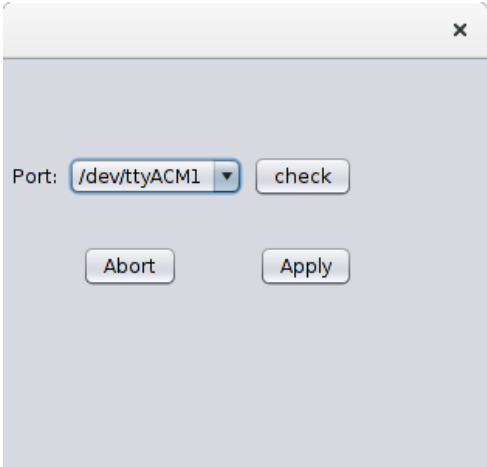


Figure 51: Configuration window

After this step the software is ready to communicate with the device.

### 7.3.4 Measure values

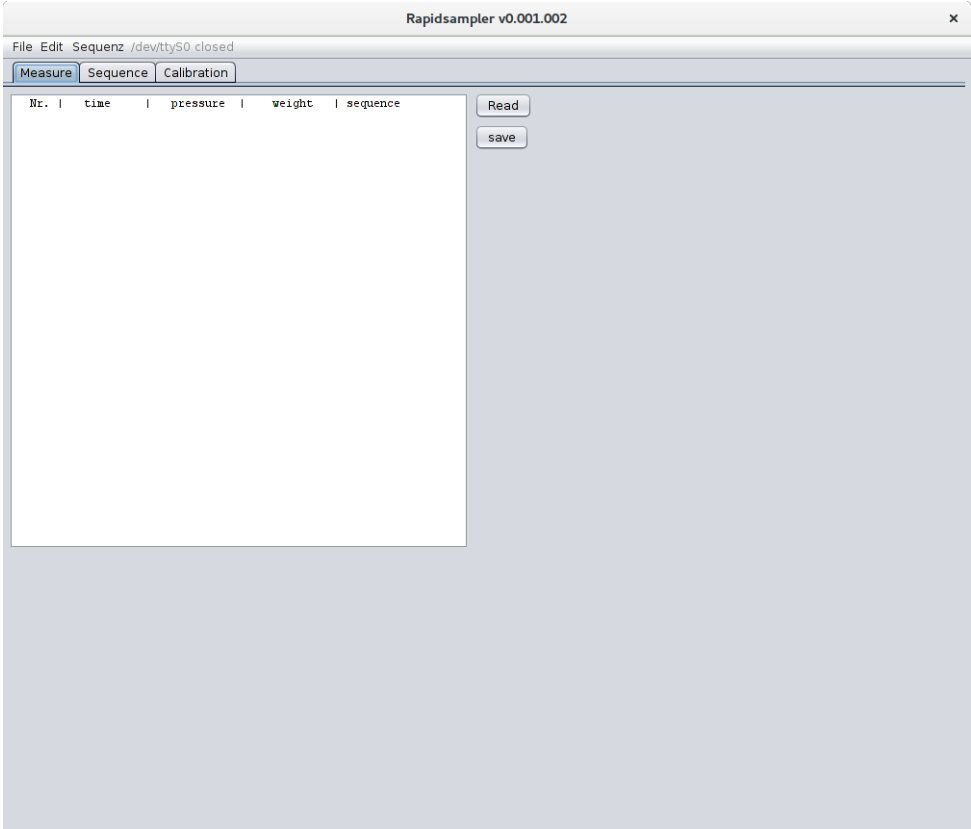


Figure 52: Measurement tab

In the first tab (measure shown in figure 52) all stored measurements can be read by pressing the Read-button and with the Save-button they can be stored as a CSV File.

### 7.3.5 Adapting the Sequence

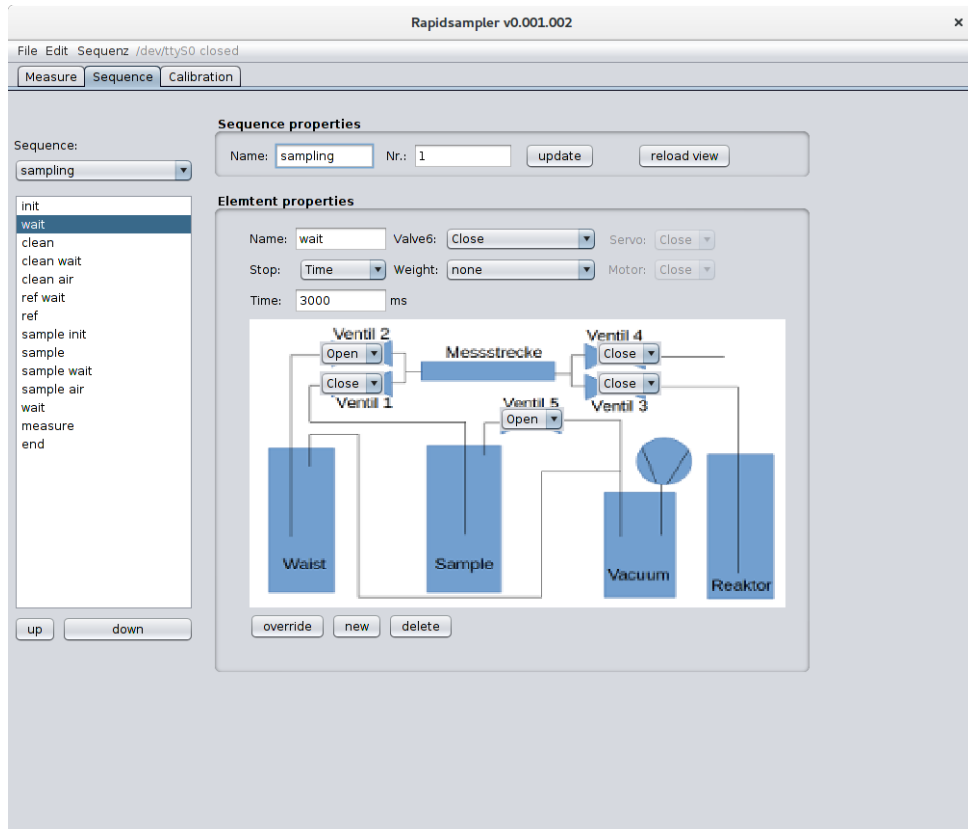


Figure 53: Sequence tab

On the second tab Sequence (Figure 53) it is possible to modify the sequences. First of all the sequence, which should be modified has to be loaded into the software.

#### Loading and storing of a sequence

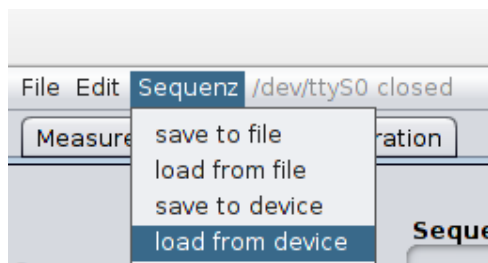


Figure 54: Loading of sequence

This can be done from a file or the device. If the sequence should be loaded from a file go to Sequence → load from file (Figure 54).

If it should be loaded from the device enter a valid number (1-9) into the Nr.-Field and then go to Sequence → load from device.

With the other two options save to file and save to device the current sequence will be stored in a file or transmitted to the device.

## Modifying the sequence

On the left upper corner there is a drop-down menu, which shows all currently loaded sequences by their names. On the right side of it there are text-boxes for entering a new name and a number. The number defines the storing position in the sampling device. After updating this values the user has to press update to apply the changes to the loaded sequence.

Under the drop-down menu there is a list of all steps in the sequence. If the user selects an element the parameters will be loaded to the right side and the configuration of the valves, mass measurement and timers will be visible.

The Valves could have 3 states open, closed and unchanged (-). The unchanged state will be changed to the state of the valve in the previous element when the sequence is stored. The state (unchanged) only exists to make it more comfortable to enter a new element to the sequence.

The Start drop down menu shows the condition to exit this state. There are 4 options:

- Button:** The state will be exit when the OK-button is pressed.
- Pressure:** The state will be exit when the OK-button is pressed and the pressure is below 2000 Pascal.
- Time:** The state will be exit after the time specified in the timer field (value in milliseconds) will be elapsed.
- Detect:** Is not implemented.

For the weight measurement three states are possible.

- none:** The weight measurement is deactivated.
- reference:** The reference value will be optioned.  
This state should be at least 1000ms long.
- weight:** The weight value will be obtained.  
This state should be at least 1000ms long.

At the end of the sequence the reference value will be subtracted from the weight value and multiplied by the calibration factor to obtain the real value.

If something is changed in this section the user has to press Override to apply the changes. With the New-button the current element will be duplicated and added at the end of the list. The Delete-button can be used to remove the current element from the sequence. With the Up- and Down-button the order of the elements in the sequence can be changed.

When modifying the sequence the user has to be careful to check if only one valve changes per element. The other should stay the same. If two valves should change their status, they should be switched with a small delay (50ms). The advantage of this method is that the user always knows which valve changes first and the peak power consumption is lower.

The reload view button can be used if the screens seems to be buggy like loading no new elements or sequences.

### 7.3.6 Calibration

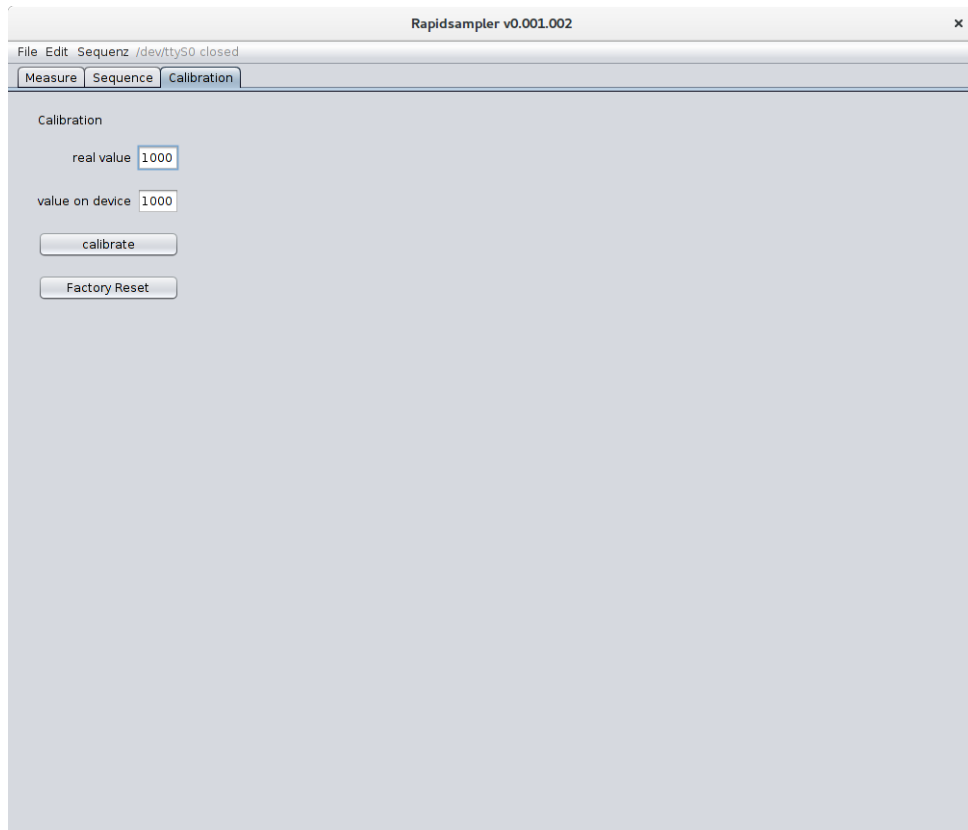


Figure 55: Calibration of the device

The third tab Calibration (Figure 55) is used for calibration of the device. There are two text boxes where the real mass value and the measured value from the device should be entered. The values can be entered in g or mg, as long as they use the same unit. It is also possible (and recommended) to insert the values without a coma, as long as they have the same amount of digits after the comma. It is recommended to enter the values with 5 significant figures (e.g. 1234.5mg).

To obtain a good reliability of the calibration there should be 10 samples drawn and averaged.

$$accuracy = \frac{stddev}{\sqrt{averaged}} = \frac{0.8\%}{\sqrt{10}} = 0.25\% \quad (58)$$

To transmit the values press calibrate.

If the calibration does not work it is possible to reset it with the button factory reset.

It is important to calibrate the device under similar conditions, as it is used. This includes following conditions:

- same position (parts could be dislocated when device is transported)
- same temperature (1-2 degrees Celsius difference is acceptable)
- similar air pressure in the room
- same vacuum pump
- similar falcons
- a liquid with a similar density as the sampled liquid
- the same preloaded amount of liquid in the falcon
- the same sequence

## **7.4 Trouble shooting**

In this section a few possible malfunctions and the possible reason for any malfunctions are listed

### **Display is not lighting**

- The device is not plugged in and switched on.
- The display is defect.

### **Display is flickering or display is on without showing any text**

- The power supply is insufficient. Check if the device is plugged in and switched on. Note that the USB cable can transmit power, but not enough for the correct operating of the device.
- If two valves are switched simultaneously it can also cause an insufficient power supply.

### **No or random pressure data**

- Pressure sensor is not plugged in. Switch off the device, check all cables and switch it on again.
- Pressure sensor is defect.

### **No vacuum**

- Vacuum pump is not switched on.
- The vacuum flasks are not connected correctly.
- The pipes are not connected correctly.

### **Unstable pressure**

- There is a leakage in the system.
- The Falcon-tube is not docked correctly to the docking port.
- The seal in the docking unit has to be replaced.
- The pipes are not connected correctly.

### **Invalid mass**

- The weight-sensor is not connected. Switch off the device, check all cables and switch it on again.
- There is a mistake in the sequence. The measurement needs a minimum of 1000ms to produce a correct value. This has been satisfied for reference and mass measurement.
- The weight-sensor (Instrumentation amplifier or ADC on the circuit board) is defect.

### **Unstable mass**

- There are mechanical influences. Check if the plate is placed freely on a vibration absorbing material.
- Air circulation is disturbing the weight measurement. Block the air blasts with some obstacle.
- The weight-sensor (instrumentation amplifier or ADC on the circuit board) is defect.

### **Incorrect mass**

- If the mass is stable but incorrect a new calibration is required.
- If it is wrong by roughly the factor 20, 10 or 5 the weight sensor (Instrumentation amplifier on the circuit board) is defect.

### **Valves does not switch**

- The valve box is not connected correctly.
- The sequence does not switch a valve.
- Valve or valve driver is defect.

### **No USB connection**

- The device is not plugged in and switched on.
- The USB cable is not plugged in.
- The USB port is not selected correctly.
- The USB driver is not installed properly.
- The RXTXCom is not installed correctly.